CODEE Journal

Volume 12 *Linking Differential Equations to Social Justice and Environmental Concerns*

Article 12

2-13-2019

Linking Differential Equations to Social Justice and Environmental Concerns

Linking Differential Equations to Social Justice and Environmental Concerns

A Special Issue of the CODEE Online Journal
In honor of its founder, Professor Robert Borrelli

Volume 12, Issue 1, 2019

TABLE OF CONTENTS

DEDICATION

Robert Borrelli (1932-2013), who taught at Harvey Mudd College from 1963-2013, was the founder of CODEE in 1992 and ever after its most fervent advocate. In 2013 he was still active as an Emeritus Professor of Mathematics and Emeritus Director of the Mathematics Clinic at Harvey Mudd College (https://www.math.hmc.edu/clinic/).

Borrelli had a special interest in Differential Equations, and he sought throughout his career to link DE's to real word problems. In particular, in 1972, he helped start the Math Clinic, where industries and government agencies work with groups of advanced undergraduate students on unsolved real-world problems that require imaginative, numerically oriented problem-solving skills. The Math Clinic is designed to educate engineers and scientists who will have a knowledge of the society in which they live and whose contributions after graduation reflect an understanding of society's needs.

On the human side, Robert Borrelli was known for his deep interest in equity issues. Early in his career, he established endowments at Harvey Mudd and Stanford to help minority and underprivileged students afford a college education. In this way he could pass on the gift from his older brother James, who had secretly made Bob's education possible.

FOREWORD

About two months ago, towards the end of the semester, I sat in a Differential Equations classroom conducting an interview with a group of students. We talked about many things that were connected to learning how to solve differential equations and systems of differential equations in a student-centered classroom. But the most exciting aspect of the conversation was about how differential equations uses mathematics to address the issues of our world. The students, many mathematics majors, but also other science and engineering majors, were happy to talk about how they solved the differential equations, but the discussion did not stop there! They talked with me about working together on problems of population growth, and climate change, and other questions that involve finding answers to society's and Earth's issues. These students, who were all from underrepresented groups in STEM, showed how they are developing mathematical identities that includes being mathematical problem solvers to make a difference.

I think this story illustrates why this particular new CODEE special issue is so relevant and stimulating. Differential equations and difference equations and their systems provide many answers to describing and predicting what goes on in our world. Once we can describe and predict what is happening, it leads us far into how to address important concerns. Traditionally, all this work goes on in advanced applied mathematics education and in industry. This special issue includes amazing work that highlights how using differential equations can be used for real good in undergraduate mathematics education. For example, there are differential equations which students investigate that can stir the students (and instructors) in new ways that transcend the traditional curriculum of finding closed solutions to the selected differential equations and systems that can be solved. Often for the first time, students can see that mathematics, beautiful in so many ways, also brings ways to understand and change our actual real world.

In this special issue, both social justice and the environment are investigated so that students can become invested in using mathematics to address problems. There is a paper where students investigate climate change and grow to understand how small changes in ecosystems have large overall effects. There is a paper on how spreading lies and the influence on social justice can be studied through differential equations, bringing issues of social justice to light. And there are nine more just as interesting and compelling! The chapters come from authors around the world, showing how we are all in this together--- bringing students into the splendid world of applied mathematics to make a difference. As I looked at the different inquiries addressed, and the many pedagogies and technologies that are used to provide students the means to address the inquiries, my belief that **now is the time to make a difference by teaching differential equations** has been strengthened. As I mentioned in the opening, students are challenged to use mathematics that was not considered accessible to them years ago. It provides instructors with 11 grand ideas on how to make that happen. And in the end, it affects the number of new mathematicians that are in the game to change our world.

Thank you for this new issue, all you authors and editors. Professor Robert Borrelli, to whom this issue is dedicated, would be proud. Those who read it and use the ideas cannot help but be affected for better!

Karen Allen Keene
Next CODEE Editor-in-Chief
Program Director, NSF Division of Undergraduate Education
North Carolina State University
January, 2019

PREFACE

Social Justice and Environmental Concerns are global concerns. In this special volume of the CODEE Journal we bring you eleven papers describing a variety of ways in which differential equations provide a means to study and explore a few facets of these concerns. The collection exhibits much diversity; though these papers are authored by mathematicians, several are collaborations with colleagues in other fields. Furthermore, for this 2018 Special Issue, our authors and editors hail from throughout the United States, Canada, Europe, the Mideast, and Asia. We encourage others to submit papers to the CODEE Journal on these issues.

Many involved in this special issue feel a mighty debt to Bob Borrelli. Several of us on the CODEE Editorial Board would echo what Mike Huber wrote: "Bob was a mentor to me and I respected him tremendously". See Paper IX for a nice elaboration on that theme by Dan Flath. For explicit focus on Bob's social justice theme, see Paper IV by Therese Shelton, Emma Kathryn Groves, and Sherry Adrian – their final sections describe in detail the emphasis on social justice at Southwestern University and the many programs that have resulted. Another article, Paper VIII by Bill Hackborn, squarely addresses a major factor in working toward social justice.

The papers that were submitted to CODEE for this special issue were wonderfully varied. They fall naturally into several groupings, which we enumerate as follows.

Research in assessing worldwide climate is the focus of Papers I and II. Justin Dunmyre and Tianna Bogart (Frostburg University), Nicholas Fortune (Western Kentucky University), Chris Rasmussen (San Diego State University), and Karen Keene (North Carolina State University) show how positive feedback loops and bifurcation diagrams enhance exploration of climate change. James Walsh (Oberlin College), a prominent specialist in modeling climate, uses differential equations to study the effects of changing ocean currents.

Papers III and IV work with extensions of the famous epidemiological SIR (Susceptible, Infected, Recovered) models to study diseases. Michael Huber (Muhlenberg College) offers four increasingly complex SIR models for malaria scenarios in Honduras. Therese Shelton, Emma Kathryn Groves, and Sherry Adrian (Southwestern University) modify the SIR model in the context of transmission of cholera, using data from Haiti.

Papers V, VI and VII adapt these epidemiological models to hot button topics outside of diseases. In the first of these, Lorelei Koss (Dickinson College) has found many applications under the umbrella of "Common Good"; she alerts us to many examples that include terrorism, crime, obesity and bulimia, sustainable agriculture, addiction and intellectual ideas. Authors of the second, Izabel Aguiar, Jessica Deters, and Jacqui Feuerborn, were students at the Colorado School of Mines when they cleverly applied an SRI model to gossip and discerning the truth of a rumor; they are now respectively at Stanford, Virginia Polytechnic Institute, and living in Copenhagen, Denmark. Finally, in the third paper, Selenne Banuelos, Ty Danet, Cynthia Flores, and Angel Ramos (California State University, Channel Islands) give a mathematical SIR model approach (with all compartments equal) to a political system with three parties.

Paper VIII addresses a similar political vein. William Hackborn (University of Alberta, Augustana Campus in Camrose, Alberta) with Tetiana Reznychenko (Vasyl` Stud Donetsk National University, Ukraine) and Yihang Zhang (East China Normal University, Shanghai) model building consensus to show the importance of committed agents.

We turn to economics in Paper IX. Daniel Flath (University of Arizona) uses the Kremer Economic Model to relate population, income, and technology.

Finally, we address the fact that in many regions of the world, the language of instruction is not the native tongue of the students. Many are disadvantaged by insufficient fluency in the language of formal education; they cannot learn and achieve understanding as quickly as is expected. Papers X and XI tell of some approaches to this problem: Haynes Miller (with MIT's Haiti Initiative) has found some success with differential equations (and other subjects) by providing, in native Haitian Creole (*Kreyòl*), software resources and other materials for students and teachers, and by organizing workshops for teachers. We also include a very short note by Younes KarimiFardinpour (Islamic Azad University) that references research studies showing how they are addressing a similar situation in northwest Iran with Azerbaijani students who have low proficiency in Farsi, the official language. KarimiFardinpour has found visualization to be the key to communication and understanding, an important factor in achieving equity in the DE classroom.

This collection of papers is just a beginning for linking differential equations to current issues of social justice and environmental concerns. We hope that many more will follow.

We gratefully acknowledge the top three CODEE Editorial Board members, Ron Buckmire, Ami Radunskaya, and Darryl Yong, who proposed this special issue and have worked hard to bring it to fruition – it has been a fascinating endeavor.

Samer Habre, Editor for this Special Issue
Lebanese American University, Beirut, Lebanon
Beverly West, Assistant Editor
Cornell University

December, 2018

Climate Change in a Differential Equations Course: Using Bifurcation Diagrams to Explore Small Changes with Big Effects

Justin Dunmyre
Frostburg State University

Nicholas Fortune
Western Kentucky University

Tianna Bogart
Frostburg State University

Chris Rasmussen
San Diego State University

Karen Keene
North Carolina State University

Keywords: Climate Change, Bifurcation Diagram, Hysteresis

Manuscript received on July 16, 2018; published on February 13, 2019.

Abstract: The environmental phenomenon of climate change is of critical importance to today's science and global communities. Differential equations give a powerful lens onto this phenomenon, and so we should commit to discussing the mathematics of this environmental issue in differential equations courses. Doing so highlights the power of linking differential equations to environmental and social justice causes, and also brings important science to the forefront in the mathematics classroom. In this paper, we provide an extended problem, appropriate for a first course in differential equations, that uses bifurcation analysis to study climate change. Specifically, through studying hysteresis, this problem highlights how it may be the case that damage done to the environment by a small change cannot be reversed merely by undoing that small change. In addition to the problem itself, we elaborate on the mathematics, discuss implementation strategies, and provide examples of student work. Students in a mathematics classroom do not necessarily expect to confront such issues of social justice or environmental concerns, but we see it as our moral obligation as educators to include such lessons in our classes so that our students can become well-informed global citizens.

1 Introduction

In studying climate, scientists are often concerned about positive feedback loops: two or more processes that magnify each other, creating a system of amplification that leads to an enhanced cycle [4]. One example is the interaction of water vapor with global temperature. As the global temperature increases, the capacity of the atmosphere to contain evaporated water vapor also increases. Continued relative humidity levels would result in an increased amount of water vapor in the atmosphere. Water vapor is a greenhouse gas. Thus, if a climate system has more water vapor in the atmosphere, the global temperature will elevate due to the increased insulation of the atmosphere. These positive feedback loops will eventually equilibrate at a higher temperature. In a high emission scenario, scientists predict that a global increase in average temperature would be enough to kick off a system of positive feedback loops that would equilibrate, by the end of the 21st century, to a temperature between 2.6 and 4.8 degrees Celsius higher than in the years between 1986 to 2005 [7]. The result of this increase would be enough to melt ice caps, completely shift ecological systems, and contribute to species extinction due to significant changes in temperature, precipitation, and ocean acidification [7]. It may even redistribute the areas of the world that can support human life, making previously uninhabitable places like the northern reaches of Siberia and Canada habitable (though they may not support agriculture), and previously habitable places, like coastal zones [6] and southwest Asia [8], uninhabitable.

This environmental phenomenon can be studied in a first course in differential equations using bifurcation diagrams. In this paper, we provide an extended problem that has been implemented in an inquiry differential equations course. We also provide a discussion of the relevant mathematics, implementation strategies, and examples of student work. This extended problem has important mathematical concepts, namely bifurcation analysis (i.e., the effect of varying a parameter in a differential equation) and practical implications related to understanding societies' and governments' impact on the climate. Specifically, this problem highlights how it may be the case that damage done to the environment by a small change cannot be reversed merely by undoing that small change. Instead, reversing the damage may require dramatic changes in policy. The environmental phenomenon discussed here is of crucial importance to today's society. It is our ethical obligation to make clear that the rate at which the global temperature is rising is itself increasing [2] and after a certain point this will cause irreparable damage to our environment. Further to cultivate globally-minded citizens, we believe it is our moral obligation to engage students with these environmental issues in the mathematics classroom.

2 Introducing Climate Change to a Differential Equations Course

In this section, we provide our climate change problem, interspersed with connections to climate science research, the necessary mathematical background and experiences for students to be able to engage with these tasks, and a discussion of the mathematical solutions to the tasks. Following this section, we briefly describe implementation strategies

for this problem and provide examples of student work.

2.1 Classroom Context

Importantly, prior to this extended problem, our students have reinvented a bifurcation diagram as a result of their work through modeling units [11]. These modeling units are part of a full course on differential equations taught from an inquiry-oriented perspective using our materials [12]. By inquiry-oriented we mean mathematics learning and instruction such that students are actively inquiring into the mathematics, while teachers, importantly, are inquiring into student thinking and are interested in using it to advance their mathematical agenda [9, 10]. An inquiry oriented differential equations (IODE) course is problem focused, with problems being experientially real, meaning students can utilize their existing ways of reasoning and experiences to make progress [3], and class time is devoted to a split of small group work and whole class discussion. Whole class discussion is facilitated by the instructor who focuses on generating student ways of reasoning, building on student contributions, developing a shared understanding, and connecting to standard mathematical language and notation [5].

2.2 Extended Problem Exposition and Introduction

In service of these aforementioned goals, our climate change problem begins with the following exposition and extended problem:

> *In studying climate, scientists are often concerned about positive feedback loops: two or more processes that amplify each other, creating a system of amplification that leads to a vicious cycle. One example is the interaction of water vapor with global temperature. If global temperature increases, the capacity of the atmosphere to contain evaporated water vapor also increases. If water resources are available, this would result in an increased amount of water vapor in the atmosphere. Water vapor is a greenhouse gas, thus if a climate system has more water vapor in the atmosphere, the global temperature will increase due to the increased insulation of the atmosphere. This positive feedback loop will eventually equilibrate at a higher temperature. Some scientists predict that a global increase in average temperature of just two degrees would be enough to kick off a system of positive feedback loops that would equilibrate at a temperature at least 6 degrees higher than we have now. This 6-degree increase would be enough to turn rainforests into deserts and melt ice caps. It may even redistribute the areas of the world that can support human life, i.e. making previously uninhabitable places, like the northern reaches of Siberia and Canada, inhabitable (though they may not support agriculture) and previously inhabitable places, like coastal cities, uninhabitable.*
>
> *1. A modern pre-industrial average temperature at the equator is about 20 degrees Celsius. Assuming that our current global climate system has not undergone this vicious cycle, model this system with a phase line. What are the essential features of that phase line?*

This enhanced water vapor greenhouse effect is only one example of the of known climate feedback loops, some of which will act to further enhance or somewhat counteract the modern warming. For example, as more terrestrial heat is reradiated to the surface by the increased levels of water vapor in the atmosphere, less of the earth will be covered by glaciers and sea ice. The reduced surface area of light colored surfaces leads to increased absorption of solar radiation into the surface, thus magnifying the warming. However, with the presence of more water vapor there may also be more clouds. Low-level clouds dampen warming since they reflect a portion of incoming solar radiation back to space. This complex system of feedback loops acts to maintain an equilibrium in the climate system, however when there is a large enough external perturbation a new state of equilibrium is achieved [1].

Phase lines are standard mathematical tools used in qualitative analysis of one-dimensional autonomous systems. Previously, our students worked through various modeling tasks to reinvent the phase line for themselves. The important features of the phase line associated with this problem are two stable equilibria at 20 and 26 degrees Celsius, and an unstable equilibria at 22 degrees Celsius.

The problem continues with the next two tasks:

> *2. What is a simple differential equation that corresponds to your above phase line?*
>
> *3. A group of scientists came up with the following model for this global climate system:* $\frac{dC}{dt} = \frac{1}{10}(C-20)(22-C)(C-26) - k$*, where* C *is the temperature, in Celsius, and* k *is a parameter that represents governmental regulation of greenhouse gas emissions. Assume the baseline regulation corresponds to* $k = 0$*, increasing regulation corresponds to increasing* k*, and the current equatorial temperature is around* 20 *degrees. To what equatorial temperature will the global climate equilibrate?*

In task 2, students create their own differential equation to model this scenario. For the remainder of the extended problem, to facilitate classroom cohesion, students work with the equation given in task 3. In the context of climate science and government regulation, we specifically desired a *negative* k value to correspond to *less regulation*, that is, *deregulation.* Doing so necessitated the differential equation contain a "$-k$" so that a negative k results in a positive shift of the average equatorial temperature. While this differential equation does not capture the complexity of climate change science, it captures the long-term behavior described in the exposition to the extended problem.

2.3 Transition to Bifurcation Diagrams

After students have considered the long-term average equatorial temperature they identify important values of the bifurcation parameter:

> 4. Sketch a bifurcation diagram and use it to describe what happens to the global temperature for various values of k.

Briefly, for a one dimensional system, a bifurcation diagram is a plot of the equilibrium points as a parameter is varied. A bifurcation point is a value of the bifurcation parameter

where a qualitative change in the structure of solution space occurs. In the climate change model there are two such points where the branch of unstable equilibria meets either branch of stable equilibria, resulting in saddle-node (or fold) bifurcations (see Figure 1). In

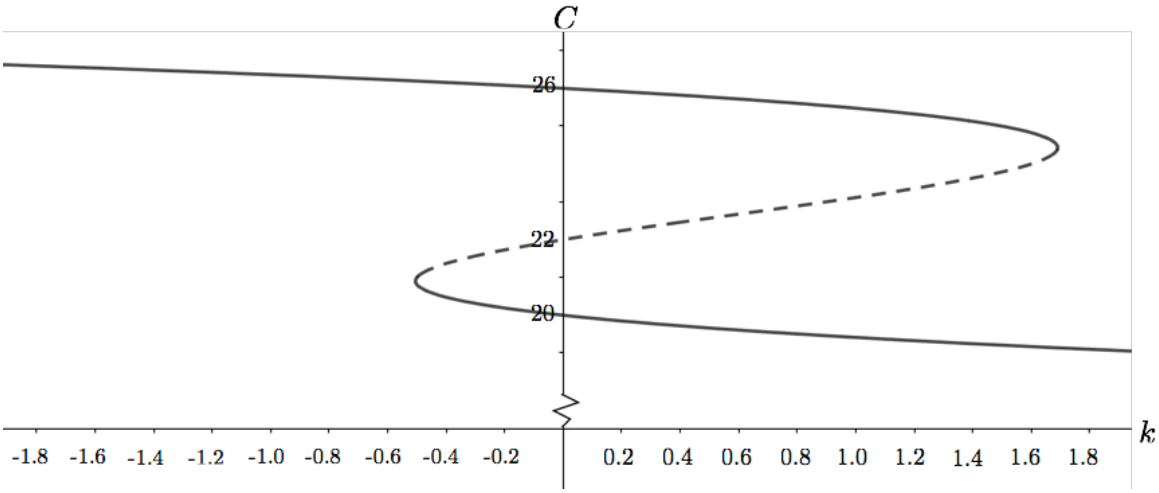

Figure 1: Bifurcation diagram for $\frac{dC}{dt} = \frac{1}{10}(C-20)(22-C)(C-26) - k$ with solid lines for stable equilibria and dashed for unstable equilibria

an effort to provide an answer to what happens for various values of k, we can see that, for instance, for values of k between approximately -0.505 and 1.69, the system is bistable. As described above, at these special values of k the branch of unstable critical points meets the stable branches of equilibria in saddle-node bifurcations. For more extreme values of k the system has a globally attracting equilibrium point (approximately 19 or 26 degrees Celsius depending on the extreme value of k).

2.4 Small Changes with Big Effects

After orientation to the bifurcation diagram, the next task contains the pivotal moment of the problem, that is, how subtle parameter variation (in this case, government deregulation) can have dramatic impact that cannot be readily undone:

> *5. Suppose at the start of a new governmental administration, the temperature at the equator is about 20 degrees Celsius, and $k = 0$. Based on the model and other economic concerns, a government decides to deregulate emissions so that $k = -0.5$. Later, the Smokestack Association successfully lobbied for a 5% change, resulting in $k = -0.525$. Subsequently, a new administration undid that change, reverting to $k = -0.5$, and eventually back to $k = 0$. What is the equilibrium temperature at the equator after all of these changes?*

For this differential equation, we chose the k values of -0.5 and -0.525 because they straddle one of the bifurcation points in the diagram and have only a seemingly insignificant difference between them. Initially, for both $k = 0$ and $k = -0.5$, the global average equatorial temperature equilibrates at the lower of the two stable equilibria, namely 20 and

approximately 21 degrees Celsius, respectively. However, the change to $k = -0.525$ moves the system beyond the bifurcation point, resulting in a globally attracting equilibrium corresponding to a significantly elevated average equatorial temperature, in this case approximately 26.2 degrees Celsius.

The bifurcation diagram indicates that, to undo the change to the average equatorial temperature, it is not mathematically viable to simply undo the change from k=-0.525 back to k=-0.5. This is known as a hysteresis effect. For $k = -0.5$, an initial condition near 26.2 degrees Celsius would be in the basin of attraction for the upper equilibria. Indeed, for $k = -0.5$, any initial condition exceeding 21 degrees Celsius would equilibrate near 26.2 degrees Celsius. Moreover, returning to the baseline regulation ($k = 0$) also fails to return average equatorial temperature to the initial 20 degrees Celsius. Therefore, at the end of these changes to k, the global average equatorial temperature equilibrates to 26 degrees Celsius.

In the course of this exploration, students may have already discussed the final task:

> *6. Use your bifurcation diagram to propose a plan that will return the temperature at the equator to 20 degrees Celsius.*

To have the global average equatorial temperature return to 20 degrees Celsius requires extreme government regulation (i.e., a k in excess of approximately 1.69). Such a value of k would shift the autonomous derivative graph down far enough to result in a globally attracting equilibria near 19.1 degrees Celsius. After reaching this equilibrium, k could be returned to the baseline of $k = 0$, so that the global average equatorial temperature would equilibrate to 20 degrees Celsius.

3 Implementation and Student Work

In this section, we provide a general discussion on the implementation of the extended problem that we have used in our classrooms. Further, we provide examples of student work to highlight the power of this extended problem and its impact on student understanding. We also highlight how students come to interpret the problem in the significant moral landscape of climate change.

Two of the authors implemented this extended problem at their home universities, during an inquiry-oriented differential equations course as described above. The extended problem appeared about halfway through the semester and served as a capstone on the study of one-dimensional differential equations.

Students formed small groups and worked through series of problems. The tasks were spread across several handouts with tasks 3, 5, and 6, strategically placed to avoid spoiling answers to previous tasks. To cover the problem, one author devoted two class days to the climate change problem while the other author devoted one class day and assigned the remaining tasks as homework with a written report. During class time the instructors circulated the room working with small groups to facilitate deep engagement in the tasks. For example, one student supplemented their bifurcation diagram with a sequence of autonomous derivative graphs with values of k corresponding to task 5, and the instructor

built on that student contribution to develop a shared understanding of the hysteresis effect among the whole class.

Importantly, we highlight examples of student work to showcase the rich potential that students have to engage with a culturally and ethically significant problem such as climate change. For example, when drawing bifurcation diagrams for task 4, Figure 2 shows a carefully labeled, qualitatively accurate, bifurcation diagram. Similarly, Figure 3 shows a contextualized understanding of "safe and unsafe zones" for temperature. Note, however, the idea of safe and unsafe zones should be restricted to the bistable region, as opposed to the shading shown that suggests, for instance, that a temperature of 19 degrees Celsius is unsafe when $k = 0$. When discussing task 5, one student wrote:

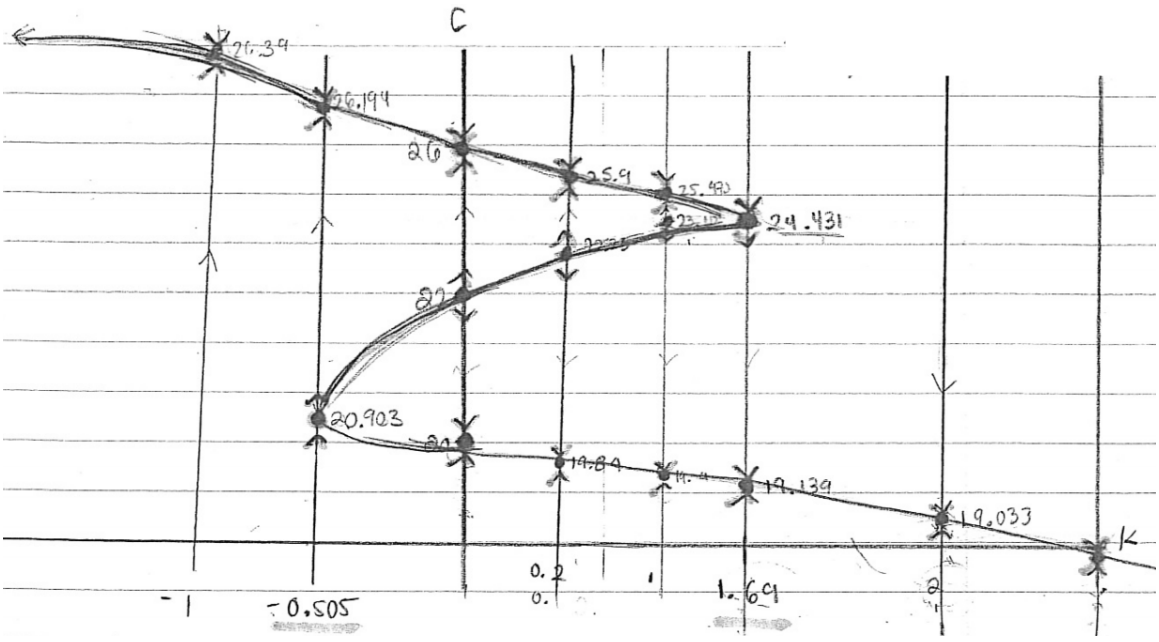

Figure 2: Example of student work.

> After we get $k = -0.525$, we lose two equilibrium points and are forced to jump to the highest equilibrium point $y = 26$. Even after going back to $k = 0$ we still have to settle at $y = 26$ because we already jumped passed the repeller $y = 22$, which is sort of the "over-the-hill" point.

From an expert's point of view, this student is discussing the hysteresis effect. The small change to $k = -0.525$ (i.e., deregulation) causes the global average equatorial temperature to equilibrate near 26 degrees Celsius as previous equilibrium points no longer exist. Further, the student highlights an understanding of the way in which the unstable equilibrium (22 degrees Celsius) serves as a threshold between the other equilibria, providing an opportunity for the instructor to introduce the formal term hysteresis.

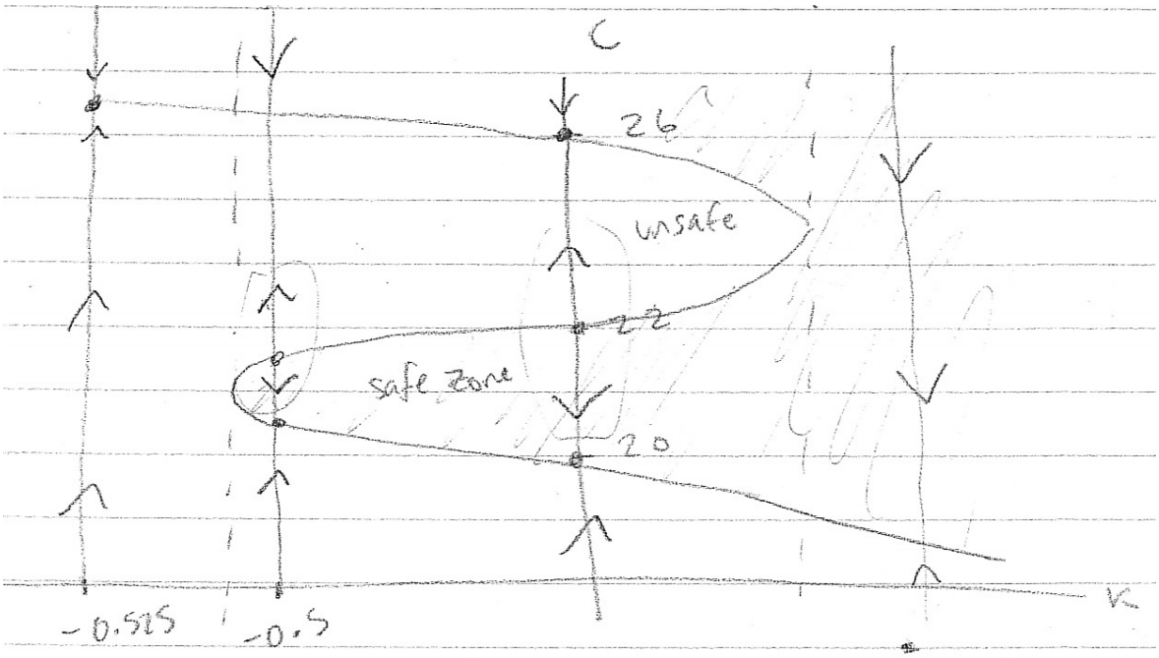

Figure 3: Example of student work.

4 Discussion and Conclusion

In this paper, we presented an extended problem that orients students to the hysteresis effect, one in which a subtle change in a parameter can have drastic implications for long-term behavior of solutions to a differential equation. We framed this mathematical lesson within a moral imperative to engage mathematics students with important modern and global environmental issues.

Our students appreciated the relevance and immediacy of this extended problem. Many were surprised in task 5 that the temperature would not return to 20 degrees Celsius when baseline regulation is reestablished. They were also concerned about the implications of needing a much larger, in absolute value, k to undo the damage done by the deregulation in task 5. One student was particularly excited that, as a dual major in mathematics and political science, this was the first time his two majors ever coincided. Another student wrote the following as a reflection on their work in the climate change problem:

> I found the climate change problem particularly interesting because it shows how bifurcation diagrams can be used in real-world scenarios. Initially I thought the phase line for this problem would only have 2 or 1 equilibrium solutions because I could not comprehend how we could stray away from an attractor far enough to jump to another attractor point, but this problem helped me see that it actually could happen. Also, I like this problem because the context makes sense. If there is too much government deregulation, we would lose our "safe zone" and our repelling equilibrium solution, forcing us to jump up to high average temperatures. This is what I would expect to happen in the real world. However, this problem also shows me if this

> were to happen, it is not necessarily irreversible. Initially, I figured if we were to lose our safe zone, we would jump up to the highest equilibrium point and we would be screwed, but this problem showed me we actually could reset temperatures with very strict government regulation of pollution. This problem is a nice illustration of bifurcation diagrams and bifurcation values in the real world.

Of course, the model in task 3 is simple and could not possibly capture the complexity of climate science. However, it is a powerful model because in task 2, students actually develop a very similar model for themselves. This affords the opportunity to fully understand the model and facilitates engagement with the surrounding lesson. Predictions about global average temperature at the equator made sense to our students. Therefore, the drastic changes to these temperatures, resulting from small changes in the parameter, were surprising but also easy to grasp as exemplified in the student quote above. Therein lies the power of the model, it's simplicity allowed students to grasp the consequences of the regulation/deregulation scenario and also to imagine how such consequences could arise in more complicated and scientifically accurate models.

The environmental phenomenon of climate change science discussed in this paper is of immediate concern to our society. It is our ethical obligation to make clear that the rate at which the global temperature is rising is itself increasing [2] and after a certain point that will cause irreparable damage to our environment. In particular, such damage may redistribute habitable areas in such a way that raises serious concerns regarding equity and social justice. We used differential equations to explore this phenomenon and what it might take to undo certain damages. Students in a mathematics classroom do not necessarily expect to confront such issues of social justice or environmental concerns, but we contend that it is our moral obligation as instructors to include such lessons in our classes so that our students will be well-informed global citizens.

References

[1] Jean-Louis Dufresne and Marion Saint-Lu. Positive feedback in climate: Stabilization or runaway, illustrated by a simple experiment. *Bulletin of the American Meteorological Society*, 97(5):755–765, 2016.

[2] Robert J.H. Dunn, Dale F Hurst, Nadine Gobron, and Kate M Willett. Global climate [in "state of the climate in 2016"]. *Bulletin of the American Meterological Society*, 98 (8):S5–S62, 2017.

[3] Koeno Gravemeijer and Michiel Doorman. Context problems in realistic mathematics education: A calculus course as an example. *Educational studies in mathematics*, 39 (1-3):111–129, 1999.

[4] William W Kellogg and Stephen H Schneider. Climate stabilization: For better or for worse? *Science*, 186(4170):1163–1172, 1974.

[5] George Kuster, Estrella Johnson, Karen Keene, and Christine Andrews-Larson. Inquiry-oriented instruction: A conceptualization of the instructional principles. *PRIMUS*, 28(1):13–30, 2018.

[6] Gordon McGranahan, Deborah Balk, and Bridget Anderson. The rising tide: assessing the risks of climate change and human settlements in low elevation coastal zones. *Environment and urbanization*, 19(1):17–37, 2007.

[7] Rajendra K Pachauri, Myles R Allen, Vicente R Barros, John Broome, Wolfgang Cramer, Renate Christ, John A Church, Leon Clarke, Qin Dahe, Purnamita Dasgupta, et al. *Climate change 2014: synthesis report. Contribution of Working Groups I, II and III to the fifth assessment report of the Intergovernmental Panel on Climate Change*. IPCC, 2014.

[8] Jeremy S Pal and Elfatih AB Eltahir. Future temperature in southwest asia projected to exceed a threshold for human adaptability. *Nature Climate Change*, 6(2):197, 2016.

[9] Chris Rasmussen and Oh Nam Kwon. An inquiry-oriented approach to undergraduate mathematics. *The Journal of Mathematical Behavior*, 26(3):189–194, 2007.

[10] Chris Rasmussen, Karen Marrongelle, Oh Nam Kwon, and Angie Hodge. Four goals for instructors using inquiry-based learning. *Notices of the AMS*, 64(11), 2017.

[11] Chris Rasmussen, Justin Dunmyre, Nicholas Fortune, and Karen Keene. Modeling as a means to develop new ideas: The case of reinventing a bifurcation diagram. *PRIMUS*, in-press(just-accepted):1–27, 2018.

[12] Chris Rasmusssen, Karen Keene, Justin Dunmyre, and Nicholas Fortune. Inquiry oriented differential equations (course materials). URL https://iode.wordpress.ncsu.edu.

The Ocean and Climate Change: Stommel's Conceptual Model

James A. Walsh
Oberlin College

Keywords: Overturning circulation, density gradients, stable nodes, bifurcation
Manuscript received on December 19, 2018; published on February 13, 2019.

Abstract: The ocean plays a major role in our climate system and in climate change. In this article we present a conceptual model of the Atlantic Meridional Overturning Circulation (AMOC), an important component of the ocean's global energy transport circulation that has, in recent times, been weakening anomalously. Introduced by Henry Stommel, the model results in a two-dimensional system of first order ODEs, which we explore via *Mathematica*. The model exhibits two stable regimes, one having an orientation aligned with today's AMOC, and the other corresponding to a reversal of the AMOC. This material is appropriate for a junior-level mathematical modeling or applied dynamical systems course.

1 Introduction

That our climate is changing is difficult to dispute. The most recent assessment report of the Intergovernmental Panel on Climate Change (IPCC AR5) concludes [8]:

> Warming of the climate system is unequivocal, and since the 1950s, many of the observed changes are unprecedented over decades to millennia. The atmosphere and ocean have warmed, the amounts of snow and ice have diminished, sea level has risen, and the concentrations of greenhouse gases have increased.

IPCC AR5 also provides strong evidence indicating that human activities, such as the burning of fossil fuels, have contributed significantly to this warming trend.

The ocean plays a major role in our climate system. For example, the ocean has a remarkable capacity for absorbing large amounts of atmospheric CO_2, a potent greenhouse gas. It is estimated that the ocean has absorbed 40% of all anthropogenic CO_2 emissions since the beginning of the industrial era, with the rate of uptake by the ocean increasing in the 2000s [3].

The focus in this article, however, will be placed on a second crucial aspect of the ocean's role in shaping our climate, namely, its capacity for transporting vast amounts of energy. The Thermohaline Circulation (THC) is the major global ocean circulation

pattern, with the rate of flow determined by density contrasts which, in turn, are functions of temperature and salinity (*thermo*–heat; *haline*–salt).

The Atlantic Meridional Overturning Circulation (AMOC), one component of the THC, consists of the northward flow of warm, upper-ocean waters to the North Atlantic, and the deep southward return flow of denser water that forms through the process of cooling and sinking at high latitudes (this latter phenomenon is known as *deep water formation*). Changes in the strength of the AMOC alter this important process of heat transport to northern latitudes, with cooling in the subtropical North Atlantic and colder climates along coastal areas of Europe being potential consequences.

The AMOC has indeed weakened over the past 150 years, a change that is anomalous relative to the preceding 1500 years [10]. Thornalley et al suggest that enhanced freshwater fluxes from melting glaciers into the North Atlantic in the middle of the 19th century—at the end of a cool period known as the Little Ice Age—resulted in less dense water and reduced deep water formation, weakening the AMOC. Currently, with ongoing reductions in the mass of the Greenland ice sheet (along with other factors), scientists believe further slowing of the AMOC is very likely in the coming decades [7]. As it stands, the current weakening of the AMOC is playing an essential role in distressing several marine species in the Gulf of Maine [2].

Changes in the strength of the AMOC have a profound effect on climate. Going back further in time, the last ice age saw repeated, millennial climate oscillations—relatively colder and warmer periods within the ice age itself—the most pronounced occurring between twenty-five and sixty thousand years ago. Analysis of data from ocean sediment cores shows the AMOC weakened during every colder phase, while relatively warmer periods followed a reinvigoration of the overturning circulation [4]. This work of L.G. Henry et al provides direct evidence of the central role played by the ocean, and the AMOC in particular, in significant climate change.

The AMOC is driven by density contrasts, with water density a decreasing function of temperature and an increasing function of salinity. In his pioneering 1961 paper [9], Henry Stommel introduced a conceptual 2-reservoir ocean box model to investigate the density-driven flow between the boxes. The water flows through a connecting, bottom capillary, with a compensating overflow at the top (in sum representing the "overturning circulation"). Interestingly, Stommel found coexisting stable regimes, one for each direction of flow through the capillary. The fact these two distinct stable regimes can occur in such an idealized model lead Stommel to wonder if a similar situation might occur in nature. If the AMOC, for example, possessed a stable motion having a direction of flow the reverse of that which we have today, might a sufficient perturbation of our climate system cause the AMOC to jump to this other regime?

Stommel's model results in a pair of first order ODEs and, as such, its study is appropriate for a modeling course or a class focusing on the qualitative and/or numerical investigation of planar systems of ODEs. (I present Stommel's model in a climate modeling course having the sophomore-level ODE course as a prerequisite.) While providing no real predictive power, Stommel's conceptual model does allow for investigations into the manner in which fundamental factors such as water temperature and salinity influence density contrasts, and thus the strength and direction of an idealized flow between two basins.

Motivating 1-box models are introduced in Sections 2 and 3 to investigate the interactions between temperature, salinity, and flow rate as they influence the density of a water parcel over time. In particular, these simple models help set the stage for Stommel's more sophisticated 2-box model, presented in Section 4. As mentioned above, there is a feedback in the sense that flow rate in turn affects the density. To introduce this feedback, a second reservoir is added to the model and the corresponding 2-dimensional system of ODEs is derived in Section 4. The dynamics of the model are investigated, with the aid of *Mathematica*, in Section 5. We discuss bifurcations and the associated hysteresis exhibited by the model in Section 5 as well. Concluding remarks are presented in the final section.

2 A 1-Basin Model

Consider a well-mixed reservoir of water with uniform temperature $T = T(t)$ (°C) and uniform salinity $S = S(t)$. The quantity S is defined as a concentration and is measured in practical salinity units (psu), a dimensionless unit. Porous walls separate the basin from an outer vessel having constant temperature T^* and constant salinity S^* (Figure 1). The outer vessel might, for example, represent a neighboring ocean.

Assume the transfer of heat and salt between the reservoir and outer vessel is modeled simply by

$$\begin{aligned} \frac{dT}{dt} &= c(T^* - T) \\ \frac{dS}{dt} &= d(S^* - S), \end{aligned} \tag{2.1}$$

where $c > 0$ and $d > 0$ are constants. Students can be asked to show the general solution of (2.1) is

$$(T(t), S(t)) = (T^* + (T_0 - T^*)e^{-ct},\ S^* + (S_0 - S^*)e^{-dt}), \quad (T_0, S_0) = (T(0), S(0)).$$

Every solution of (2.1) converges to the equilibrium (T^*, S^*) as $t \to \infty$ in this setting.

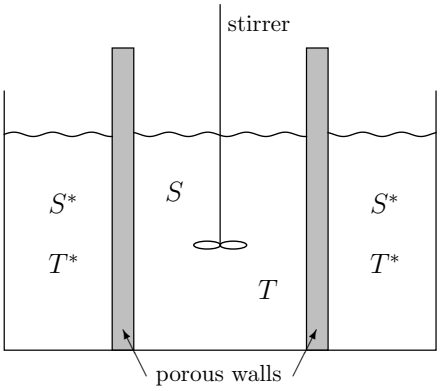

Figure 1: The outer vessel has constant salinity S^* and temperature T^*. Heat and salinity are exchanged with the outer vessel through porous walls.

2.1 Nondimensionalization

Note system (2.1) contains the four parameters c, d, T^* and S^*. The number of parameters can be reduced by *nondimensionalizing*; letting $x = S/S^*$, we have

$$\frac{dx}{dt} = \frac{1}{S^*}\frac{dS}{dt} = \frac{1}{S^*}(d(S^* - S)) = d(1 - x).$$

Similarly, setting $y = T/T^*$ yields

$$\frac{dy}{dt} = \frac{1}{T^*}\frac{dT}{dt} = \frac{1}{T^*}(c(T^* - T)) = c(1 - y).$$

Note variables x and y are dimensionless; additionally, we now only have two parameters.

A further simplification can be realized by rescaling time; setting $\tau = ct$ yields

$$\frac{dx}{d\tau} = \frac{dx}{dt}\frac{dt}{d\tau} = \frac{1}{c}(d(1 - x)) = \delta(1 - x) \quad \text{and} \quad \frac{dy}{d\tau} = \frac{dy}{dt}\frac{dt}{d\tau} = \frac{1}{c}(c(1 - y)) = (1 - y),$$

where $\delta = d/c$ is the (dimensionless) ratio of the rates at which salinity and temperature approach equilibrium. Letting "$'$" denote $\frac{d}{d\tau}$, we have

$$\begin{aligned} x' &= \delta(1 - x) \\ y' &= 1 - y, \end{aligned} \tag{2.2}$$

a system with the single parameter δ. Given that thermal energy generally transfers on a faster time scale than does salinity, Stommel chooses $\delta = 1/6$, so that temperature equilibrates much more quickly than does salinity (Figure 2).

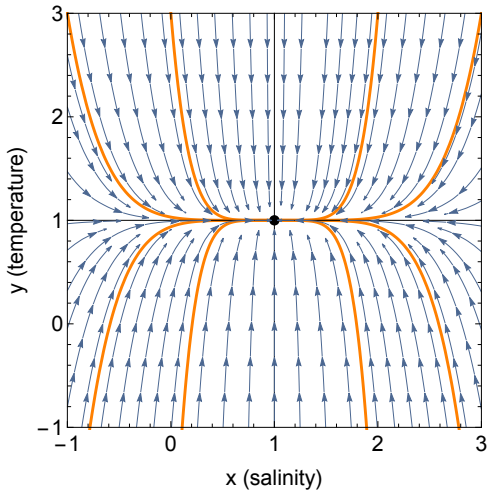

Figure 2: Phase plane for system (2.2) with $\delta = 1/6$. All solutions tend to $(1, 1)$, with y (temperature) equilibrating more quickly than x (salinity).

2.2 Density Anomaly

Recall that temperature and salinity work in an opposing fashion in determining density. One might ask what happens to the density over time if, for example, salinity and temperature each increase toward equilibrium. Let Γ denote the solution to system (2.2) with initial condition $(x(0), y(0)) = (0, 0)$ (so that $x(t)$ and $y(t)$ each increase toward 1 as $t \to \infty$). Given that density is an increasing function of salinity and a decreasing function of temperature, a simple approach is to let

$$\rho = \rho_0(1 - \alpha T + \beta S), \tag{2.3}$$

where ρ (gm/cm^3) is the density, ρ_0 is a reference density (here corresponding to the density at $T = S = 0$), and α ($^\circ$C^{-1}) and β (psu^{-1}) are positive constants. Using $T = yT^*$ and $S = xS^*$, we have

$$\rho = \rho_0(1 - \alpha y T^* + \beta x S^*) = \rho_0(1 + \alpha T^*(-y + Rx)), \tag{2.4}$$

where $R = \beta S^*/\alpha T^*$ is a positive, dimensionless constant measuring the relative effect of salinity and temperature on density.

At the equilibrium point $(x, y) = (1, 1)$, $\rho' = \rho_0(1 + \alpha T^*(-1 + R))$. The density at equilibrium will thus be greater than at $(x, y) = (0, 0)$ if $R > 1$; following Stommel, we set $R = 2$.

One might then ask if the density increases monotonically along Γ as x and y approach equilibrium. Using (2.4) and equations (2.2), note

$$\rho' = \rho_0 \alpha T^*(-y' + Rx') = \rho_0 \alpha T^*(-1 + y + R\delta(1 - x)).$$

When $x = y = 0$, $\rho' = \rho_0 \alpha T^*(-1 + R\delta) < 0$ since $R = 2$ and $\delta = 1/6$. Thus, starting at $(x, y) = (0, 0)$, the density first decreases, due to the larger time constant for temperature, as T rapidly approaches equilibrium. Given sufficient time, however, salinity becomes the dominant factor as it increases toward equilibrium (via long-term evaporation, say), resulting in an eventual increase in density.

The interplay between temperature and salinity vis-à-vis density described above can be viewed in the (dimensionless) *density anomaly*

$$\sigma = \frac{1}{\alpha T^*}\left(\frac{\rho}{\rho_0} - 1\right) = -y + Rx, \tag{2.5}$$

which follows from (2.4). The term anomaly is used as σ is proportional to $\rho - \rho_0$ so that, starting at $x = y = 0$, whether the water becomes more or less dense over time is indicated by whether $\rho - \rho_0 > 0$ or $\rho - \rho_0 < 0$. Level sets of σ, along with the trajectory Γ, are plotted in Figure 3. Note the density anomaly $\sigma < 0$ on $(0, \hat{t})$ due to the influence of increasing temperature, and $\sigma > 0$ on $(\hat{t}, \infty)$ as salinity continues to increase ($\hat{t}$ as in Figure 3).

While model (2.1) has been introduced to investigate the dynamics of the density as temperature and salinity evolve in the simplest of settings, the following section presents an augmented model incorporating flow rate and the effect flow rate has on density.

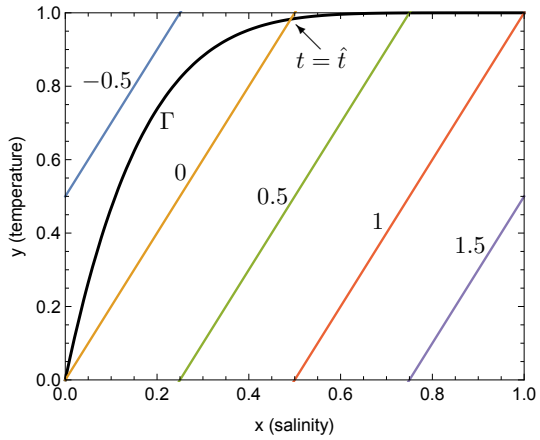

Figure 3: Level sets of the density anomaly σ (2.5) (colored lines) and the trajectory of the solution Γ starting at $(x, y) = (0, 0)$. The water in the basin is less dense than at $(x, y) = (0, 0)$ for $t \in (0, \hat{t})$, and more dense for $t > \hat{t}$.

3 A 1-Basin Model with Inflow and Outflow

To consider the effects flow rate may have on density, imagine an external inflow of water having fixed temperature $T = T_{in}$ and fixed salinity $S = S_{in}$ at a rate q (s^{-1}). Basin water having temperature T and salinity S exits the reservoir at the same rate q (see Figure 4). The equation for the temperature of the basin water is now

$$\frac{dT}{dt} = c(T^* - T) + q\,T_{in} - q\,T.$$

To simplify matters, shift the origin of the temperature axis to T_{in} by setting $u = T - T_{in}$. Note

$$\begin{aligned}\frac{du}{dt} = \frac{dT}{dt} &= c(T^* - u - T_{in}) + q\,T_{in} - q(u + T_{in}) \\ &= c(u^* - u) - qu,\end{aligned}$$

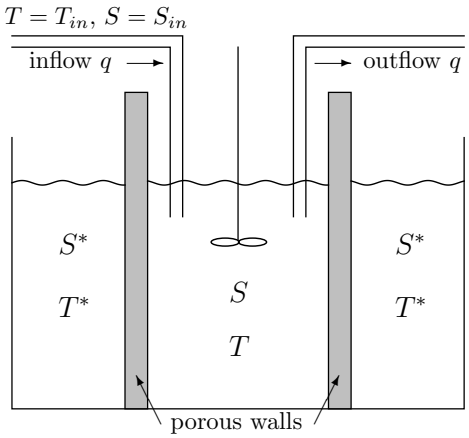

Figure 4: The 1-box, inflow/outflow model. The incoming water has fixed temperature $T = T_{in}$ and fixed salinity $S = S_{in}$.

where $u^* = T^* - T_{in}$. Similarly, after setting $v = S - S_{in}$ and letting $v^* = S^* - S_{in}$, the salinity equation becomes

$$\frac{dv}{dt} = d(v^* - v) - qv.$$

Note that in the (u, v)-coordinate system it is the evolution of temperature and salinity relative to T_{in} and S_{in}, respectively, that is being modeled.

As above, we nondimensionalize by letting $x = v/v^*$, $y = u/u^*$ and $\tau = ct$ to reduce the number of parameters. One can easily check these substitutions result in the system

$$\begin{aligned} x' &= \delta - (\delta + f)x \\ y' &= 1 - (1 + f)y, \end{aligned} \tag{3.1}$$

where $\delta = d/c$ as before, and $f = q/c$ is a (new) dimensionless flow rate.

Note the equilibrium solution of (3.1) has the form

$$(x^*, y^*) = \left(\frac{\delta}{\delta + f}, \frac{1}{1 + f}\right). \tag{3.2}$$

Let ρ_0 denote the density of the basin water when $(u, v) = (0, 0)$, that is, when $(T, S) = (T_{in}, S_{in})$. Setting $\rho = \rho_0(1 - \alpha u + \beta v)$ and proceeding as in the previous section, the density anomaly at equilibrium becomes

$$\sigma^* = \frac{1}{\alpha u^*}\left(\frac{\rho}{\rho_0} - 1\right) = -y^* + Rx^* = -\frac{1}{1 + f} + \frac{R\delta}{\delta + f}. \tag{3.3}$$

Note that we have made use of (3.2).

If we set $f = 0$ in (3.2) and (3.3) (so $q = 0$ and the inflow and outflow are turned off), we recover $(x^*, y^*) = (1, 1)$ and $\sigma^* = -1 + R = 1 > 0$, as in Section 2. As the flow rate $f \to \infty$, however, $(x^*, y^*) \to (0, 0)$ and $\sigma^* \to 0$. We thus see that the density anomaly at equilibrium varies with the flow rate. Indeed, plotting the density anomaly at equilibrium σ^* as a function of the flow rate f (Figure 5), we see the outflow is more dense than the inflow water if $f \in (0, 1/4)$, while the outflow is less dense than the inflow water if $f \in (1/4, \infty)$.

This simple model illustrates the role flow rate plays in determining water density in the basin. For a very slow inflow/outflow, an incoming parcel of water resides in the basin for an extended time, during which the salinity comes to dominate the density as discussed in Section 2. For fast inflow/outflow rates, temperature has the dominating short-term effect and the outflow water is then less dense than the inflow.

The AMOC is driven by density contrasts, as mentioned above. In this section we have seen the flow rate influences density, so that there is a feedback between flow rate and density. To investigate this feedback a second basin will be added to the model, as described in the following section.

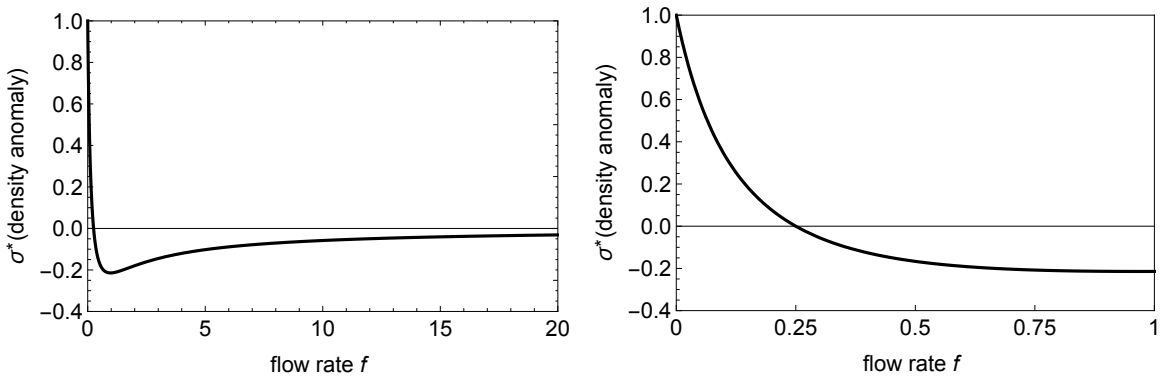

Figure 5: The density anomaly at equilibrium as a function of flow rate f. *Left*: $0 < f < 20$. *Right*: $0 < f < 1$. Small flow rates lead to outflow more dense than the inflow; larger flow rates lead to outflow less dense than the inflow.

4 Stommel's 2-Box Model

4.1 Model Equations

Consider two well-mixed basins of water connected at the bottom by a capillary, with a corresponding overflow at the top so as to maintain constant volume in each basin. There is an exchange of heat and salinity with outer vessels having constant temperature T_i^* and salinity $S_i^*,\ i = 1, 2$ (see Figure 6).

Let $T_i(t)$ and $S_i(t)$ denote the temperature and salinity of the water in box $i,\ i = 1, 2$. The direction and strength of the flow through the capillary is driven by the difference in densities of the two boxes. If $S_1 = S_2$, for example, the colder box will contain denser water and the flow will be from the colder to the warmer box. This would then correspond to a flow of water from the cooler high latitudes to the warmer low latitudes (as is currently the case with deep water formation and the AMOC).

If $T_1 = T_2$, however, then salinity will determine the difference in densities. Due to

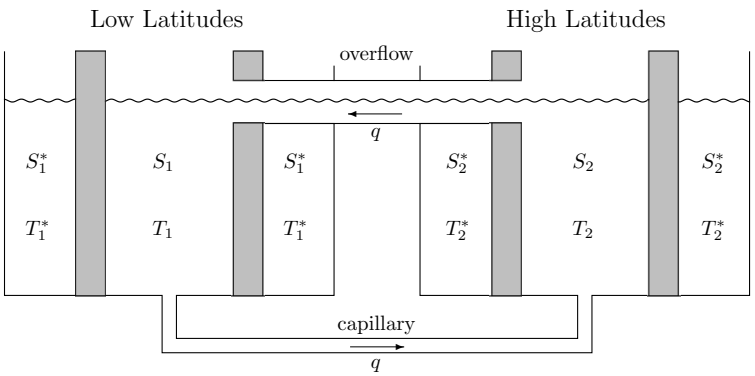

Figure 6: Stommel's 2-box model. The direction of flow through the capillary is driven by density differences. As pictured here, the capillary (deep water) flow is from the low latitude (warm) box to the high latitude (cold) box.

increased evaporation in lower latitudes, with a resulting increase in salinity of the ocean water, the lower latitude box will be the saltier of the two. Hence if $T_1 = T_2$, the saltier box will contain denser water and the flow will be from the warmer to the colder box. This would then correspond to a flow of water from the warmer low latitudes to the cooler high latitudes.

We note that water in the high latitude box is colder but less salty, while the water in the low latitude box is warmer but saltier, so the direction of the flow is, generally, not clear.

Let's first derive the temperature equations for the 2-box model. Referring to Figure 6, the equations are

$$\begin{aligned} \frac{dT_1}{dt} &= c(T_1^* - T_1) + q\,T_2 - q\,T_1 \\ \frac{dT_2}{dt} &= c(T_2^* - T_2) - q\,T_2 + q\,T_1. \end{aligned} \tag{4.1}$$

Note equations (4.1) remain unchanged if the direction of the flow is reversed, due to the compensating overflow at the top of the basins. We thus have

$$\frac{dT_1}{dt} = c(T_1^* - T_1) + |q|(T_2 - T_1) \tag{4.2a}$$

$$\frac{dT_2}{dt} = c(T_2^* - T_2) - |q|(T_2 - T_1). \tag{4.2b}$$

It is once again convenient to shift the temperature axes, here setting $u_i = T_i - T^*_{ave}$, $i = 1, 2$, where $T^*_{ave} = \frac{1}{2}(T_1^* + T_2^*)$. Equation (4.2a) becomes

$$\begin{aligned} \frac{du_1}{dt} = \frac{dT_1}{dt} &= c(T_1^* - u_1 - T^*_{ave}) + |q|(u_2 + T^*_{ave} - u_1 - T^*_{ave}) \\ &= c(T_1^* - T^*_{ave} - u_1) + |q|(u_2 - u_1), \end{aligned}$$

while (4.2b) becomes

$$\begin{aligned} \frac{du_2}{dt} = \frac{dT_2}{dt} &= c(T_2^* - u_2 - T^*_{ave}) - |q|(u_2 + T^*_{ave} - u_1 - T^*_{ave}) \\ &= c(T_2^* - T^*_{ave} - u_2) - |q|(u_2 - u_1). \end{aligned}$$

Let $u^* = T_1^* - T^*_{ave}$, and note $T_2^* - T^*_{ave} = -u^*$. Hence in (u_1, u_2)-coordinates the temperature equations become

$$\frac{du_1}{dt} = c(u^* - u_1) + |q|(u_2 - u_1) \tag{4.3a}$$

$$\frac{du_2}{dt} = c(-u^* - u_2) - |q|(u_2 - u_1). \tag{4.3b}$$

The net effect of the (u_1, u_2)-change of variables is that one may assume the temperatures in the outer vessels are the opposite of each other.

In an entirely analogous manner, the salinity equations are

$$\frac{dS_1}{dt} = d(S_1^* - S_1) + |q|(S_2 - S_1) \tag{4.4a}$$

$$\frac{dS_2}{dt} = d(S_2^* - S_2) - |q|(S_2 - S_1). \tag{4.4b}$$

If we let $v_i = S_i - S_{ave}^*$, $i = 1, 2$, where $S_{ave}^* = \frac{1}{2}(S_1^* + S_2^*)$, and $v^* = S_1^* - S_{ave}^*$, the salinity equations in the (v_1, v_2)-coordinate system become

$$\frac{dv_1}{dt} = d(v^* - v_1) + |q|(v_2 - v_1) \tag{4.5a}$$

$$\frac{dv_2}{dt} = d(-v^* - v_2) - |q|(v_2 - v_1). \tag{4.5b}$$

Note that addition of the equations in system (4.3) yields $\frac{d}{dt}(u_1 + u_2) = -c(u_1 + u_2)$. We see that for any initial condition, $(u_1 + u_2)(t) \to 0$ as $t \to \infty$. We will thus simplify matters by assuming $u_1 = -u_2 = u$ in all that follows.

In a similar fashion, addition of the equations in system (4.5) yields $\frac{d}{dt}(v_1 + v_2) = -d(v_1 + v_2)$. Hence, given that $(v_1 + v_2)(t) \to 0$ as $t \to \infty$ for any initial condition, we assume $v_1 = -v_2 = v$ henceforth. Making these substitutions into (4.3a) and (4.5a) results in the two dimensional system of equations

$$\begin{aligned} \frac{du}{dt} &= c(u^* - u) - 2|q|u \\ \frac{dv}{dt} &= d(v^* - v) - 2|q|v. \end{aligned} \tag{4.6}$$

Solving system (4.6) will yield the temperature and salinity of the water in basin one as a function of time, with each of the temperature and salinity of the water in basin two then the opposite of that in basin one.

As in previous sections, nondimensionalizing proves helpful. Letting $x = v/v^*$, $y = u/u^*$ and $\tau = ct$, the reader is invited to show that system (4.6) becomes

$$\begin{aligned} x' &= \delta(1 - x) - |f|x \\ y' &= 1 - y - |f|y, \end{aligned} \tag{4.7}$$

where "$'$" denotes $\frac{d}{d\tau}$, $\delta = d/c$, and $f = 2q/c$ is a nondimensionalized flow rate.

4.2 Density Driven Flow

The reader may note (4.7) and the 1-basin model (3.1) each contain a "flow" parameter. The advantage of incorporating a second basin is that f in (4.7) can now be made to depend upon density, which in turn is a function of x and y. Following Stommel, assume the flow rate is proportional to the difference in densities in the two boxes, that is, $kq = \rho_1 - \rho_2$, where k (s gm/cm^3) is a positive constant (we take the capillary flow orientation depicted

in Figure 6 to represent $q > 0$). Recalling relation (2.3) and our symmetry assumption $u_2 = -u_1$ and $v_2 = -v_1$, we have

$$\begin{aligned} kq &= \rho_0(1 - \alpha u_1 + \beta v_1) - \rho_0(1 - \alpha u_2 + \beta v_2) \\ &= \rho_0(-\alpha(u_1 - u_2) + \beta(v_1 - v_2)) \\ &= 2\rho_0(-\alpha u + \beta v) \\ &= 2\rho_0 \alpha u^*(-y + Rx), \end{aligned} \tag{4.8}$$

where we have used $x = v/v^*$, $y = u/u^*$ and $R = \beta v^*/\alpha u^*$.

Notably, we see the flow rate q is a function of salinity x and temperature y. If $y > Rx$, so that temperature dominates the density difference, $q < 0$ and the deep water flow is the reverse of that pictured in Figure 6, from the cold box to the warm box. In this case water flows from the colder high latitudes to the warmer low latitudes. For $Rx > y$, however, salinity plays the leading role and the capillary flow is as in Figure 6 ($q > 0$), now from the saltier to the less salty box. In this scenario water moves from the warmer low latitudes to the colder high latitudes, the reverse of the current orientation of the AMOC.

The dependence of the flow rate f on salinity x and temperature y in system (4.7) can be made explicit. To that end, since $f = 2q/c$ we have $kq = kcf/2$, from which it follows via (4.8) that

$$-y + Rx = \lambda f, \quad \text{where} \quad \lambda = \frac{kc}{4\rho_0 \alpha u^*}. \tag{4.9}$$

System (4.7) becomes

$$\begin{aligned} x' &= \delta(1 - x) - \tfrac{1}{\lambda}|y - Rx|\, x \\ y' &= 1 - y - \tfrac{1}{\lambda}|y - Rx|\, y. \end{aligned} \tag{4.10}$$

We note that, while not continuously differentiable, the vector field defined by (4.10) is Lipschitz continuous so (4.10) admits a unique solution for any initial condition $(x(0), y(0))$.

While a qualitative approach to the analysis of the nonlinear system (4.10) is feasible in an upper-level course (see [5], Chapter 6), here we make use of the *Mathematica* notebook in the Appendix to determine model behavior.

5 Dynamics of the 2-Box Model

With a bit of algebra, one can show solving system (4.10) for equilibrium solutions reduces to the finding of roots of a cubic polynomial in x; hence (4.10) will typically have one or three real equilibrium solutions (x^*, y^*). Looking to keep the flow rate involved, note that at equilibrium

$$\begin{aligned} x' &= \delta(1 - x) - |f|x = 0 \\ y' &= 1 - y - |f|y = 0, \end{aligned}$$

from which it follows an equilibrium point satisfies

$$x^* = \frac{\delta}{\delta + |f|} \quad \text{and} \quad y^* = \frac{1}{1 + |f|}. \tag{5.1}$$

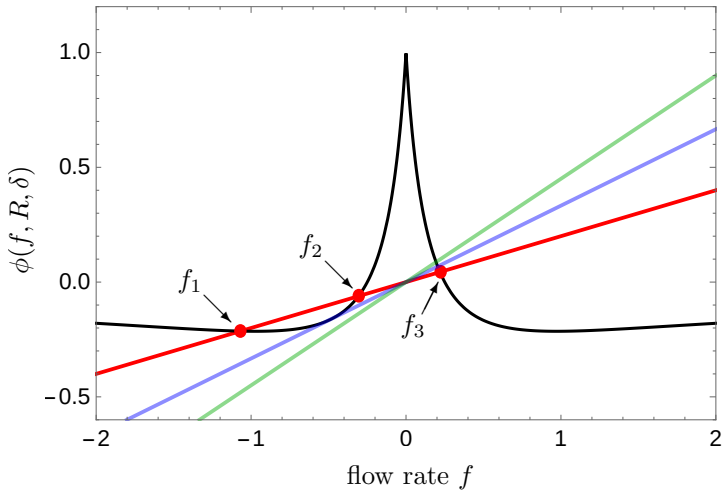

Figure 7: *Black*: Plot of $\phi(f, R, \delta)$ with $R = 2$, $\delta = 1/6$. Lines are plots of λf with $\lambda = 1/5$ (*red*), $\lambda = 1/3$ (*blue*) and $\lambda = 2/5$ (*green*). The f_i are equilibrium flow rates, $i = 1, 2, 3$.

From equation (4.9),

$$\lambda f = -y^* + Rx^* = -\frac{1}{1 + |f|} + \frac{R\delta}{\delta + |f|} \equiv \phi(f, R, \delta). \tag{5.2}$$

Solutions of equation (5.2) for the flow rate f can then be substituted into (5.1) to determine the equilibrium point(s) (x^*, y^*).

The black curve in Figure 7 is the graph of $\phi(f, 2, 1/6)$, while the red line in Figure 7 is the graph of λf for $\lambda = 1/5$; the intersection of these two curves will yield f-values satisfying (5.2). We see for the given parameters equation (5.2) has three real solutions, which we label $f_1 < f_2 < f_3$, while the corresponding equilibrium solutions of system (4.10) will be denoted (x_i^*, y_i^*), $i = 1, 2, 3$.

Given that $f_i < 0, i = 1, 2$, temperature dominates density differences and the flow through the capillary is from the cold box to the warm box when the system is in equilibrium states (x_i^*, y_i^*), $i = 1, 2$. At equilibrium (x_3, y_3), however, $f_3 > 0$ and salinity dominates density differences; the capillary flow is now from the warm box to the cold box as in Figure 6.

We use *Mathematica* to investigate the stability of each equilibrium solution via the file appended to this article. Presented in Table 1 are the eigenvalues of the Jacobian matrices $J(x_i^*, y_i^*)$ when $\lambda = 1/5, R = 2$ and $\delta = 1/6$ (we fix $R = 2$ and $\delta = 1/6$ in all that follows). For $\lambda = 1/5$, we see (x_1^*, y_1^*) is a stable node and (x_3^*, y_3^*) is a stable spiral, while (x_2^*, y_2^*) is a saddle. This conceptual model exhibits two stable regimes, one in which temperature drives the density difference and the deep water flow is from the cold box to the warm box, the other having salinity dominate the density difference with the capillary flow going from the warm box to the cold box. As mentioned above, this result caused Stommel to wonder whether such a situation might occur in nature.

To further investigate the dynamics of (4.10), we plot the xy-phase plane in Figure 8. The green line in Figure 8 corresponds to $f = 0$; above this line the flow is from the cold box to the warm box, with temperature dominating, and below the flow is from the

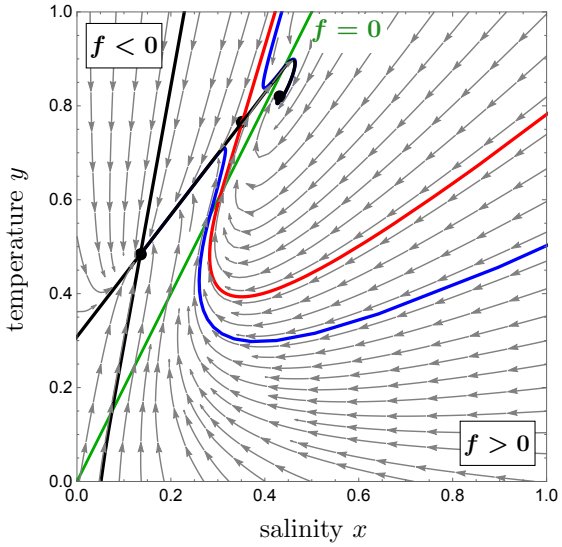

Figure 8: The xy-phase plane for $\lambda = 1/5, R = 2, \delta = 1/6$. The black dots are equilibria (x_i^*, y_i^*), with $x_1 < x_2 < x_3$. The red curve is the stable separatrix for the saddle point. The flow through the capillary reverses direction on each of the blue trajectories.

warm box to the cold box with salinity dominating. Note in particular the existence of trajectories that cross the $f = 0$ line (the blue curves in Figure 8 are two such trajectories). Hence there are initial conditions for which the deep water flow slows down and then reverses over time.

f equilibrium values	(x^*, y^*) equilibrium values	Jacobian $J(x^*, y^*)$ eigenvalues	equilibrium type
$f_1 = -1.068$	$(x_1^*, y_1^*) = (0.135, 0.484)$	$-3.609,\ -0.761$	stable node
$f_2 = -0.307$	$(x_2^*, y_2^*) = (0.352, 0.765)$	$-2.849,\ 0.761$	saddle
$f_3 = 0.219$	$(x_3^*, y_3^*) = (0.432, 0.820)$	$-0.921 \pm 1.823\, i$	stable spiral

Table 1. Parameters $\lambda = 1/5,\ R = 2,\ \delta = 1/6$.

5.1 Bifurcations and Hysteresis

In this section we briefly discuss bifurcations and associated hysteresis exhibited by the model. To set the stage, denote by $\mathcal{B}_i$ the set of initial conditions for which the corresponding solution of (4.10) converges to (x_i^*, y_i^*) as $t \to \infty, i = 1, 2, 3$ (the sets $\mathcal{B}_i$ are called *basins of attraction*). Note the stable separatrix of the saddle (the red curve in Figure 8) separates $\mathcal{B}_1$ and $\mathcal{B}_3$, the basins of attraction of the two stable equilibria. For the parameter values used in Figure 8, the system would require a large perturbation to enable a solution near the stable node (x_1^*, y_1^*) to jump over to $\mathcal{B}_3$ (and so cause a reversal of the deep water flow).

What happens if we vary the parameter λ, a proportionality constant for the flow rate f via (4.9)? An increase in λ, which may correspond to factors such as increased bottom friction or greater wind-driven surface turbulence [5], makes it more difficult for the water to flow from one basin to the other. A decrease in λ, on the other hand, would make it easier for water to flow through the capillary.

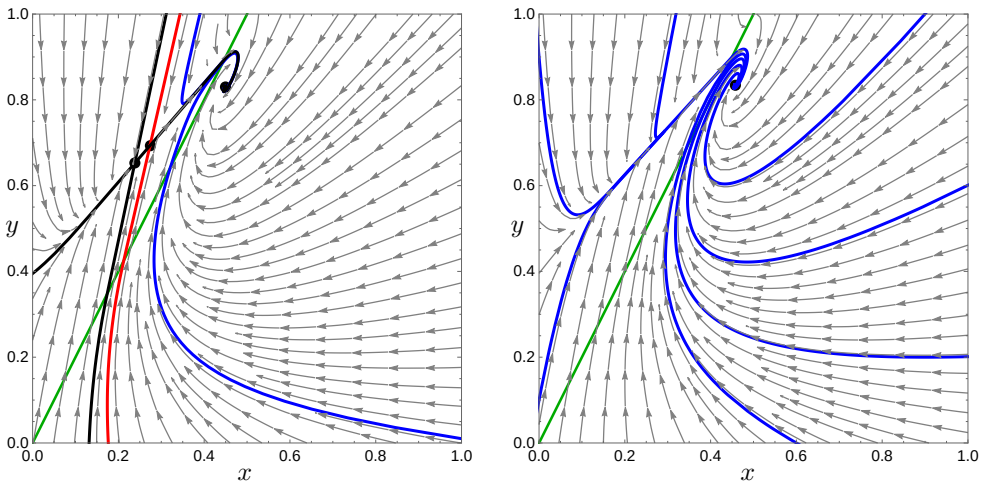

Figure 9: The xy-phase planes for $\lambda = 1/3$ (left) and $\lambda = 2/5$ (right).

The blue line in Figure 7 is the plot of λf for $\lambda = 1/3$. While difficult to discern in this image, there are again three equilibrium flow rates $f_1 < f_2 < 0 < f_3$ (f_1 and f_2 are quite close together). The stability type of equilibria (x_i^*, y_i^*), $i = 1, 2, 3$, remains unchanged from the $\lambda = 1/5$ case, as can be investigated via the *Mathematica* file in the Appendix.

The left plot in Figure 9 is the xy-phase plane for $\lambda = 1/3$. Note the stable node (x_1^*, y_1^*) and the saddle (x_2^*, y_2^*) are close to merging. Here, a solution near (x_1^*, y_1^*) within $\mathcal{B}_1$ would need but a slight nudge to jump to $\mathcal{B}_3$, with a corresponding reversal of the flow.

The green line in Figure 7 is the graph of λf for $\lambda = 2/5$. There is now but one equilibrium flow rate $f_1 > 0$. The stable node (x_1^*, y_1^*) and the saddle (x_2^*, y_2^*) merge at some $\lambda_0 \in (1/3, 2/5)$, disappearing as λ increases through λ_0 via a *saddle-node bifurcation* ([1], §9.3). For $\lambda = 2/5$ the system is permanently stuck in the regime in which the deep water flow is from the warm box to the cold box, with salinity dominating the density difference (right plot in Figure 9).

The *bifurcation plot* in Figure 10, in which the equilibrium flow rate is plotted as a function of the flow resistance λ, summarizes the above discussion. The red and green portions of the curve correspond to stable equilibria for system (4.10) (stable node and stable spiral, respectively), while the blue portion corresponds to the unstable saddle point. As λ increases through λ_0, the flow rate jumps to the green curve; such a bifurcation is often referred to as a *tipping point* by climate scientists.

Interestingly, the model also exhibits the following behavior. If we start on the stable red curve in Figure 10 at $\lambda = 1/5$, and first increase λ through λ_0 so that f jumps to the green stable curve, and then decrease λ back to $\lambda = 1/5$, f remains on the stable green curve. That is, the system is in a different stable regime than the one in which it started, even though the parameter values are the same. This phenomenon, known as *hysteresis*, is presented in [10] as a possible explanation for evidence suggesting that the AMOC has yet to recover from the weakening of the flow that began at the end of the Little Ice Age.

The appearance of hysteresis in Stommel's model is perhaps suggestive of the possibility that, were the AMOC to slow down and switch orientation due to climate change, any future return to the current transport of warm surface waters to the North Atlantic will be difficult to realize.

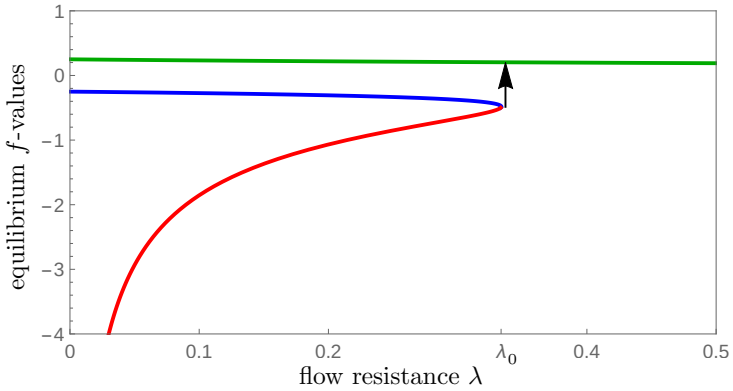

Figure 10: f-equilibrium values as a function of λ. *Red*: stable node (x_1^*, y_1^*). *Blue*: saddle (x_2^*, y_2^*). *Green*: stable spiral (x_3^*, y_3^*). System (4.10) has a saddle-node bifurcation at $\lambda = \lambda_0$.

6 Discussion

Stommel's 2-box model is conceptual in nature, a greatly simplified model of but one component of the global ocean circulation. No consideration is given to the coupling of the subpolar North Atlantic ocean with other oceans or with the atmosphere. Nevertheless, that such a simple model exhibits stable regimes having oppositely oriented circulation patterns, and that the passing from one circulation mode to the other can be induced by changing forcing parameters, has had a significant impact on climate science and oceanography [5].

L.G. Henry et al found that repeated weakening of the AMOC on a millenial time scale during cycles of temperature fluctuations in the last ice age occurred during each of the relatively colder periods, the latter coinciding with immense discharges of freshwater from melting ice in Canada into the subpolar North Atlantic [4]. Similarly, the work of Thornally et al suggests that increased freshwater fluxes from melting glaciers and sea ice roughly 150 years ago served to weaken the AMOC, anomalously so with respect to the past 1,500 years [10].

The effect of these "freshwater forcings" can be seen in Stommel's model: assuming the capillary flow is from the colder to the warmer box, imagine that a parcel of water is removed from the high latitude box, replaced by a cold, salt-free parcel having the same volume. Recalling $R > 1$, where $R = \beta S^*/\alpha T^*$ measures the relative effects of salinity and temperature on density, the reduced salt content will lead to lower density water in the cold box and hence a weaker circulation through the capillary.

The focus in this article has been placed on model development, with somewhat less attention given to the analysis of the system of ODEs (4.10). When teaching this material in the junior-level course MATH 305 *Mathematics and Climate*, I start with the pencil-and-paper approach presented in Chapter 6 in [5], teaching linearization at equilibria and the determination of the eigenvalue type via the trace and determinant of the Jacobian matrix along the way. Students then reinforce this analysis through their use of *Mathematica*.

Students are also exposed to introductory bifurcation theory in MATH 305, in which the Implicit Function Theorem plays an important role. Bifurcations of saddle-node,

Hopf, and cusp types are typically covered. In terms of Stommel's 2-box model, using *Mathematica* to see that one of the eigenvalues of the Jacobian matrix at the stable node (x_1^*, y_1^*) approaches 0 as the stable node and saddle point (x_2^*, y_2^*) merge in a saddle node bifurcation serves to reinforce the theory.

The bifurcation parameter λ is the proportionality constant for the flow rate through the capillary in Stommel's 2-box model. The flow resistance increases with λ, eventually leading to a single stable spiral equilibrium with an associated deep water flow from the low latitude box to the high latitude box. In this scenario the density difference is dominated by salinity. Insight into this behavior can be gleaned from the 1-basin model, where it was seen that salinity is the determining factor if the flow rate is sufficiently small (that is, λ is sufficiently large in the 2-box model setting).

While not presented here, it would be of interest to investigate how the model behaves as λ decreases toward 0, so that the flow resistance *decreases*. Does temperature then play the dominant role in determining density contrasts, as it does for increased flow rates in the 1-basin model?

Stommel's model provides for a wonderful introduction to the fundamental concepts of ocean circulation patterns. The corresponding ODEs are best analyzed via a combination of junior-level ODE analysis and the use of technology. This topic would make for an engaging addition to an upper-level mathematical modeling course.

Acknowledgment. Lecture notes on Stommel's model from a course offered by Professor Richard McGehee at the University of Minnesota served to frame the discussion of the model in MATH 305 as well as the presentation in this article. Professor McGehee's entire course on a mathematical approach to conceptual climate modeling—slides and lecture videos—can be found online [6].

Appendix

One can analyze Stommel's two-vessel model with the following *Mathematica* file. (We make no claims as to the efficiency of the code!)

```
(* Set λ here. We use δ = 1/6, R = 2 throughout. *)
Clear[λ]
λ = 0.2;

(* Here one can find the equilibrium flow rates fᵢ by solving equation (5.2)
  in the article for f. The value λ_0 =
 0.333801 is the saddle-node bifurcation value indicated in Figure 10 in the
   article.  *)
Clear[fequilibria, f1, f2, f3]
fequilibria = NSolve[λ * f == -1 / (1 + Abs[f]) + (2 / 6) / ((1 / 6) + Abs[f]), f];
If[ λ < 0.333801, {f1, f2, f3} = {fequilibria[[1]], fequilibria[[2]],
   fequilibria[[3]]}, f3 = fequilibria[[1]] ]
{{f → -1.06791}, {f → -0.307027}, {f → 0.21909}}

(* Here one finds the equilibria ((x*)ᵢ,(y*)ᵢ)
 corresponding to fᵢ via equation (5.1) in the article. *)
Clear[x1, y1, x2, y2, x3, y3]
If[ λ < 0.333801,
 {{x1, y1}, {x2, y2}, {x3, y3}} = {{(1 / 6) / ((1 / 6) + Abs[f]), 1 / (1 + Abs[f])} /. f1,
   {(1 / 6) / ((1 / 6) + Abs[f]), 1 / (1 + Abs[f])} /. f2,
   {(1 / 6) / ((1 / 6) + Abs[f]), 1 / (1 + Abs[f])} /. f3},
 {x3, y3} = {(1 / 6) / ((1 / 6) + Abs[f]), 1 / (1 + Abs[f])} /. f3]
{{0.134999, 0.48358}, {0.351845, 0.765095}, {0.432051, 0.820284}}

(* Here is the vector field given in equation (4.10) in the article *)
g[x_, y_, δ_] := δ * (1 - x) - Abs[(1 / λ) * (-y + 2 * x)] * x
h[x_, y_] := 1 - y - Abs[(1 / λ) * (-y + 2 * x)] * y

(* We split the vector field into the cases f =
 (1/λ)*(-y+2*x) < 0 and f = (1/λ)*(-y+2*x) ≥ 0 *)
gneg[x_, y_, δ_] := δ * (1 - x) - (- (1 / λ) * (-y + 2 * x)) * x
hneg[x_, y_] := 1 - y - (- (1 / λ) * (-y + 2 * x)) * y

gplus[x_, y_, δ_] := δ * (1 - x) - ((1 / λ) * (-y + 2 * x)) * x
hplus[x_, y_] := 1 - y - ((1 / λ) * (-y + 2 * x)) * y
```

```
(* Here's the Jacobian when f < 0 *)
MatrixForm[Jneg = {{D[gneg[x, y, 1 / 6], x], D[gneg[x, y, 1 / 6], y]},
   {D[hneg[x, y], x], D[hneg[x, y], y]}}]
```

$$\begin{pmatrix} -\frac{1}{6} + 10.\,x + 5.\,(2\,x - y) & -5.\,x \\ 10.\,y & -1 + 5.\,(2\,x - y) - 5.\,y \end{pmatrix}$$

```
(* Here's the Jacobian at (x1,y1) when f < 0 *)
If[λ < 0.333801, MatrixForm[J1 = Jneg /. {x → x1, y → y1}],
 Print["There are no equilibria with f < 0"]]
```

$$\begin{pmatrix} 0.115414 & -0.674995 \\ 4.8358 & -4.48581 \end{pmatrix}$$

```
(* Here are the evalues/evectors at (x1,y1) when f < 0 *)
If[λ < 0.333801, Eigenvalues[J1], Print["Only one equilibrium (x3,y3)"]]
If[λ < 0.333801, Eigenvectors[J1], Print["Only one equilibrium (x3,y3)"]]
```

```
{-3.60951, -0.760883}
```

```
{{0.178306, 0.983975}, {0.610234, 0.792222}}
```

```
(* Here's the Jacobian at (x2,y2) when f < 0 *)
If[λ < 0.333801, MatrixForm[J2 = Jneg /. {x → x2, y → y2}],
 Print["There are no equilibria with f < 0"]]
```

$$\begin{pmatrix} 3.04476 & -1.75922 \\ 7.65095 & -5.1325 \end{pmatrix}$$

```
(* Here are the evalues/evectors at (x2,y2) when f < 0 *)
If[λ < 0.333801, Eigenvalues[J2], Print["Only one equilibrium (x3,y3)"]]
If[λ < 0.333801, Eigenvectors[J2], Print["Only one equilibrium (x3,y3)"]]
```

```
{-2.84863, 0.760883}
```

```
{{0.286036, 0.958219}, {0.610234, 0.792222}}
```

```
(* Here's the Jacobian when f ≥ 0 *)
MatrixForm[Jplus = {{D[gplus[x, y, 1 / 6], x], D[gplus[x, y, 1 / 6], y]},
   {D[hplus[x, y], x], D[hplus[x, y], y]}}]
```

$$\begin{pmatrix} -\frac{1}{6} - 10.\,x - 5.\,(2\,x - y) & 5.\,x \\ -10.\,y & -1 - 5.\,(2\,x - y) + 5.\,y \end{pmatrix}$$

```
(* Here's the Jacobian at (x3,y3) when f > 0 *)
MatrixForm[J3 = Jplus /. {x → x3, y → y3}]
```

$$\begin{pmatrix} -4.70627 & 2.16025 \\ -8.20284 & 2.88233 \end{pmatrix}$$

```
(* Here are the evalues/evectors at (x3,y3) when f > 0 *)
Eigenvalues[J3]
Eigenvectors[J3]

(* Here is a plot of the equation f = 0 (green line),
the equilibria and the flowlines. Above the green line f <
 0 (temperature dominates density contrast),
while below the green line f > 0 (salinity dominates density contrast).
     The direction of the flow through the capillary stops and reverses
    along any trajectory crossing the green line. The value λ =
 0.333801 is the saddle-node bifurcation value indicated in Figure 10 in
    the above article. *)
If[λ ≤ 0.333801, Show[ContourPlot[(1 / λ) * (-y + 2 * x) == 0,
    {x, 0, 1}, {y, 0, 1}, ContourStyle → Directive[Darker[Green], Thick],
    FrameLabel → {"x (salinity)", "y (temperature)"}, LabelStyle → Bold],
  Graphics[{Red, Disk[{x, y} /. {x → x1, y → y1}, 0.01],
     Disk[{x, y} /. {x → x2, y → y2}, 0.01], Disk[{x, y} /. {x → x3, y → y3}, 0.01] }],
  StreamPlot[{g[x, y, 1 / 6], h[x, y]}, {x, 0, 1}, {y, 0, 1}]],
 Show[ContourPlot[(1 / λ) * (-y + 2 * x) == 0, {x, 0, 1}, {y, 0, 1},
    ContourStyle → Directive[Darker[Green], Thick],
    FrameLabel → {"x (salinity)", "y (temperature)"}, LabelStyle → Bold],
  Graphics[{Red, Disk[{x, y} /. {x → x3, y → y3}, 0.01] }],
  StreamPlot[{g[x, y, 1 / 6], h[x, y]}, {x, 0, 1}, {y, 0, 1}]]
]
```

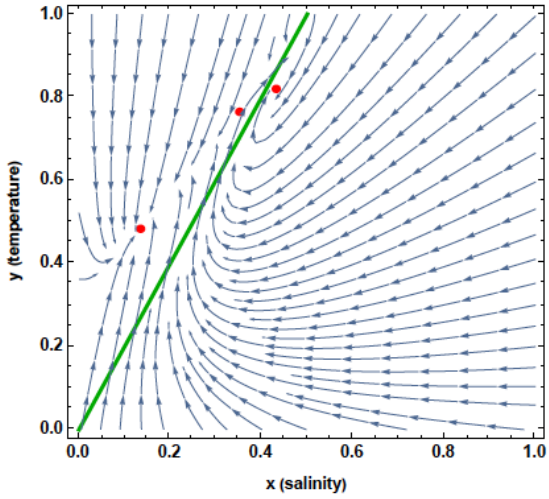

References

[1] R. Borrelli and C. Coleman. *Differential Equations: A Modeling Perspective*. Wiley, 2nd edition, 2004.

[2] M. Carlowicz. Watery heatwave cooks the Gulf of Maine. *NASA Global Climate Change Vital Signs of the Planet*, September 12, 2018. URL https://climate.nasa.gov/news/2798/watery-heatwave-cooks-the-gulf-of-maine/.

[3] T. DeVries, M. Holzer, and F. Primeau. Recent increase in oceanic carbon uptake driven by weaker upper-ocean overturning. *Nature*, 542:215–218, 2017.

[4] L.G. Henry, J.F. McManus, W.B. Curry, N.L. Roberts, A.M. Piotrowski, and L.D. Keigwin. North Atlantic ocean circulation and abrupt climate change during the last glaciation. *Science*, 353:10.1126/science.aaf5529, June 2016.

[5] H. Kaper and H. Engler. *Mathematics and Climate*. SIAM, 2013.

[6] R. McGehee. Math 5490 Fall 2014. URL http://www-users.math.umn.edu/~mcgehee/teaching/Math5490-2014-2Fall/lectures.html.

[7] M. Rhein, S.R. Rintoul, S. Aoki, E. Campos, D. Chambers, R.A. Feely, S. Gulev, G.C. Johnson, S.A. Josey, A. Kostianoy, C. Mauritzen, D. Roemmich, L.D. Talley, and F. Wang. *Observations: Ocean. In: Climate Change 2013: The Physical Science Basis. Contribution of Working Group I to the Fifth Assessment Report of the Intergovernmental Panel on Climate Change [Stocker, T.F., D. Qin, G.-K. Plattner, M. Tignor, S.K. Allen, J. Boschung, A. Nauels, Y. Xia, V. Bex and P.M. Midgley (eds.).* Cambridge University Press, 2013.

[8] T.F. Stocker, D. Qin, G.-K. Plattner, M. Tignor, S.K. Allen, J. Boschung, A. Nauels, Y. Xia, V. Bex, and P.M. Midgley (eds.). *IPCC, 2013: Summary for Policymakers. In: Climate Change 2013: The Physical Science Basis. Contribution of Working Group I to the Fifth Assessment Report of the Intergovernmental Panel on Climate Change*. Cambridge University Press, 2013.

[9] H. Stommel. Thermohaline convection with two stable regimes of flow. *Tellus*, 13(2): 224–230, 1961.

[10] D. Thornalley, D. Oppo, P. Ortega, J. Robson, C. Brierley, R. Davis, I. Hall, P. Moffa-Sanchez, N. Rose, P. Spooner, I. Yashayaev, and L. Keigwin. Anomalously weak Labrador Sea convection and Atlantic overturning during the past 150 years. *Nature*, 556:227–230, 2018.

Modeling the Spread and Prevention of Malaria in Central America

Michael Huber
Muhlenberg College

Keywords: Malaria, differential equations, chemoprophylaxis, SIR models, Laplace transforms
Manuscript received on October 1, 2018; published on February 13, 2019.

Abstract: In 2016, the World Health Organization (WHO) estimated that there were 216 million cases of Malaria reported in 91 countries around the world. The Central American country of Honduras has a high risk of malaria exposure, especially to United States soldiers deployed in the region. This article will discuss various aspects of the disease, its spread and its treatment and the development of models of some of these aspects with differential equations. Exercises are developed which involve, respectively, exponential growth, logistics growth, systems of first-order equations and Laplace transforms. Notes for instructors are included.

1 Introduction

In 2016, the World Health Organization (WHO) estimated that there were 216 million cases of Malaria reported in 91 countries around the world. This number was five million more than that reported in 2015 [14]. More importantly, the WHO estimates that of those cases, there were 445,000 deaths reported (similar to the 446,000 from 2015). As another data point, in 2006, there were 247 million cases of malaria world-wide, causing nearly one million deaths. Approximately half of the world's population is at risk of malaria. Malaria is predominantly endemic to the tropic and subtropic regions of the globe. More than 90% of malaria cases occur on the African continent, with the remainder concentrated in parts of the Pacific, Latin America, and Asia (see Figure 1).

Inhabitants of malaria-infected countries are not the only ones at risk. Soldiers deployed to these regions are susceptible to infection. From 1995 to 2004, military clinicians reported an average of 42 cases of malaria per year in United States soldiers, with the majority of these cases developed while serving in the Republic of Korea [13]. Although this incidence rate and the epidemiological pattern have been relatively stable over the past two decades, outbreaks associated with an increase in the number of military troops deployed to malarial areas have occurred and may continue to account for an increase in malaria cases imported into the United States.

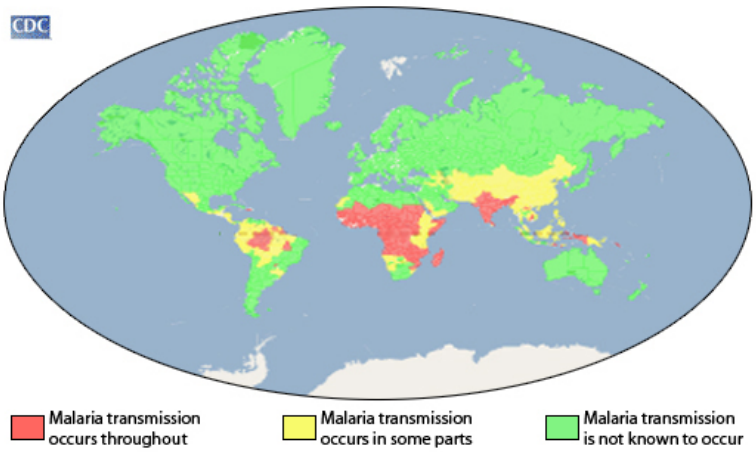

Figure 1: Malaria Map (from [8])

Most United States service members currently deployed in war zones are in Afghanistan or Iraq where malaria transmission is seasonal and varies geographically. Further, many service members have had "multiple, relatively short assignments to malaria-endemic areas" [3]. Malaria is caused by *Plasmodium* parasites, which are spread to people when an infected female Anopheles mosquito, called a malaria vector, bites the human. Believe it or not, there are more than 400 different species of the Anopheles mosquito [14], and studies show that all of the important malaria vectors bite their prey between dusk and dawn. Further, in many locations, transmission of the disease is seasonal, with peak transmission occurring during and immediately after an area's rainy season. There are five different parasite species which can cause malaria in humans [14], but two of them—*Plasmodium falciparum* and *Plasmodium vivax*—are believed to pose the greatest threat of transferring malaria. While *Plasmodium vivax* historically accounts for 80% to 90% of indigenous cases in Afghanistan and 95% of cases in Iraq, with *Plasmodium falciparum* causing the majority of the remaining cases, these numbers are likely to be inaccurate due to unreliable reporting in recent years from these war-torn areas.

According to [13], "The United States Army directs soldiers operating in these areas to consume antimalaria chemoprophylaxis and use personal protective measures, to include minimizing exposed skin through proper wear of the uniform and use of bed nets, impregnating uniforms and bed nets with permethrin, and frequently applying topical insect repellent (33% diethyltoluamide—DEET) to exposed skin. Although bed nets are an integral component of this directive, front-line soldiers, like those described in this study, may be afforded only limited protection through this measure because nighttime patrols and vigilance during dusk and dawn (when mosquitoes are prevalent) often preclude their intended use." Additionally, an injectable vaccine (RTS,S or commonly known as Mosquirix) is being evaluated in sub-Saharan Africa, in the countries of Ghana, Kenya and Malawi. Results of the pilot programs are not yet available.

The United States Army has deployed soldiers to the Central American country of Honduras for several decades, beginning in the late 1980s, to support Joint Task Force-Bravo operations in the region. JTF-B headquarters is located at Soto Cano (formerly

known as Palmerola) Air Base, Honduras, just outside the capital of Tegucigalpa. In January 1989, the 37th Engineer Battalion (Combat)(Airborne Corps) deployed as part of a task force in support of Operation *Ahuas Tara*. The unit's three-month mission was to construct a 5200-foot flight landing strip (an airfield), complete with a taxiway and parking apron, to allow C-130 aircraft to take off and land in the region. The engineer battalion's area of operations was in southwest Honduras, near the Pacific Ocean, between El Salvador and Nicaragua; its base camp was just outside the town of San Lorenzo, which lies east of the El Salvador border and north of the Bay of San Lorenzo (which feeds into the Gulf of Fonseca), a marshy region which allows the mosquito population to thrive. In addition to the airfield construction project, the engineers also conducted road construction and repair operations in the surrounding countryside. The battalion task force accomplished humanitarian projects as well, which included building an orphanage, upgrading a local school, and drilling wells to provide water for local inhabitants. Military missions involved training with the Honduran armed forces, participating in joint field operations with a host engineer battalion and conducting several airborne training operations with the Honduran Special Forces Battalion. Many American soldiers earned the Honduran Parachutist Badge after making five such jumps with the *Paracadista*.

As one might imagine, the soldiers of the 37th traveled extensively throughout southwestern and central Honduras. Malaria is known to be present throughout the country at altitudes below 1000 meters ($< 3,281$ ft), which included the 37th's Area of Operations (see Figure 2). This meant that preventive measures were taken to protect American soldiers from malaria infection. Figure 2 shows the area of operations of the battalion. This exposed the soldiers to the local population, animals, and, unfortunately, diseases.

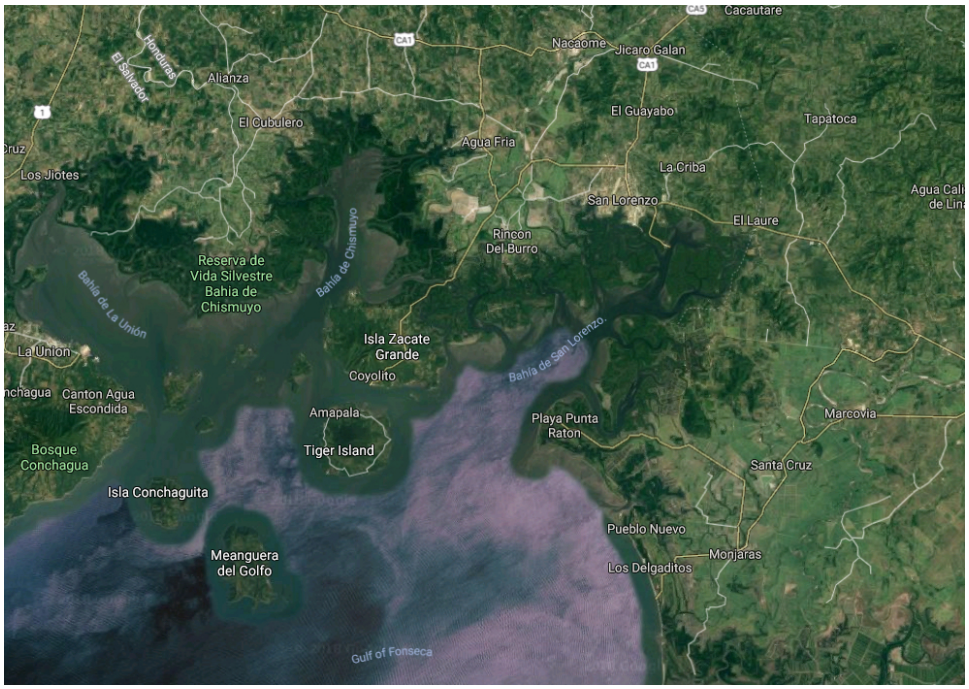

Figure 2: Area of Operations in Honduras (from [1])

Joint Task Force-Bravo is still in operation today. Its mission, "as guests of our Honduran partners at Soto Cano Air Base and as the senior representative for the United States Southern Command, maintains a forward presence and conducts and supports joint operations, actions and activities throughout the Joint Operations Area in order to enhance regional security, stability and cooperation" [11]. As such, its soldiers are exposed to the potential dangers of malaria.

This article will discuss various aspects of the disease, its spread and its treatment and the development of models of some of these aspects with differential equations. Each of the following four sections would make a nice project for an ODE class—an instructor can choose one appropriate to the level of the class. The exercises involve, respectively, exponential growth, logistics growth, systems of first-order equations and Laplace transforms. In each case students should be encouraged to dig deeper. The problems were motivated by my deployment to Central America as part of different Army operations.

2 Antimalaria Chemoprophylaxis

Malaria symptoms may include fever, chills, sweats, headache, body aches, nausea and vomiting, and fatigue [10]. Malaria symptoms will occur usually seven to ten days after being bitten (but in some cases could take up to several months) by an infected mosquito. Fever in the first week of travel in a malaria-risk area is unlikely to be malaria; however, you should see a doctor right away if you develop a fever during your trip. Malaria may cause anemia and jaundice. Malaria infections with *Plasmodium falciparum*, if not promptly treated, may cause kidney failure, coma, and death. Despite using the protective measures outlined above, travelers may still develop malaria up to a year after returning from a malarious area.

The first problem we study is one of pharmacokinetics. Malaria can be prevented through chemoprophylaxis, which basically suppresses the blood stage of malaria infections, logically preventing the disease. There are a few anti-malarial drugs currently considered for use for preventing malaria in Honduras: Atovaquone/proguanil, chloroquine, doxycycline, or mefloquine hydrochloride (see [9]). In order to understand the kinetics of any drug dosing regimen, we need to know a few things, such as the amount of the initial dosage, the drug's rate of absorption in the body, the volume of distribution, and the rate of elimination. To simplify this problem, we will assume that there is one rate of metabolism, so that we only consider one rate of elimination (each soldier's rate of absorption and rate of elimination is the same). Some pharmacists believe that malaria can be adequately prevented if three times the dosage is achieved in the bloodstream in a relatively short period and five times the dosage amount is achieved in a longer period [5, 4]. In 1989, soldiers of the 37th Engineer Battalion took one tablet of chloroquine (Aralen or its generic equivalent) once each week, usually after the Friday breakfast meal. The dosage was 300 mg per tablet. Soldiers began taking one tablet per week two weeks before deploying to the region. In this section, we will ignore the possibility of resistance to antimalarial medicines, although that can be a recurring problem [14].

Exercises

1. As a first requirement, suppose the body's system breaks down the chemicals in chloroquine at a rate that, in the absence of any new dosage, declines at a rate proportional to one-fourth of the amount of drug present. If the soldiers take the anti-malarial drug once per week, when are they getting the required dosage to prevent malaria and maintain an immunity? When is "three times the dosage" achieved? How much of the drug is in the body after several weeks (i.e., does $a(t)$ reach an equilibrium value)? Plot the amount of Aralen in the bloodstream if the regimen is continued for a half-year deployment.

2. What does the body's absorption rate x need to be to take a 300 mg tablet once each week and build up to five times the dosage (1500 mg) in the bloodstream in the long term? With this new absorption rate, when is three times the dosage achieved?

3 How Many Mosquitoes Are There?

By some estimates, in heavily infected regions, the number of mosquitoes that can be sustained by the environment is equal to one hundred million times the number of humans. For every 10 people, there are one billion mosquitoes [6]. Not all of them are capable of transmitting the disease, but one billion is a very large number.

Suppose the population $p(t)$ of mosquitoes in Central America can be modeled with the logistics equation:

$$\frac{dp}{dt} = rp\left(1 - \frac{p}{M}\right), \tag{3.1}$$

where r is the net growth rate per unit population and M is the carrying capacity of the environment. Honduras covers an area of just over 112,000 square kilometers, with an estimated population of almost eight million people. Assuming a sparse density of 60 people per square kilometer in the southwest region (the possible infected area) of the country, that would translate to a carrying capacity of mosquitoes of six billion (6,000,000,000) mosquitoes.

Exercises

1. Consider an initial mosquito population near San Lorenzo that numbers four billion. Plot and discuss the number of mosquitoes that will be present as time increases if the net growth rate per unit population is 0.1, 0.01, and 0.001.

2. What effect would lowering the carrying capacity of the environment to below the initial amount have on the population? Plot examples for both $M > p(0)$ and $M < p(0)$.

3. When is the rate of change of the mosquito population the greatest?

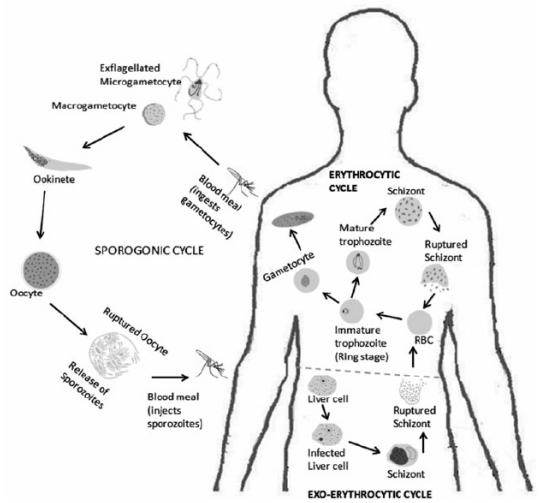

Figure 3: The malaria infection cycle (from [7])

4 Modeling Susceptibility, Infection and Recovery of Humans

One of the most important interactions being studied regarding malaria is whether immunity can be a consequence of infection. Several studies are taking place with the goal of inducing artificial immunity through the use of vaccines. These studies have led to the further investigation of the natural dynamics of immunity to the disease. According to Anderson [2, 12], both the maintenance of immunity and the degree of immunity depend on reinfections. The standard characterization of the epidemiology of malaria is what is termed an "age-prevalence" curve, which shows the proportion of each age group whose blood have the parasites present. Models are needed to study whether the effects of malaria on the human host depend on the infection's intensity, rather than whether or not the infection is present.

Malaria is caused by the multiplication of parasitic protozoa of the family *Plasmodiidae* within the blood cells of other tissues of the host. From [2]:

> Infection of a human host begins with the bite of a female mosquito and the injection of sporozoite stages into the bloodstream. These stages of the parasite are carried to the liver where they develop in the parenchymal cells. After an incubation period of several days, these exoerythrocytic stages grow, divide and release merozoites back into the bloodstream. The merozoites penetrate red blood cells, where they grow and subdivide to produce more merozoites that rupture host cells and invade other red blood cells....A portion of the merozoites develop into sexual stages, the gametocytes. Only gametocytes are infective to the mosquito. When a vector mosquito bites a human and ingests male and female gametocytes, these are freed from the blood cell, the female gamete is fertilized, and develops into an oocyst on the wall of the mosquito's gut. After 10 days or so (the actual development time is temperature-dependent), immature sporozoites migrate from the ruptured oocyst to the mosquito's salivary glands, mature to infectivity, and the cycle is ready to repeat itself. (See Figure 3 from [7].)

We could model this scenario with just two variables. For example, let $x(t)$ denote the population who have contracted a disease and $y(t)$ denote those who have not yet been exposed. If we assume that $\frac{dx}{dt}$ models the rate at which the malaria spreads, we could also assume that the rate is proportional to the number of interactions, and we get a differential equation: $\frac{dx}{dt} = kxy$, where k is a constant of proportionality that scales the number of interactions between $x(t)$ and $y(t)$.

Instead, let's study a compartment model which just treats the infection among humans. The case where everyone is born susceptible, becomes infected, and then recovers to become permanently immune has been often called the SIR model. Let $s(t)$ represent the susceptible class of the population, $i(t)$ the infected class, and $r(t)$ the recovered class. If the infection rate is α and the constant rate of recovery is β, then we can describe the dynamics of the disease by the following differential equations:

$$\frac{ds}{dt} = -\alpha s \tag{4.1a}$$

$$\frac{di}{dt} = \alpha s - \beta i \tag{4.1b}$$

$$\frac{dr}{dt} = \beta i. \tag{4.1c}$$

By scaling, we can assume that the entire population is susceptible and immediately thereafter, infection of the population occurs, and that $s(t) + i(t) + r(t) = 1$ as well, for all times t.

Perhaps a better model can be expressed as an SIRS model. Susceptible members of the population are repeatedly infected, recover, become *temporarily* immune, and then become susceptible again. Introduce γ as the average rate of movement out of the immune state. In other words, it is the inverse of the average time spent with immunity. The coupled differential equations become:

$$\frac{ds}{dt} = \gamma r - \alpha s \tag{4.2a}$$

$$\frac{di}{dt} = \alpha s - \beta i \tag{4.2b}$$

$$\frac{dr}{dt} = \beta i - \gamma r. \tag{4.2c}$$

4.1 Exercises

1. Plot solutions to the system of equations (4.1). Use typical values for α of 2 year^{-1}; allow β to vary between 0.07 and 0.03 year^{-1}. Use Equations 4.1 to plot the solutions for each class. Assume, with scaling, that the initial population is 100% of the soldiers and that five percent are infected when the study begins.

2. Plot solutions to the system of equations (4.2). Let $\beta = 0.5$ year^{-1} and $\gamma = 0.5$ year^{-1}. The parameter α can vary between 0.2 and 5 year^{-1}. Further, an important assumption is that the parameters β and γ are independent of the parameter α. Explain why. As α increases, what happens to the immunity of the population?

5 Controlling the Mosquito Population

Let's examine a small part of the base camp; in particular, we will model the number of mosquitoes that existed in the area of the battalion tent city. Imagine that we could track the number of mosquitoes with some device. Assume that the mosquito population in the area surrounding the tents grows at a rate of 5% per day. They are drawn to the living quarters by many factors. To combat the mosquitoes, the operations section of the battalion tasks a platoon to spray insect repellent throughout the area. This causes a 1000-mosquito drop in the population over the next 24 hours after spraying. The platoon sprays the area on the 3rd, 6th, 9th, 12th, etc., days after the operations section begins tracking mosquitoes.

Exercises

1. If there are initially 5000 mosquitoes, what happens to the population over time? Approximately how many mosquitoes will there be after two weeks? Plot both the effects of the spraying (the forcing function) and the overall mosquito population.

2. Is this strategy effective or should it be adjusted, and how?

6 Some Solutions to Exercises

Note for Instructors

These are problems used in an introductory course in Differential Equations. In the first section, a simple, first-order equation is used to model and predict the amount of drug in the bloodstream. The twist involves finding the absorption rate. The second section involves a logistics equation for modeling rates of change for populations. The third section uses the well-known SIR and SIRS models and is effective for incorporating computer-algebra systems to see long-term behavior. The instructor could also adjust the equations to introduce interaction. The final section involves the use of Laplace transforms to model and solve. In each section, try to incorporate student writing to add to the solutions.

Section 2: Antimalaria Chemoprophylaxis

1. First, let's assume a continuous situation and that small variations for individual soldiers can be ignored. Let $a(t)$ equal the amount of drug in the bloodstream (measured in mg) at time t (measured in weeks). The soldiers take 300 mg each week for two weeks before deploying. The initial value problem is

$$\begin{aligned} \frac{da}{dt} &= -\frac{1}{4}a + 300 \\ a(0) &= 300 \end{aligned}$$

Solving, we obtain $a(t) = 1200 - 900e^{-t/4}$. Plot this. Each soldier should have 900 mg in the bloodstream at approximately $t = 4.39$ weeks, or sometime between the second and third week after arrival in country. After 10 weeks ($t = 12$) in country, $a(12) = 1155.19$ mg, closing in on the equilibrium value of 1200 mg.

2. In order to reach an equilibrium point of five times the 300 mg dosage, the amount of drug needs to get to 1500 mg, so the rate needs to decline (so the body retains more drug). At equilibrium, $a(t) = 1500$ and $\frac{da}{dt} = 0$, so we solve $0 = x * 1500 + 300$ for x, obtaining $x = -0.2$. Solving

$$\begin{aligned} \frac{da}{dt} &= -\frac{1}{5}a + 300 \\ a(0) &= 300 \end{aligned}$$

we find $a(t) = 1500 - 1200e^{-\frac{t}{5}}$. Each soldier should have 900 mg in the bloodstream at approximately $t = 3.47$ weeks, or sometime between the first and second week after arrival in country.

Section 3: How Many Mosquitoes Are There?

1. Solve Equation (3.1) with $M = 6{,}000{,}000{,}000$ and the three net growth rates. With the highest rate ($r = 0.1$) we obtain

$$p(t) = \frac{12000000000}{2 + e^{-\frac{t}{10}}}$$

A plot is shown in Figure 4. Solve the logistics equations with the other values of r. As r decreases, so does the number of mosquitos over time. For Requirements 2 and 3, try various values for M and discuss the behavior.

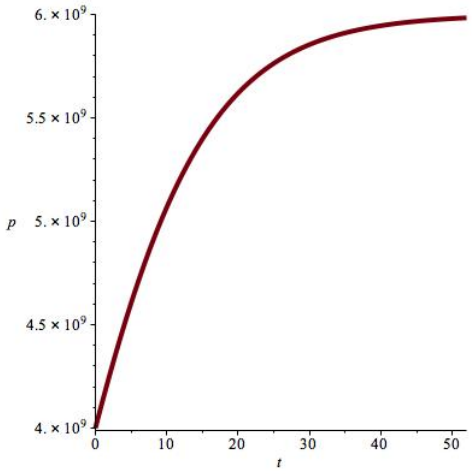

Figure 4: The population of mosquitos with $r = 0.1$

Section 4: Modeling Susceptibility, Infection and Recovery of Humans

1. Using Equations (4.1abc) with the values provided, the behaviors for each class over a 20-week period are shown in Figure 5a.

2. Using Equations (4.2abc) with the values provided (start with $\alpha = 2.5$), the behaviors for each class over a 20-week period are shown in Figure 5b. Vary the parameters to see how the behaviors change.

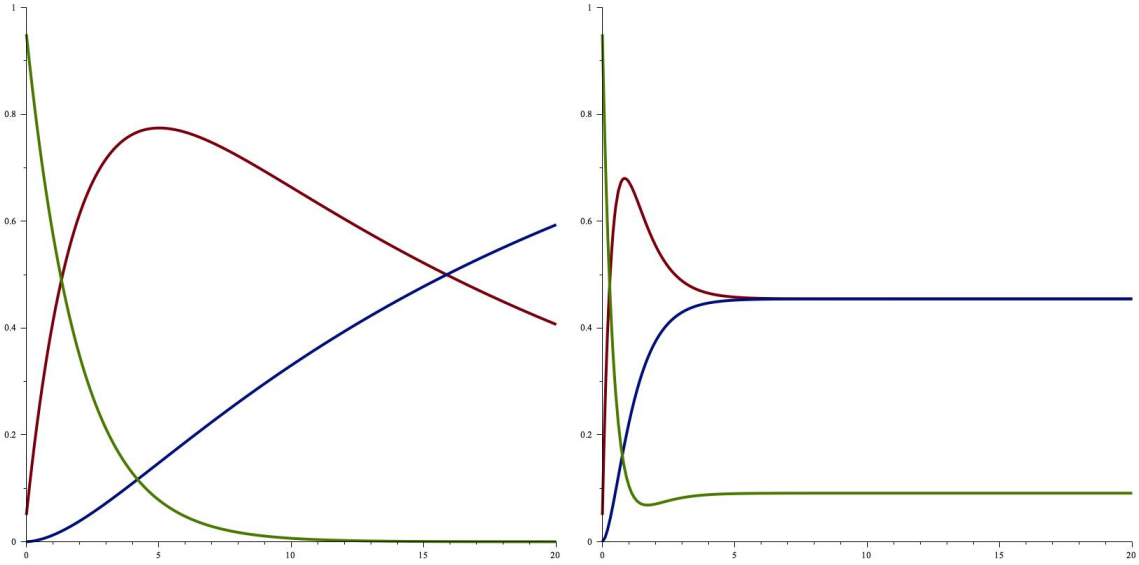

Figure 5: The susceptible (green), infected (red), recovered (blue) populations using the SIR model (4.1) on the left, and the SIRS model (4.2) on the right.

Section 5: Controlling the Mosquito Population

1. We assume that it takes 24 hours for the spraying to have an effect, so it appears to be an instantaneous reduction in the number of mosquitos. The forcing function (caused by the spraying) can be viewed as a step function, as seen in Figure 6.

   Define $m(t)$ to be the number of mosquitos in the base camp at day t. The differential equation becomes

   $$\frac{dm}{dt} = 0.05M + \text{forcing}$$

   Using Laplace transforms, we solve the differential equation with an initial condition of $m(0) = 5000$. A plot of the solution is shown in Figure 7. After 14 days with this scenario, there are approximately 4593 mosquitos in the base camp.

2. There appears to be a downward trend in Figure 7, but it might not be drastic enough. In some sense, it almost keeps the mosquito population in a status quo. Possible recommendations include increasing the frequency of spraying, finding an alternative to spraying that might be more effective, etc. Students can discuss environmental issues as well.

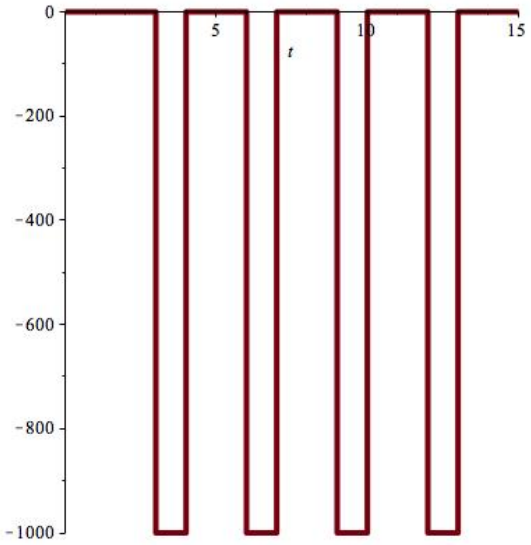

Figure 6: The forcing function

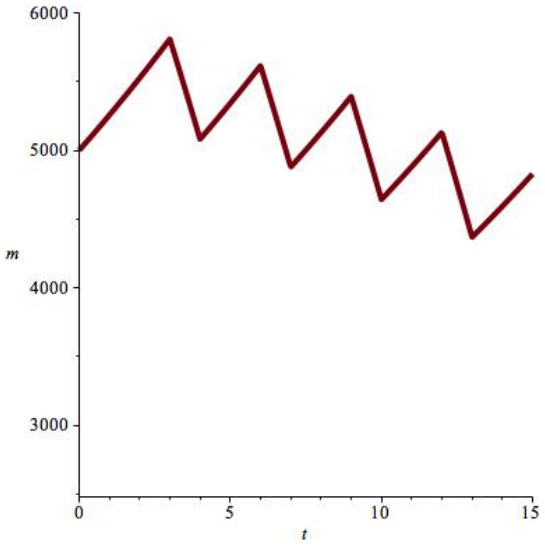

Figure 7: The number of mosquitos in the base camp

References

[1] URL http://maps.google.com.

[2] R.M. Anderson. *The Population Dynamics of Infectious Diseases: Theory and Applications*. Chapman and Hall: London, 1982.

[3] Paul Ciminera and John Brundage. Malaria in U.S. Military Forces: A Description of Deployment Exposures From 2003 Through 2005. *Am. J. Trop. Med. Hyg.*, 76(1), 2007.

[4] Dr. (Captain) Paul Arguin, Chief, Domestic Response Unit of the Malaria Branch, Division of Parasitic Diseases, Center for Disease Control and Prevention. Personal interview, January 2010.

[5] Dr. Chrys Cronin, Director of Public Health Program, Muhlenberg College. Personal interview. September 2010 and April 2018.

[6] Dr. Marten Edwards, Department of Biology, Muhlenberg College. Personal interview. January 2010 and May 2018.

[7] Janez Ferluga and Uday Kishore. *Microbial Pathogenesis: Infection and Immunity (Host-pathogen interaction: Plasmodium and Trypanosomes)*. Springer-Landes: London, 2014.

[8] Center for Disease Control and 2017 Prevention fact sheet dated March 17. Where malaria occurs, March 2017. URL https://www.cdc.gov/malaria/about/distribution.html.

[9] International Association for Medical Assistance to Travellers (IAMAT). Country health advice: Afghanistan-suppressive medication guide, June 2018. URL https://www.iamat.org/country/afghanistan/risk/malaria.

[10] International Association for Medical Assistance to Travellers (IAMAT). Malaria: Symptoms, June 2018. URL https://www.iamat.org/risks/malaria.

[11] Joint Task Force-Bravo. Joint task force-bravo, 2018. URL http://www.jtfb.southcom.mil/About-Us/Who-We-Are/.

[12] M.J. Keeling and P. Rohani. *Modeling Infectious Diseases in Humans and Animals*. Princeton University Press: Princeton, NJ, 2009.

[13] Russ S. Kotwal, Robert B. Wenzel, Raymond A. Sterling, William D. Porter, Nikki N. Jordan, and Bruno P. Petruccelli. An Outbreak of Malaria in US Army Rangers Returning From Afghanistan. *Journal of the American Medical Association*, 293(2), January 2005.

[14] 2018 World Health Organization fact sheet dated June 11. Malaria, June 2018. URL http://www.who.int/news-room/fact-sheets/detail/malaria.

A Model of the Transmission of Cholera in a Population with Contaminated Water

Therese Shelton
Southwestern University

Emma Kathryn Groves
North Carolina State University

Sherry Adrian
Southwestern University

Keywords: Cholera, differential equations, social justice, global health, sanitation, force of infection, SIR model, SIRB model, Haiti, SIMIODE
Manuscript received on December 4, 2018; published on February 13, 2019.

Abstract: Cholera is an infectious disease that is a major concern in countries with inadequate access to clean water and proper sanitation. According to the World Health Organization (WHO), "cholera is a disease of inequity—an ancient illness that today sickens and kills only the poorest and most vulnerable people…The map of cholera is essentially the same as a map of poverty." [27] We implement a published model [9] of a SIR model that includes a bacterial reservoir. Bacterial concentration in the water, λ, or the "force of infection," is modeled by the Monod Equation in microbiology. We investigate the sensitivity of the models to some parameters. We use parameter values for cholera in Haiti that are consistent with the ranges in meta-analysis [9] and other sources. We show the results of our numerical approximation of solutions. Our goal is to use this system of nonlinear ordinary differential equations to raise awareness among the mathematics community of the dynamics of cholera. We discuss the enhancement of undergraduate experiences by motivating learning with a real-world context in social justice implications of global health.

1 Overview

Cholera is a well-established waterborne disease that spreads through populations of people who are already overly burdened. Controlling cholera will require investment of monetary and human resources, issues beyond the scope of this paper. Here, we seek to understand and illustrate more about the disease through a mathematical model. We begin with an overview of the disease and of the outbreak in Haiti. We review the basic

disease model and its parameters, introduce and analyze a model for the force of infection, and examine the combined system of differential equations. We show the results of our numerical solution with respect to the compartments of the population and to the level of bacteria in the water supply, and we examine the sensitivity of the model to parameter values. We share perspectives about teaching mathematics with and about social justice, and we point to the broader view of experts as well. As we indicate in Section 8, two of the authors are novices or near-novices in teaching mathematics with social justice, and one author is well versed in social justice in general. We describe the context of and support for our work at our institution. We discuss several mathematical communities with resources available to anyone wishing to include projects in teaching differential equations. Some are venues to which new work may be contributed. Greater sharing of materials and pedagogies also constitutes engagement in social justice.

2 Cholera is a Dreadful Disease

The world is dealing with the seventh pandemic of cholera in the past two hundred years, and it has lasted for almost sixty years: "Cholera is a 'genie that escaped from the bottle' and is proving very difficult to put back in." [31] We summarize relevant information about cholera from [27, 26, 2, 12]. Humans throughout the world can contract cholera, an infectious diarrhoeal disease. The majority have few or no symptoms but can still spread the disease. Treatments are usually quite effective when administered promptly. Preventative measures include vaccination, drinking clean water, and washing hands well – all of which assumes that people have easy access to these resources. Consider, however, that one million to over four million people contract cholera each year, with deaths estimated between twenty thousand to nearly one hundred fifty thousand annually.

People mostly become infected by eating food or drinking water that is contaminated with the bacteria *Vibrio cholerae*. The bacteria can brew in someone's system for up to twelve days before she or he develops diarrhea, which can lead to dangerous dehydration. Most deaths occur on the first day of illness; in fact, death can occur within hours without treatment. "[T]he bacteria are present in their faeces for 1-10 days after infection and are shed back into the environment, potentially infecting other people." [26] In a layperson's terms, the poop of people who are sick is full of bacteria, and if bacteria gets into food that others eat, or a water supply from which people drink, others also get sick, and a cycle of infection develops. The dynamics of the disease indicate that it is intimately linked to inadequate access to clean water and to improper treatment of human waste.

Unfortunately, many people across the globe live with inadequate sanitation and clean water. We report some 2015 estimates about the global situation [28]: 71%, or 5.2 billion people, used a safely managed drinking water service; (that is, one located on premises, available when needed and free from contamination); 263 million people spent over 30 minutes per round trip to collect water from an improved source; 844 million people still lack even a basic drinking water service.

For sanitation, the situation is even worse; only 39%, or 2.9 billion people, used a safely managed sanitation service in which excreta are safely disposed of in situ or treated off-site; 2.3 billion people still lacked even a basic sanitation service; 600 million people

shared improved facilities with other households; 892 million people worldwide still practiced open defecation; more than 2 billion drink water from sources that are faecally contaminated, and 2.4 billion are without basic sanitation facilities, exposing them to a range of water-related diseases including cholera. Moreover, "Half the world lacks access to essential health services, [and] 100 million [are] still pushed into extreme poverty because of health expenses." [32]

The case of Haiti has raised attention to cholera and demonstrates that cholera can become entrenched very quickly. Haiti had been essentially cholera-free until the unintentional introduction in the fall of 2010 by a United Nations (U.N.) peacekeeping team: "A panel of experts appointed by the U.N. found that the strain of cholera that popped up in Haiti was 'a perfect match' for a strain found in Nepal. Nepalese peacekeepers were staying at the U.N. camp, and poor sanitation sent sewage from the camp into local waterways." [8] How ironic that some who came to help with security made general conditions more dire. The response of the U.N. Secretary-General [24] to the legal determination of the U.N.'s responsibility is a poignant illustration of the magnitude of suffering experienced by those with cholera, as well as the general situation of many countries in which cholera is endemic.

> The Haitian people have faced enormous hardships and obstacles over the years: endemic poverty; political instability; and, of course, the devastating earthquake of 2010. The cholera epidemic that soon followed added a deeper layer of tragedy and suffering. Most recently this was compounded by the horrendous hurricane that put the country under new serious strains. [From 2010 through 2016], cholera has afflicted nearly 800,000 people and claimed the lives of more than 9,000 Haitians.

According to [4], 57.7% of Haiitians had access to a drinking water source in 2015, and 27.6% had access to improved sanitation, or just 19.2% of the rural population. The report of the appointed panel of experts, [6], describes the conditions in Haiti in 2010 that can help us understand multiple factors contributing to this tragic outbreak. This includes what had formerly been fairly safe "human activity along [the Meye Tributary System of the Artibonite River], with women washing, people bathing, people collecting water for drinking, and children playing," [6], as well as regular exposure of agricultural workers to irrigation water from the river. The report describes leaky pipes that allowed cross contamination at the U.N. camp, even though there were no reported cases of cholera at the camp, as well as open pits of human waste that could wash elsewhere in rains. Other conditions also contributed to the "explosive cholera outbreak:" lack of immunity, "optimal environmental conditions for rapid proliferation" of the bacteria in the river, movement of infected people to other areas, an extra-potent strain of bacteria, and poor sanitation conditions in treatment centers and across Haiti. Although the U.N. has subsequently been held responsible, "[t]he Independent Panel conclude[d] that the Haiti cholera outbreak was caused by the confluence of circumstances ... and was not the fault of, or deliberate action of, a group or individual." [6]

3 Basic SIR Model and Meaning of Parameters

We remind the reader of a basic SIR model of the spread of a disease. See [21] for an easily accessible, straightforward, general introduction of a simpler model than we cover here, or [10] for an SIR model of Avian flu in birds. We provide some indications of the need for an improved model in the case of cholera.

We consider N people who are either "susceptible", "infectious", or "removed" from getting the disease. The variables S, I, R are often transformed into fractions of N for mathematical convenience. We consider the following general model with notation and parameter values from [9], acknowledging the issue of non-integer numbers of people for unscaled S, I, R variables.

$$\frac{dS}{dt} = -\lambda\ S + \mu_b\ N - \mu_d\ S \tag{3.1a}$$

$$\frac{dI}{dt} = \lambda\ S - \gamma\ I - (\mu_c + \mu_d)\ I \tag{3.1b}$$

$$\frac{dR}{dt} = \gamma\ I - \mu_d\ R \tag{3.1c}$$

$$N = S\ +\ I\ +\ R \tag{3.1d}$$

Parameters μ_b, μ_d, and μ_c represent the rates at which people are born, die from general causes, and die from cholera, respectively. A common form of the SIR model uses a net death rate by combining $\mu_c + \mu_d$, but separate parameters are needed here because cholera can greatly increase the death rate. In the case of Haiti, an intensive study of four sites indicated that, during the first seven months of the epidemic, "the crude mortality rate increased by an estimated 2.9–fold (2.1 – 4.0–fold across sites) compared with baseline data." [12]

The parameter γ represents the rate at which people who are infectious recover, with $1/\gamma$ representing the length of time that an infected person is ill. Generally, in the basic model, these are all constants for a particular disease and population.

The term $\lambda\ S$ in Equations (3.1 a, b) is often modeled as $\alpha\ S\ I$ where α has a constant value, as in [21] and [10]. In this system, then, λ is often considered as a function only of the number of infected people.

For cholera, the disease dynamics indicate that λ include the interplay between people and the bacterial reservoir, capturing the "force of infection" (FOI), which is well explained in [9]. Both [9] and [1] present a meta-analysis of multiple research sources for models of cholera, particularly related to the outbreak in Haiti. The main article in [9], primarily for healthcare practitioners, also has a supplement that states the differential equations, describes the parameters, and provides ranges of parameter values with units. Five models of cholera of increasing complexity are included in [1], as well as ranges of parameter values. We use both sources for our parameter values in the expanded model.

We first share how we have led undergraduate students through an understanding of the new FOI model as related simply to bacteria – not to the SIR components. We then describe the expanded SIR model expanded to include bacterial growth and interaction

with humans, and we show the results of our numerical solution of the SIRB system. We discuss the enhancement of undergraduate experiences by motivating learning with a real-world context with social justice implications of global health.

4 Force of Infection Model and Effect of Parameter Values

In the model from microbiology described by [9], λ is the *force of infection (FOI)*, the per capita rate of infection experienced by susceptible individuals. It is reasonable to assume that the chance of any one person becoming infected by *V. cholerae* rises with the concentration of the bacteria in the water. Let B represent this changing level of contamination of the water supply. The force of infection, *lambda*, increases with B but has a maximal level, β, the "contact rate" of the susceptible population with contaminated water. The concentration of bacteria for which the infection rate is half of its maximum is κ, which is a shape parameter in the model. Measured in bacterial cells per mL water, this is the concentration of *V. cholerae* that yields 50% chance of infection [9, Table S5]; this is also referred to as the half-saturation constant of vibrios [1].

$$\lambda = \beta \frac{B}{B + \kappa} \tag{4.1}$$

We use the following parameter values within the ranges provided by [9]: a contact rate of the susceptible population with contaminated water 0.07 per day and a level of 10^5 cells of *V. cholerae* per mL water at which there is a 50% chance of infection. We use these parameter values for Figure 1, with an exaggerated scale for B to see the mathematical meaning of the definition of κ and how κ relates to β.

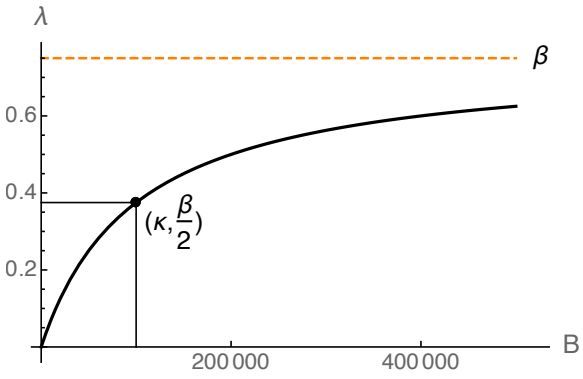

Figure 1: Role of Parameters in the Force of Infection Model

Equation (4.1) has Michaelis-Menten dynamics, a term that may be familiar to our readers; it is the Monod equation in microbiology. Translating the epidemiological statements, we can verify that

$$\lambda\Big|_{B=\kappa} = \frac{\beta}{2} \tag{4.2}$$

and λ has limiting value β as the bacteria level, B, increases.

The FOI is a function of B with parameters κ and β; this is four dimensional if we consider all variable quantities. We will examine this in two and three dimensions. The different asymptotic behaviors of the FOI functions for multiple values of β, all with $\kappa = 10^5$ cells/mL, are apparent in Figure 2. We see the FOI functions for multiple values of κ, all with $\beta = 0.07$/day, in Figure 3; the curves have the same asymptote. Our 2D graphs are traces of the 3D graph, which include the points defined by Equation (4.2). We can see that cholera worsens for larger values of β and smaller values of κ.

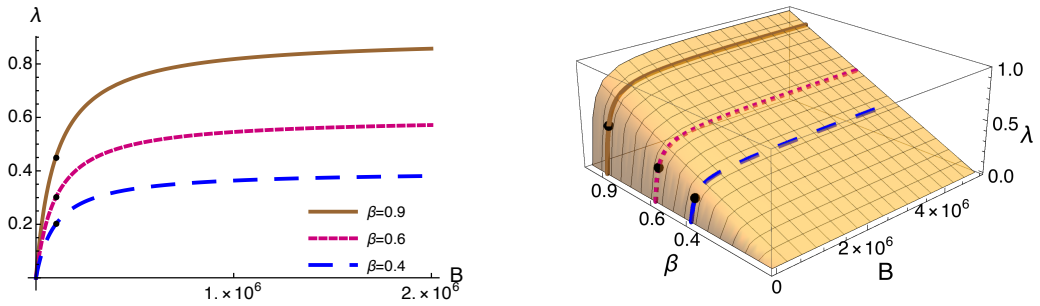

Figure 2: Effect on FOI of Varying β with constant κ

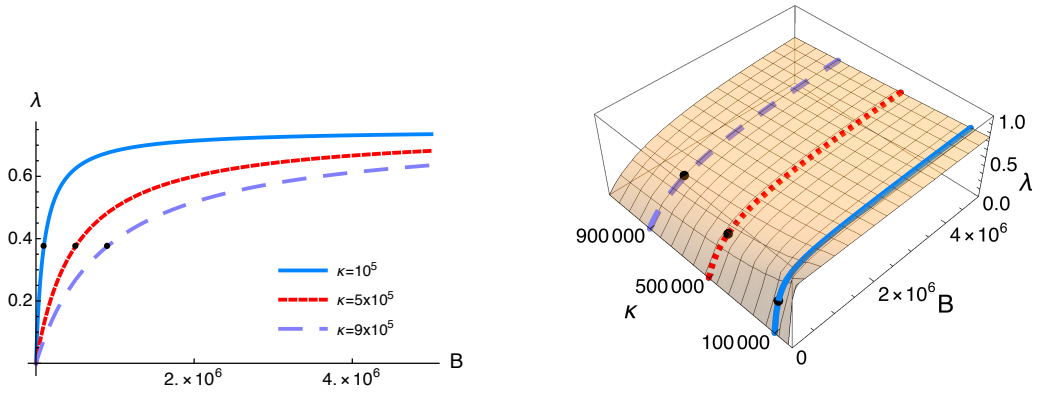

Figure 3: Effect on FOI of Varying κ with constant β

Note that in Figures 1, 2, and 3, the bacteria level is thought of as increasing. In our system of differential equations, the bacteria level can rise and fall, leading the FOI to rise and fall. We remind students that these graphs do not show time.

The parameters β and κ are on very different scales, so comparing how sensitive the FOI is to each is not clear from Figure 2 and Figure 3. We employ the method in [14]: for a function f with parameter p, the *sensitivity function* is defined as $S(f;p) = \frac{df}{dp} \Big/ \frac{p}{f}$. This is based on $\triangle f/f$ representing the average proportion of change in f, which would be divided by $\triangle p/p$ representing the average proportion of change in p. The sensitivity function is like a ratio of relative rates of change. We evaluate $S(f;p)$ at baseline values of the independent variables and parameters. $B = 1000, \beta = 0.07, \kappa = 10^5$. The result can be interpreted as an approximate rate of change of the function value with respect to a one percent increase in the parameter value.

The sensitivity of FOI to the half-saturation constant is $S(\lambda;\kappa) = -\kappa/(B+\kappa)$, which is approximately -0.96 for our baseline values. The sensitivity of the force of infection to the contact rate of the susceptible population with contaminated water is $S(\lambda;\beta) \equiv 1$.

The FOI is barely more sensitive to the rate at which susceptible people contact the bacteria in the reservoir than to the half-saturation constant of vibrios. FOI decreases by about 1% for a 1% increase κ near its baseline value, and FOI increases by 1% as β increases 1%. FOI is a bit more stable with changes in β than it is to changes in κ. Even if we vary the bacterial concentration from $B = 100$ to $B = 9000$, $S(\lambda;\kappa)$ only varies between -0.92 and 1.

5 Disease Model with Bacterial Reservoir

5.1 SIRB Model

Now we consider the combined system of Equations (3.1) with Equation (4.1), with the additional differential equation modeling bacteria in the water reservoir. Infected persons contribute to the vibrio concentration at rate ξ, and the bacteria die at rate δ.

$$\frac{dS}{dt} = -\beta \frac{B}{B+\kappa} S + \mu_b (S + I + R) - \mu_d S \tag{5.1a}$$

$$\frac{dI}{dt} = \beta \frac{B}{B+\kappa} S - \gamma I - (\mu_c + \mu_d) I \tag{5.1b}$$

$$\frac{dR}{dt} = \gamma I - \mu_d R \tag{5.1c}$$

$$\frac{dB}{dt} = \xi I - \delta B \tag{5.1d}$$

We can see from our SIRB model in Equations (5.1) that cholera worsens for larger values of β, ξ, and μ_c, as well as with smaller values of γ, δ, and κ.

5.2 Our Simulation of a Moderately Severe Outbreak

We return to the parameter set that was used in Figure 1: $\beta = 0.07$/day and $\kappa = 10^5$ cells/mL. These model a fairly severe cholera situation, being on the worse end of the ranges in [9]. The duration of cholera infection for a person is $1/\gamma$ days, which is a little over two weeks for this parameter set. The natural lifespan of cholera in a water reservoir is $1/\delta$ days, which is a little over seven weeks for this parameter set.

We include additional parameter values to enable a numerical solution. We model a subpopulation of size $N = 15,000$, which is similar to the sizes of subpopulations of study sites within Cap-Haïtien and North Department considered in [12]. Haiti is divided into ten Departments, which are geographic subdivisions like states or provinces. [4, 1] For the daily birth rate, we convert the 2017 estimate from [4] of 23 births per thousand people annually to a daily rate of $\mu_b = 23/1000/365$. We base our death rates on [1]: $\mu_d = 9/1000/365$ for deaths unrelated to cholera, and $\mu_c = 25/1000/365$ for deaths related to cholera. We base our other parameter values on [9]: $\xi = 10.0$ cells per mL water per

day shed into the water source by infectious individuals, and $\kappa = 10^5$ cells per mL water as the half-saturation rate. We modeled through 100 days, which is about 14 weeks as in [29, Figure 2].

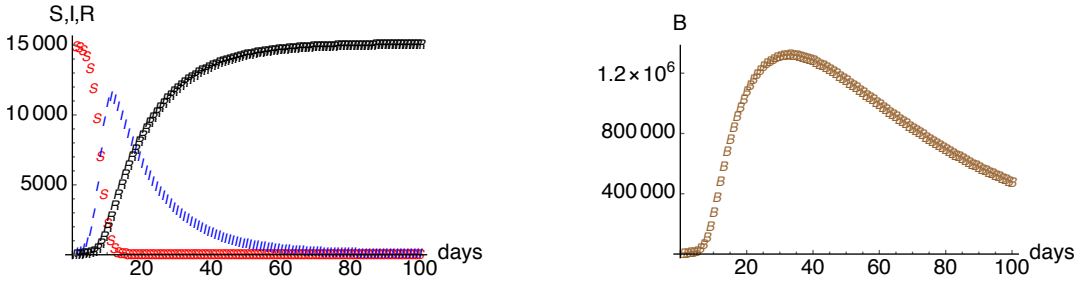

Figure 4: Simulation of Moderately Severe Outbreak: left SIR, right B.

Figure 4 shows the results of our numerical solution. The graph of "Infected" is slightly skewed to the right; the SIRB model indicates that people are infected more quickly than in an SIR model. The rapidity of infection in our model is reasonable, given the following about the outbreak in Haiti: "The first cases were confirmed on October 22nd, 2010. As of April 17th, 2011, 285,931 cases of cholera had been reported, with 154,041 (54.0%) patients hospitalized, and 4,870 (1.7%) deaths." [6] Furthermore, a single hospital had under a total of 70 hospitalizations for cholera and no deaths from October 8 through October 19 in 2010, and then had 404 hospitalizations and 44 deaths *on the next day!* [6]

The graphs of "Recovered" and "Susceptible" indicate a speedier recovery than we might expect in a subpopulation of Haiti. That is reasonable because ours is still a simple model. The simulation of "Bacteria" concentration in the water reservoir seems consistent with the values and description in [16] of Haitian cholera bacteria levels.

5.3 Effect of Parameter Values: Less Severe Outbreak

The SIRB model can yield widely different results, which can be useful in modeling a different situation. We changed some parameter values, still within the ranges determined by [9]: $\beta = 0.75 \longrightarrow 0.6$, $\gamma = 0.07 \longrightarrow 0.12$, $\delta = 0.02 \longrightarrow 0.15$, $\xi = 10 \longrightarrow 5$.

Here, the contact rate, β of the susceptible population with contaminated water is lower; a person is sick with cholera for $1/\gamma = 8.3$ days instead of over two weeks; cholera lives in the water reservoir for $1/\delta = 6.7$ days instead of over seven weeks; and infected people shed bacteria into the water source at half the rate. We see in Figure 5 that this second parameter set models a much less severe outbreak. Although the graph of those who recover looks quite similar, the the number of susceptible people decreases more slowly, and the peak number of people infected is much lower. The peak bacterial level in the water is dramatically lower.

Consider the following parameter set with values all still within ranges given by [9]: the contact rate with contaminated water, duration of infectiousness, and lifespan of bacteria in the water are all significantly smaller. $\beta \longrightarrow 10^{-4}$, $\gamma \longrightarrow 0.20$, $\delta \longrightarrow 0.20$, $\xi \longrightarrow 5$. Not one person in our simulation of a small population contracted cholera.

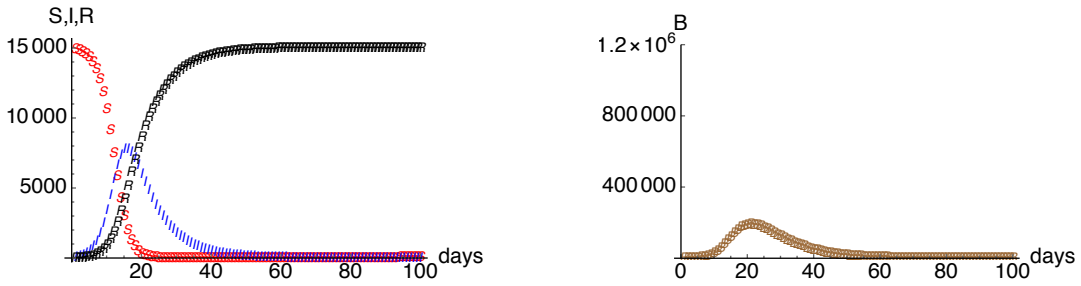

Figure 5: Simulation of Less Severe Outbreak: left SIR, right B.

Our choice of the basic SIRB model for a short-term analysis is affirmed by the assessment of multiple models by [1]: "We find that within the majority of the individual Haitian departments, for the timeframe of about 15 months, the simple SIRB model enjoys the most support."

5.4 Simulation Methods

The simulations are produced with Euler's Method. We chose this for multiple reasons: simplicity; intuition for students; and sufficient accuracy. Figure 6 shows the results of another numerical solution, using *Mathematica's* sophisticated numerical differential equation solver, NDSolve. Figure 4 is comparable, indicating the adequacy of Euler's Method for this system.

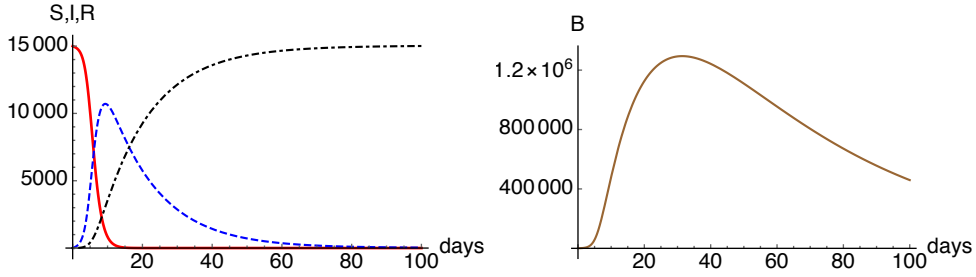

Figure 6: Solution using NDSolve

6 Relating to Social Justice

6.1 Data Collection and Choices of Model and Parameters

We used a fairly simple model with published data and information about parameter values. These choices are appropriate for teaching undergraduates about mathematical modeling in general, or about differential equations. Estimating parameters can be within the realm of undergraduate mathematics, if information is carefully prepared. We can indicate the use of sophisticated statistical methods used in parameter estimation, such as

the maximum likelihood methods in [1]. Whatever the level of complexity that instructors choose to engage students in modeling, it is appropriate for students – and instructors – to understand the variation in, power of, and limitations in, modeling.

"Models are simple, but not simplistic representations of the real world. They are used to capture the 'essence' of a complex phenomenon." [9] Models can illustrate the effect of vaccinations, as in [9] with cholera, or [10] with Avian flu. Models might help in setting public policy about the frequency and extent of vaccinations. Waning immunity is included in [9]. These models are more complex than our simple SIRB model. Other models consider subpopulations, which may be defined by a geographical region, age structure, sex, or health condition, some of which are issues of social justice. Five models with various subpopulation structures according to level of susceptibility, etc. are considered in [1], along with other models that take into account movement between the Departments of Haiti. Models can be spatiotemporal, as in [16], to account for the seasonal effects of flooding. Accurate models for Haiti over a longer time period than ours would require considering that: "Rainfall possibly increased surface water prone to infection (possibly through open defecation) and dissemination through runoff. The mountainous eastern areas ... are prone to both, as sanitation conditions are extremely poor and the topography increases the risk of transmission through runoff." [3] Departments in Haiti vary in population and poverty levels. [1, Table 2] "Considering its high population density and poor sanitation, there is a high risk for continued cholera transmission in [the vast Artibonite estuary]." [3] (Multiple maps are also included in [3].) Notice how intimately linked the modeling process is to inequities. The mathematical model chosen can lead to more or less appreciation for the severity of the social justice issue because models vary in the degree of "explanation" for the spread of the outbreak and the severity on the populations.

So, which model do we use? "There is tremendous disagreement throughout both kinds of research, biological and mathematical, about what parameter values are realistic and what modelling assumptions are important." [1] Both [9] and [1] include tables with a wide range of possible parameter values for SIR and variant models. Model misspecification and parameter uncertainty are explicitly discussed in [9].

Models and data influence public policy. Public policy influences the type, amount, and quality of data collected. An epidemiological model and its parameters can be based somewhat on theoretical information about a disease and its transmission, but the ability to validate our choices for the model and the parameters requires reliable data. Evidence of issues with data collection in the case of Haiti is offered in [3].

> [M]issing data at the epidemic's beginning led to a difference of over 20,000 patients compared with the number of patients reported by [Haiti's Ministry of Health]. ... In addition, approximately 2% of registered patients had no geographic information, or had geographic information that could not be traced. ... [D]ata are [based on health facilities], and patients who did not seek care were not included, ... [which] would be particularly important in the remote mountains regions where access to care is the most limited.

Haiti had 0.7 hospital beds per 1,000 people in 2013 [4], hardly enough to manage the tremendous number of cholera cases, let alone to ensure high quality healthcare or to

handle accurate data collection. Moreover, "decentralization of healthcare structures in Haiti was and remains difficult in very remote areas such as some villages in North Department that require a *10-hour walk* to get to the nearest healthcare facility." [12] "[A]ssessment of cholera-related deaths ... estimated that *87% of deaths were not recorded* in the hospital records." [12] (Emphases added.)

The difficulty in data accuracy and in modeling is well described by [1]:

> [I]n addition to the expected surveillance errors given the setting, there were surely additional errors in representing the data numerically. We believe that these errors are typical, and that the data will have noise in any large-scale cholera study. As a result, if there were a 'true' model that could describe the surveillance data in such an epidemiological setting, then that 'true' model would not be a 'true' representation of the actual disease dynamics. This is simply unavoidable, and we assume that the model which best describes the noisy data would be the best model to describe the actual data if it were possible to discover that data.

Good modeling demands good data. That, in and of itself, assumes that someone has the resources – and the authority (though not necessarily the "right") – to collect data on individuals, as well as to report at least aggregate information to public agencies.

6.2 Teaching and Learning of Differential Equations, and Mathematical Communities, as Contributions to Equity

Our model of a recent and real cholera epidemic is inherently interdisciplinary, incorporating differential equations, mathematical modeling, epidemiology, social justice, and more. The process of mathematical modeling necessitates honing in on a small part of a larger issue, ignoring detail to grapple with a tractable problem. Mathematicians frequently re-scale variables and eliminate parameters for mathematical convenience. Note that we explicitly included N, the total population, in Equation (3.1d), but in Equations (5.1) we eliminated N in the equations, although the initial population is indicated in Figures 4 and 5. How much more impactful might it be to show the cumulative number of cholera cases, or the number of deaths?

First among the nationally recognized Cognitive Recommendations for all mathematics courses calls for all undergraduate mathematics programs to "promote students' progress in learning to identify and model essential features of a complex situation, modify models as necessary for tractability, and draw useful conclusions." [13, Ref A] However, formerly for some undergraduates, this was a sterile situation, with focus on the mathematical process with problems that are totally devoid of meaning beyond the mathematics.

Many have been working to restore meaning to the math. We mention some related to differential equations. (See 8 for a description of author interactions with these communities.) SIMIODE supports a resurgence of a *modeling-first* approach to the study of differential equations because "[m]odeling engages and motivates students; it makes them curious," [23], which makes students engaged. Peer-reviewed classroom materials for the study of differential equations are offered freely by SIMIODE, IODE [17], and CODEE

[5, Ref B]. CODEE has a long history of working to make differential equations more understandable and visual. In fact, CODEE was originally founded by Bob Borrelli and Courtney Coleman as a Consortium for ODE Experiments, emphasizing the newfound ability to vary parameters and see the results. The introduction of computer graphics in the late 1980s suddenly gave a lot more power to the modeling approach to differential equations. IODE materials focus on conceptual aspects of differential equations. SIMIODE has teacher and student versions of modeling scenarios to facilitate adaptation to individual teaching styles and situations. SIMIODE also points to a number of free e-texts. Both CODEE and SIMIODE accept submissions for peer-review. The National Science Foundation (NSF) has supported each of these communities with grants: SIMIODE 2018-2021, IODE 1999-2003 and 2014-2017, and CODEE 1992-1997 and 2007-2011. All have organized sessions at professional meetings. All promote teaching with a focus on modeling, which is a form of inquiry-oriented learning. SIMIODE has offered multiple professional development opportunities for faculty to learn to teach with a modeling-first approach, as well as to author new materials for publication at the SIMIODE site.

"Mathematical modeling can be used to motivate curricular requirements and can highlight the importance and relevance of mathematics in answering important questions. It can also help students gain transferable skills, such as habits of mind that are pervasive across subject matter." [20] In this way, when taught in context, modeling may be a way to level the playing field for students. The free availability of high quality resources levels the playing field for instructors. Mathematical modeling in differential equations, and the mathematical communities that support its use, are part of a more general social justice context.

6.3 Broader Ideas of Teaching with/for Social Justice

Many different audiences study differential equations, and the course must offer materials and pedagogy to meet their needs. The differential equations course is undergoing great change because of advances in teaching with technology, which has increased the diversity of our students. Differential equations is taught at community colleges as well as four-year institutions, [13, Ref D], and at least one preporatory high school [7] in the United States. The relatively new contest for students, the SIMIODE Challenge Using Differential Equations Modeling (SCUDEM) [23, Ref C], has seen multiple teams of high school students, including one from West Lake High School in Austin, Texas that participated in SCUDEM III at Austin Community College, November 2018. The West Lake students had completed through multivariate calculus, and one was learning differential equations through the OpenCourseWare at the Massachusetts Institute of Technology. [15]

Our readers may consist primarily of those teaching mathematics at the undergraduate level, yet there is much to learn from work at all levels on math and social justice, as well as from the broader context of social justice education. Teachers at all levels can be catalysts for social justice by choosing to exemplify "critical mathematics", designing lessons to examine the world and expose students to inequities. One small but important step is to use person-first language, such as referring to people "who are infectious" rather than the quicker "infecteds."

Consider four possible components of mathematics for social justice [11]:

1. High quality mathematics instruction for all students.
2. Re-centered curriculum around the experiences of students from marginalized communities, while exploring issues of social justice through mathematics.
3. Mathematics as a critical tool for understanding social life; people's positions in society; and issues of power, agency, and oppression.
4. The use of mathematics to radically reconfigure society so that it might be more just.

We argue that the mathematical communities that we describe in Sections 6.2 and 8 contribute to the first of these. The second and third components are fulfilled, in part, by our system of differential equations model of cholera model *when* meaningful examinations of parameter values and model results are informed by the context of the real-world situation, along with a discussion of the limitations of the model.

We make no claims about our adherence to the last component - yet. Movement toward that goal would mean that we go beyond teaching the mathematical models and processes, beyond simply identifying the factors in Haiti that contribute to cholera outbreaks, beyond modeling how quickly cholera spreads or the numbers of individuals who sicken and die. We would have to allow time to examine what factors - systemic, racial, sociopolitical, etc. - have contributed to the poverty, poor sanitation, poor access to health care, that result in outbreaks and contribute to the high number of deaths. We would also need to examine the under-reporting that is based on limited staff and access to healthcare. For many mathematicians, this seems out of our training and areas of expertise. As we describe in Section 8, we have been making strides in that direction.

We do believe we have exhibited the following: "Mathematics becomes a tool used to examine social environments, increase awareness of social injustice, and serves as a valued language that can be used to further an agenda of social change towards a more just society." [11, P 25]

7 Final Thoughts

The development and analysis of our cholera model are informed by, and highlight inequities in, access: "[H]ouseholds in cholera-affected countries are largely below the global mean with regard to access to basic water and sanitation services." [27] The outbreak of cholera in Haiti in 2010 was the world's largest at the time. However, "in 2017, cholera continues to impact communities already made vulnerable by tragedies such as conflicts and famines. Yemen currently faces the world's largest cholera outbreak, with over 600,000 suspected cases and more than 2,000 deaths reported" between April 2017 and October 2017." [27] Researchers from many disciplines have been involved in identifying and understanding the dynamics of the disease and various situations under which cholera and other devastating diseases thrive. The models that researchers and instructors investigate and create, and the instruction methods that we employ, can

prepare the current and future generations to meet the continuing challenges that face our communities and our world.

8 Author Interactions and Acknowledgements

We point to multiple situations that enabled the authors' collaborations. This is to acknowledge others, as well as to encourage our readers to take advantage of opportunities.

Shelton and mathematical colleague John Ross wove social justice assignments into an Introductory Statistics course and produced the article [19], which includes thoughts, supported by a partial literature review about our journey as novices to teaching with social justice, as well as a link to our modules. This began at the 2016 Associated Colleges of the South (ACS) workshop, *Mathematics for Social Justice*. Southwestern University is a member of the ACS consortium. We gratefully acknowledge the organizers (C. Buell, Z. Teymuroglu, J. Wares, C. Yerger) and participants of this conference. They formed a community of mathematicians who care deeply about the issues of social justice within and beyond mathematics/statistics classroom.

Southwestern University has a well-established environment that fosters attention to social justice. The Core Principle: "Fostering a liberal arts community whose values and actions encourage contributions toward the well-being of humanity." The Core Values include "Respecting the worth and dignity of persons," and "Encouraging activism in the pursuit of justice and the common good." [22, Ref A] Southwestern University requires each student to take a course with a significant social justice component to "connect their learning to issues of diversity and inequality." [22, Ref B] Although no math course currently carries the social justice credit, Ross and Shelton made strides in that direction with the statistics modules.

Adrian has extensive experience incorporating social justice into her courses in Education, as well as designing entire courses with such a focus. Shelton began learning from Adrian in 1997 while being one of those to teach a course that all first year students took and that Adrian designed: "Disability, Society, and Ethical Issues." This was when Shelton first learned "person first" language. Southwestern has a long-standing initiative of intentionally making connections, known as *Paideia*^{TM}. [22, Ref C] Adrian has been a leader in *Paideia* since 2012 and served as *Paideia* Director (2014-2018). In this role, Adrian has continued to inform Shelton about social justice, including for the previously mentioned article about introductory statistics.

Two grants to Southwestern University aided Shelton and Groves. The Howard Hughes Medical Institute funds (2012-2016) formed the Inquiry Initiative in the Natural Sciences, supporting the eight-week 2015 Summer Collaborative Opportunities (SCOPE) Faculty-Student Research for Groves, an undergraduate at the time, and Shelton, the faculty supervisor. The W. M. Keck Foundation, Undergraduate Education Program, funds (2015-2018) fostered the integration of molecular biology across the Natural Sciences, supporting Shelton in creating a course module of the force of infection.

Shelton has worked with the SIMIODE [23] community since a 2015 faculty development workshop. Shelton is a co-Principal Investigator in the 2018-2021 NSF grant, was a 2018 DEMARC Fellow (Differential Equations Model and Resource Creator) to author

modeling scenarios in differential equations, and co-led a 2018 workshop for MINDE Fellows (Model INstructors in Differential Equations) to guide faculty in practicing a modeling-first approach. These two workshops are the primary purpose of the NSF grant, in order "to promote the use of modeling in motivating and teaching differential equations in high schools and undergraduate institutions." [23, Ref B] Shelton worked with the IODE [17] community as a 2015 and 2016 TIMES Fellow (Teaching Inquiry-oriented Materials: Establishing Supports) using Inquiry-Oriented Differential Equations (IODE).

The authors are grateful for the environment at Southwestern University, to the work of a "Math for Social Justice" Community, to funding opportunities, and to multiples communities in differential equations, mathematical modeling, and general mathematics. We are grateful to the CODEE journal for encouraging this collaboration, which has raised our own awareness of social justice issues in mathematics.

References

[1] Akman, Olcay; Romadan, Marina; Schaefer, Corby; Schaefer, Elsa. (2016) Examination of models for cholera: insights into model comparison methods. *Letters in Biomathematics* 3:1, 93-118. https://www.tandfonline.com/doi/full/10.1080/23737867.2016.1211495

[2] Ali, Mohammad; Nelson, Allyson R.; Lopez, Anna Lena; and Sack, David A. (2015) Updated Global Burden of Cholera in Endemic Countries. *PLOS Neglected Tropical Diseases* 9(6): e0003832. https://doi.org/10.1371/journal.pntd.0003832

[3] Allan, Maya, et.al. (2016) High-resolution spatial analysis of cholera patients reported in Artibonite department, Haiti in 2010-2011. Epicentre Epidemics 14:1.10. http://dx.doi.org/10.1016/j.epidem.2015.08.001

[4] Central Intelligence Agency. World Fact Book. https://www.cia.gov/library/publications/resources/the-world-factbook/

[5] Community of Ordinary Differential Equations Educators (CODEE)
(A) main site https://scholarship.claremont.edu/codee/
(B) projects booklet https://www.codee.org/jmm2013minicourse/jmm-2013-project-book.pdf

[6] Cravioto, Alejando; Lanata, Claudio F.; Lantagne, Daniele S.; Nair, G. Balakrish. (est 2011) Final Report of the Independent Panel of Experts on the Cholera Outbreak in Haiti. http://www.un.org/News/dh/infocus/haiti/UN-cholera-report-final.pdf No date was in the report, but the date of 04 May 2011 was given by ReliefWeb in its posting of the report at https://reliefweb.int/report/haiti/final-report-independent-panel-experts-cholera-outbreak-haiti

[7] Creighton Preporatory High School https://www.creightonprep.creighton.edu/page.cfm?p=331

[8] Domonoske, Camila. (2016) U.N. Admits Role in Haiti Cholera Outbreak That has Killed Thousands. August 18, 2016. *National Public Radio, Inc. (US).* https://www.npr.org/sections/thetwo-way/2016/08/18/490468640/u-n-admits-role-in-haiti-cholera-outbreak-that-has-killed-thousands

[9] Fung, Isaac Chun-Hai. (2014) Cholera Transmission Dynamic Models for Public Health Practitioners. *Emerging Themes in Epidemiology,* 11:1. https://doi.org/10.1186/1742-7622-11-1. Includes Online Supplementary Material 12982_2013_119_MOESM1_ESM.pdf. *(Note: there are variations in the font used for κ.)*

[10] Galvin, Cooper J.; Rumbos, Adolfo; Vincent, Jessica I.; and Salvato, Maria. (2014) Modeling the Effects of Avian Flu (H5N1) Vaccination Strategies on Poultry. *CODEE Journal,* Vol. 10, Article 1. https://scholarship.claremont.edu/codee/vol10/iss1/1/

[11] Gonzalez, Lidia. (2009) Teaching mathematics for social justice: Reflections on Community of Practice for Urban High School Mathematics Teachers. *Journal of Urban Mathematics Education.* 2(1), 22-51.

[12] Luquero, Francisco J., et al. (2016). Mortality Rates during Cholera Epidemic, Haiti, 2010 - 2011. *Emerging Infectious Diseases*, 22(3), 410 - 416. https://dx.doi.org/10.3201/eid2203.141970

[13] Mathematical Association of America, Committee on the Undergraduate Program in Mathematics. (2015) CUPM Curriculum Guide to Majors in the Mathematical Sciences. main page: https://www.maa.org/node/790342
(A) overall guidelines: http://www.maa.org/programs/faculty-and-departments/curriculum-\department-guidelines-recommendations/cupm.
(B) biomathematics report: https://www.maa.org/sites/default/files/MathBioPASGReport.pdf
(C) mathematical modeling course report: https://www.maa.org/sites/default/files/MathematicalModeling.pdf
(D) differential equations course report: https://www.maa.org/node/790342

[14] Meerschaert, Mark. (2013) Mathematical Modeling. 4thEd., Academic Press.

[15] Miller, Haynes and Mattuck, Arthur. 18.03 Differential Equations. Spring 2010. Massachusetts Institute of Technology: MIT OpenCourseWare, https://ocw.mit.edu. License: Creative Commons BY-NC-SA.

[16] Piarroux, Renaud, et al. (2011) Understanding the Cholera Epidemic, Haiti. *Emerging Infectious Diseases*, 17(7), 1161-1168. http://doi.org/10.3201/eid1707.110059 or https://www.ncbi.nlm.nih.gov/pmc/articles/PMC3381400/pdf/11-0059_finalS.pdf

[17] Rasmussen, Chris., Keene, Karen Allen, Dunmyre, Justin, and Fortune, Nicholas (2017). Inquiry oriented differential equations: Course materials. https://iode.wordpress.ncsu.edu

[18] "Rollins360" announcement of ACS grant to Teymuroglu for workshop. https://360.rollins.edu/faculty-highlights/teymuroglu-applies-mathematics-to-social-justice

[19] Ross, John, Shelton, Therese. (2018) Supermarkets, Highways, and Natural Gas Production: Statistics and Social Justice, *PRIMUS*, DOI: 10.1080/10511970.2018.1456497 https://doi.org/10.1080/10511970.2018.1456497

[20] Society for Industrial and Applied Mathematics (SIAM) & Consortium for Mathematics and its Applications (COMAP). (2016) Guidelines for Assessment and Instruction in Mathematical Modeling Education. https://www.siam.org/Publications/Reports/Detail/guidelines-for-assessment-and-instruction-in-mathematical-modeling-education; accessible from https://www.siam.org/Publications/Reports

[21] Smith, David; Moore, Lang. (2004) The SIR Model for Spread of Disease: The Differential Equation Model. *Loci.* (originally *Convergence.*) https://www.maa.org/press/periodicals/loci/joma/the-sir-model-for-spread-of-disease-the-differential-equation-model

[22] Southwestern University.
(A) Core Purpose and Core Values. (2011 version.) https://www.southwestern.edu/about-southwestern/university-profile/mission-purpose-values/index.php
(B) Catalog. (2018)
(C) *Paideia* https://www.southwestern.edu/about-southwestern/paideia/index.php

[23] Systemic Initiative for Modeling Investigations and Opportunities with Differential Equations (SIMIODE). https://www.simiode.org/
(A) SIMIODE Challenge Using Differential Equations Modeling (SCUDEM). https://www.simiode.org/scudem
(B) October 2018 Newsletter https://www.simiode.org/newsletter/simiodenewsletteroct2018?no_html=1#nsf

[24] United Nations Press Release. (2016) Secretary-General Apologizes for United Nations Role in Haiti Cholera Epidemic, Urges International Funding of New Response to Disease. SG/SM/18323-GA/11862 December 1, 2016. https://www.un.org/press/en/2016/sgsm18323.doc.htm

[25] World Bank. https://www.worldbank.org/

[26] World Health Organization. (2018) Fact Sheet on Cholera. February 1, 2018. http://www.who.int/mediacentre/factsheets/fs107/en/

[27] World Health Organization, Global Task Force on Cholera Control. (2017) Ending Cholera: A Global Roadmap to 2030. http://www.who.int/cholera/publications/global-roadmap.pdf or from www.who.int/cholera/en.

[28] World Health Organization and the United Nations Children's Fund, WHO/UNICEF Joint Monitoring Programme for Water Supply, Sanitation and Hygiene (JMP) (2017). Progress on Drinking Water, Sanitation and Hygiene: 2017 Update and SDG Baselines. http://www.who.int/mediacentre/news/releases/2017/launch-version-report-jmp-water-sanitation-hygiene.pdf or from https://washdata.org/

[29] World Health Organization, Pan American Health Organization. (2017) Epidemiological Update: Cholera. 4 May, 2017. https://reliefweb.int/sites/reliefweb.int/files/resources/2017-may-4-phe-epi-update-cholera.pdf

[30] World Health Organization, Pan American Health Organization. (2017) Epidemiological Update: Cholera. 28 Dec, 2017. https://reliefweb.int/sites/reliefweb.int/files/resources/2017-dec-28-phe-epi-update-cholera.pdf

[31] World Health Organization. (2016) Weekly Epidemiological Record (WER). No. 23, 2016, 91, p297-304. http://www.who.int/wer/2016/wer9123.pdf

[32] World Health Organization and World Bank. (Dec 13, 2017). World Bank and WHO: World Bank and WHO: Half the world lacks access to essential health services, 100 million still pushed into extreme poverty because of health expenses. https://tinyurl.com/y5tuf38n

SIR Models: Differential Equations that Support the Common Good

Lorelei Koss
Dickinson College

Keywords: Differential equations, common good, social justice
Manuscript received on November 28, 2018; published on February 13, 2019.

Abstract: This article surveys how SIR models have been extended beyond investigations of biologically infectious diseases to other topics that contribute to social inequality and environmental concerns. We present models that have been used to study sustainable agriculture, drug and alcohol use, the spread of violent ideologies on the internet, criminal activity, and health issues such as bulimia and obesity.

1 Introduction

In 2015, UNESCO argued that "education and knowledge are common goods and represent a collective societal endeavor in a complex world based on respect for life and human dignity, equal rights, social justice, cultural diversity, international solidarity and shared responsibility for a sustainable future." [24] This article surveys how SIR models have been extended beyond investigations of biologically infectious diseases to other topics that contribute to social inequality. The goal of this paper is twofold. First, we show how the SIR model provides one lens to investigate a number of topics that broadly fall in the field of social justice. We present models that have been used to study sustainable agriculture, drug and alcohol use, the spread of violent ideologies on the internet, criminal activity, and health issues such as bulimia and obesity. Second, as an entry in a special issue dedicated to education and knowledge regarding differential equations and social justice, this paper also contributes to the common good as proposed by UNESCO.

The topics discussed here are by no means comprehensive but instead are intended to present some ways that SIR models give insight to policy makers and advocates who are interested in fostering equity. In each section, we describe the construction and conclusions of one model and then point the reader to papers investigating similar topics. The models presented get more complicated as the paper progresses.

The paper is organized as follows. We introduce the basic SIR system of differential equations described by Kermack-McKendrick in Section 2 and provide an example of how the model was used to describe the spread of smallpox on Easter Island in 1863. The basic model assumes a closed population and does not account for birth or immigration into the population. In Section 3, we present how the SIR system can be adapted to

study the spread of ideas. We focus on an application investigating the dissemination of violent topics on a terrorist web forum. This model is slightly modified from the original Kermack-McKendrick model in that it incorporates logistic growth of the population.

In Section 4, we present a model of disease transmission in plants. Clearly, this application is closely related to disease transmission in humans, but sustainable agriculture fits well with the ideals of fostering equity that are addressed in this special issue of the journal. In this model, the rate at which plants are infected can change over time. Section 5 presents a SIR model of heroin use in Ireland. This model incorporates different death rates for the susceptible population and the drug using population as well as the possibility that drug users can stop using drugs and not re-enter the susceptible population.

Section 6 describes a system in which a person's decision to start criminal activity is modeled as a socially contagious disease. This model splits the population into four groups, instead of the three groups of Kermack-McKendrick's model. Finally, Section 7 of the paper describes a model investigating whether obesity rates in the United States will plateau by using a model that splits the population into five different subgroups.

2 Kermack-McKendrick's SIR Model

Kermack-McKendrick [14] introduced the SIR system of differential equations to model the spread of infectious diseases. They applied their analysis to plague deaths in Bombay in 1905-1906. In their study, they let $S(t)$, $I(t)$, and $R(t)$ respectively be the proportion of the population susceptible, infectious, and recovered at time t. (By "recovered," we simply mean that the individual has been removed from the infectious population by recovery or death.) The SIR system is defined by the equations

$$\begin{aligned} \frac{dS}{dt} &= -bSI, \\ \frac{dI}{dt} &= bSI - kI, \\ \frac{dR}{dt} &= kI. \end{aligned} \tag{2.1}$$

The number b represents the rate at which the disease is transmitted when an infected individual interacts with susceptible individuals. The first differential equation in Equation 2.1 describes how individuals move from the susceptible group to the infected group. The constant k represents the proportion of the infected group that will recover each day, which is the reciprocal of the infectious period of the disease. So the second equation in Equation 2.1 describes how the infected group increases as susceptible people become sick but decreases as infected people recover. Finally, the recovered group grows as people move from the infected group to the recovered group.

As an example, the SIR model was used in [15] to model the spread of smallpox on Easter Island in 1863. At that time, there were approximately 2700 susceptible people living on the island when between 1 and 15 people infected with smallpox arrived. Using historical data for smallpox transmissibility and contagion length, estimates of $0.14 \leq b \leq 0.85$, $1/25 \leq k \leq 1/20$, and $1/2700 \leq I(0) \leq 15/2700$ were used to simulate the epidemic. In all

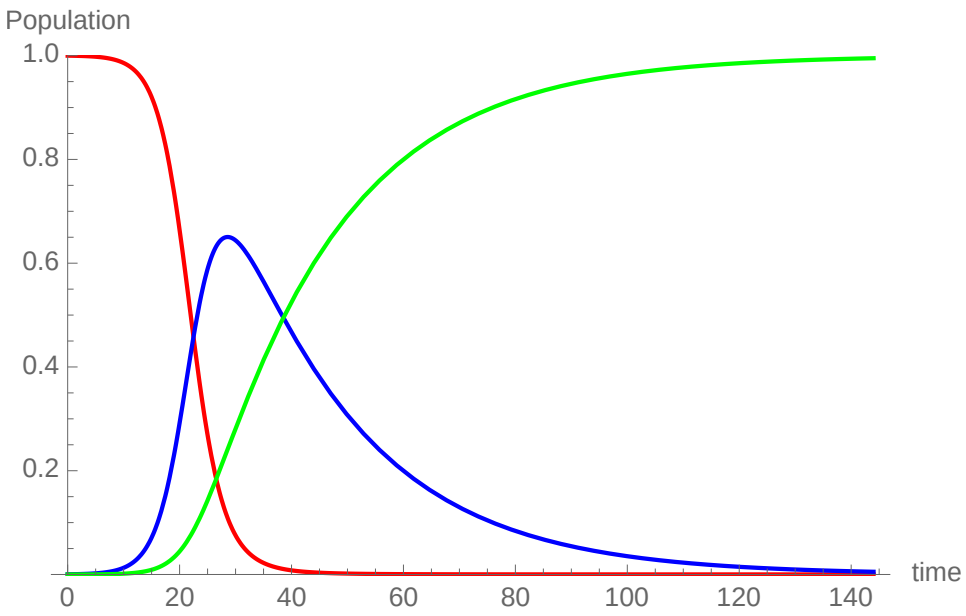

Figure 1: Simulating smallpox on Easter Island with the parameters $b = 0.4$, $k = 1/23$, and $I(0) = 1/2700$

simulations using parameters in these range, more than 90% of the islanders contracted smallpox. A simulation with $b = 0.4$, $k = 1/23$, and $I(0) = 1/2700$ is shown in Figure 1. In the figure, the red curve represents the susceptible population $S(t)$, the blue curve represents the infectious population $I(t)$, and the green curve represents the recovered population $R(t)$.

3 Intellectual ideas

The use of SIR models to understand the transmission of ideas dates back at least to 1964 when Goffman and Newill wrote a paper in Nature that explored modeling the development of ideas within a population [10]. In their model, Goffman and Newill described personal communication or publication as possible routes for the spread of infectious material. A more modern mechanism of transmission of ideas is through social media. In this section, we describe work by Woo, Son, and Chen [27] who used the SIR model to investigate the spread of violent topics on a major Jihadi web forum. Their model is very close to the system described in Section 2 except that they incorporated a variable population into their model.

In this model, $S(t)$ denotes the number of future authors, or the group of users who have interest in a topic and might read or comment on posts. The model assumes logistic population growth of the population with rate μ and carrying capacity K. Some susceptible users move in to the group of current authors $I(t)$ by writing or commenting on a thread after they have read previous posts about a topic. The constant b represents the degree of infectiousness of a topic. Authors move into the group of past authors $R(t)$ at a rate of k when their posts lose the power to infect others. The total number of authors at time t is

$N = S + I + R$. The model is given by

$$\begin{aligned} \frac{dS}{dt} &= \mu\left(1 - \frac{N}{K}\right)N - bSI, \\ \frac{dI}{dt} &= bSI - kI, \\ \frac{dR}{dt} &= kI. \end{aligned} \tag{3.1}$$

The authors collected data from a Dark Web Forum called Ummah from 2002–2010 which had over one million posts. They studied seven key topics discussed in the forum: *suicide bomb, anti-American, George Bush, wear hijab, honor killing, Bin Laden*, and *nuclear weapon*. They evaluated how well their model fit the data collected and found good results, with R-squared values ranging from 0.57 to 0.80. Of the seven topics, *anti-American* exhibited the highest infection rate, recovery rate, and growth rate, where *wear hijab* had the lowest infection rate. The authors concluded that the SIR model reasonably describes how violent topics spread on web forums.

Beyond the topics of violent ideologies, social media can also be used to spread information relevant to other social justice issues. For example, Woo, Ha, and Chen [28] modified the model given in Equation 3.1 to study the key topics of *healthcare and insurance, minimum wage and pay, stock price*, and *low price* on a Walmart discussion board. They adjusted the model by incorporating the possibility that an outside event, perhaps an important news story, could accelerate the infection rate. This paper also gave a helpful literature review of a number of studies of online information diffusion over discussion boards, computer viruses, blog connections, and other social media.

Beyond transmission by social media, Gurley and Johnson [12] used a more complicated model to investigate how sub-fields of economic theory grow or contract by exploring peer-reviewed journal publications. Similarly, Bettencourt et. al. [2] used a SIR model to investigate the spread of Feynman diagrams through the theoretical physics communities via personal communication in the period immediately after World War II.

4 Sustainable agriculture

Attention to sustainable agriculture is critical to humanity and the environment. There is a rich body of research using differential equations in this field; see [6, 8, 16, 20] as examples. Here, we describe work done by Gilligan, Gubbins, and Simons [9] in which they used a SIR system to model stem canker disease in tomatoes. This disease is caused by a fungus that attacks germinating tubers at the base of the stem, potentially destroying the stem.

Gilligan, Gubbins, and Simons set up their model by dividing the population into three categories. The population of susceptible stems is represented by $S(t)$ and the population of infected stems is $I(t)$. We use $R(t)$ to denote stems that are removed or dead. The study modeled how different levels of infection influenced the production of susceptible tissue,

called the *host response to infection load*. Their model was

$$\begin{aligned} \frac{dS}{dt} &= m(K-N) - b(t)S - f(I,S), \\ \frac{dI}{dt} &= b(t)S - kI, \\ \frac{dR}{dt} &= kI. \end{aligned} \tag{4.1}$$

Define $N = S + I + R$ to be the total number of stems. In this model, m represents the per capita rate of production of susceptible stems, k is the per capita death rate of infected stems, and K is the carrying capacity, or maximum number of stems per plant. The function $b(t)$ represents the force of infection, which involves the rate of infection of susceptible stems by the soil based fungus, the density of the fungus in the soil, and the level of host susceptibility. The function $b(t)$ can change with respect to time as the fungus becomes less infective and the host plant develops resistance.

The authors are primarily interested in determining an appropriate model for different host responses to the presence of infected stems. They consider seven different functions $f(I,S)$ that represent different responses. One of the possible functions is the null response, $f(I,S) = 0$. Another possible function is $f(I,S) = \alpha I$, where the reduction in the production of new stems changes in direct proportion to the amount of infected stems on the plant, where α is the rate of inhibition of production of susceptible stems due to infection. The other five functions $f(I,S)$ range from stronger reductions in the stem production with the presence of small amounts of fungus, to the possibility that the fungus significantly inhibits the production of more stems.

The authors fit their models to data collected Simons and Gilligan [21, 22] as well as Hide and Read [13] and Cother and Cullis [5]. They found that there is no evidence to reject the simplest SIR model where $f(I,S) = \alpha I$. In this case, disease can be controlled by reducing the initial inoculate density.

For an interesting discussion of a number of different models in sustainable agriculture, readers might look to Gilligan's paper *Sustainable agriculture and plant diseases: An epidemiological perspective* [8]. Gilligan describes a number of different SIR modifications that can be used to study agriculture on different scales, ranging from studies that focus on what happens within the plant to studies on national and continental scales.

5 Addiction

Alcoholism and drug use can be modeled as infectious diseases. In 2007, White and Comiskey [26] studied heroin use in Ireland in the hopes of gaining insight into how individuals progress through drug-using stages. White and Comiskey set up their model as follows.

The number of susceptible users, ranging from age 15–64, is given by $S(t)$. We use $I(t)$ to represent initial drug users or relapsed drug users who are not in treatment. The number of drug users in treatment is represented by $R(t)$. The number Λ represents a population growth rate resulting from individuals turning 15 during the study period and

thus entering the susceptible population, and N is the total size of the population under study. The constant b represents the probability of becoming a drug user, and k is the proportion of drug users who enter treatment. Finally, β is the probability that a drug user in treatment relapses to untreated drug usage.

In this model, individuals are removed from the population under study in a number of different ways. The natural (non-drug related) death rate is μ. The constant δ_1 represents a removal rate due to drug-related deaths of users not in treatment as well as a spontaneous recovery rate of individuals not in treatment who stop using drugs and are no longer susceptible. Similarly, the constant δ_2 represents a removal rate due to drug-related deaths of users in treatment as well as a spontaneous recovery rate of individuals in treatment who stop using drugs and are no longer susceptible.

$$\begin{aligned}
\frac{dS}{dt} &= \Lambda - \frac{bSI}{N} - \mu S, \\
\frac{dI}{dt} &= \frac{bSI}{N} - kI + \frac{\beta IR}{N} - (\mu + \delta_1)I, \\
\frac{dR}{dt} &= kI - \frac{\beta IR}{N} - (\mu + \delta_2)R.
\end{aligned} \tag{5.1}$$

The authors use the model to investigate the *basic reproduction number* R_0, the threshold value representing how many secondary infections result from the introduction of one infected individual into a population. In their model, $R_0 = b/(k + \mu + \delta_1)$. They perform a sensitivity analysis and determine that, to control the spread of habitual drug use, preventing initial drug use is more effective than increasing the number of individuals in treatment programs. Results such as these offer suggestions to policy makers about where to focus limited resources.

Njagarah and Nyabadza performed similar work analyzing drug epidemics in which they also included functions representing the roles of drug lords in the process [18]. Benedict [1] and Walters, Straughan, and Kendal [25] use SIR models to perform similar analyses of the spread of alcoholism and binge drinking.

6 Crime

A person's decision to start criminal activity can be modeled as a socially contagious disease. Mushayabasa [17] used a four function model to investigate the effects of unemployment on property crime under the assumption that criminality is a socially contagious process.

In Mushayabasa's model, the population of 15–64 year olds is divided into four subgroups: $S(t)$ is the number of unemployed individuals at time t, $W(t)$ is the group of employed individuals, $I(t)$ is the group of unemployed and undetected criminals, and $R(t)$ is the group of detected and incarcerated criminals. Note that this model assumes that an individual or either employed or a criminal, but not both at the same time. The model is given by the following system of differential equations.

$$
\begin{aligned}
\frac{dS}{dt} &= \mu - bSI - (\mu + \alpha)S + p\upsilon R, \\
\frac{dW}{dt} &= \alpha S - (1-q)bIW - \mu W, \\
\frac{dI}{dt} &= bI(S + (1-q)W) - (\mu + g + d)I + (1-p)\upsilon R, \\
\frac{dR}{dt} &= kI - (\mu + \upsilon)R.
\end{aligned} \tag{6.1}
$$

The parameter μ denotes both a constant growth rate as people age into the population as well as a natural death rate which is consistent among the different subgroups. Criminals are assumed to have an additional death rate d due to their criminal activities. Again, b represents the infection rate when individuals in the two susceptible groups S and W interact with individuals in the group I. We use α to denote the difference between employment rate and retrenchment rate. The term $1-q$ represents the assumption that employed individuals are less likely to be drawn into criminal activity. Criminals are detected and incarcerated at a rate of g. Criminals are released from incarceration at a rate υ, and a proportion p of them enter the susceptible classes while the remainder $1-p$ become criminals again. Finally, the model allows for no movement of undetected criminals into the employment group by assuming that fear of detection would prevent this move.

The author investigates the basic reproductive number,

$$
R_0 = \frac{b(\mu + (1-q)\alpha)}{(\alpha + \mu)(\mu + g + d)} + \frac{(1-p)g\upsilon}{(\mu + \upsilon)((\mu + g + d)}
$$

The basic reproduction number accounts for how new criminals are generated. The first term of R_0 measures the effects of having susceptible members interact with criminals. The second term measures the effects of relapse. Mushabaya's analysis determines that if at most 20% of released criminals relapse into criminal behavior and at most 10% of employed individuals are influenced into property crime, then property crime will die out. The author continues his analysis by modifying the model in Equation 6.1 by adding functions representing government or police policies intended to detect or incarcerate criminals, improve employment rates, or improve rehabilitation systems and seeing how that affects the long term outcome.

Sooknana, Bhatt and Comissiong performed a similar study of the spread of gang membership in Trinidad and Tobago [4]. In addition, Ormerod, Mounfield, and Smith used an SIR model to investigate burglary and violent crime in the United Kingdom [19].

7 Eating Behaviors

The SIR model can be used to model the spread of eating behaviors leading to health issues by incorporating biological, behavioral, and social factors into the model. Obesity is not an illness in itself (it is possible to be both obese and healthy), but obesity is correlated with higher risks of cancer, heart disease, disability, and mortality [7].

In 2014, Thomas et. al. [23] constructed a model to investigate whether obesity rates in the United States will plateau or continue to rise. The authors were especially interested in observing the impact of the birth rate on obesity prevalence as well as the effects of a person being raised in an obesogenic environment. The model described in this section is the most complicated in the paper, as it divides the population into six different groups, which the authors immediately simplify into a system of five equations. The susceptible group $S(t)$ are individuals consistently classified with body mass index (BMI) less than 25 at year t. The exposed group $E(t)$ describes individuals consistently classified with BMI less than 25 that have been effectively exposed by year t but are not yet overweight. Individuals with higher BMIs were split into three groups: $I_1(t)$, individuals classified as overweight ($25 \leq BMI < 30$) at year t, $I_2(t)$, individuals classified as obese ($30 \leq BMI < 40$), and $I_3(t)$, individuals classified as extremely obese ($40 \leq BMI$). The function $R(t)$ represents individuals who have reduced back to normal weight at year t, so they are susceptible but predisposed to weight regain. Again, we use $N = R + S + E + I_1 + I_2 + I_3$ to denote the entire population. Solving for R, we obtain $R = N - S - E - I_1 - I_2 - I_3$, so the authors don't use a sixth equation to describe R in the model.

The model has many parameters necessary to describe the relationships between each of the populations. The constant p represents the probability of being born in an obesogenic environment, and the birthrate and uniform death rate is μ. So the first term $(1-p)\mu N$ in the first equation in Equation 7.1 represents the proportion of births to individuals who have BMI less than 25. People in the overweight and obese classes provide social influence, or infectiousness, to susceptible individuals represented by the constants k_1 and k_2. Individuals in each class can spontaneously gain weight at rates α for the susceptible class, a for the exposed class, a_1 for overweight class, and a_2 for the obese class. The rate of weight loss is represented by β_3 moving from the extremely obese group to the obese group and β_2 for moving from the obese group to the overweight group. Overweight individuals recover at a rate ρ_1. Finally, ρ_R represents the fraction of the recovered population that move to the exposed group.

$$\begin{aligned}
\frac{dS}{dt} &= (1-p)(\mu N) - \mu S - \frac{k_1 I_1 S}{N} - \frac{k_2 I_2 S}{N} - \alpha S, \\
\frac{dE}{dt} &= p(\mu N) - \mu E - aE + \frac{k_1 I_1 S}{N} + \frac{k_2 I_2 S}{N} + \rho_R(N - S - E - I_1 - I_2 - I_3) + \alpha S, \\
\frac{dI_1}{dt} &= -\mu I_1 + aE - a_1 I_1 - \rho_1 I_1 + \beta_2 I_2, \\
\frac{dI_2}{dt} &= -\mu I_2 + a_1 I_1 - a_2 I_2 - \beta_2 I_2 + \beta_3 I_3, \\
\frac{dI_3}{dt} &= -\mu I_3 + a_2 I_2 - \beta_3 I_3
\end{aligned} \tag{7.1}$$

Thomas et. al. use data from the US and the UK to develop values for the given parameters. For example, $p = .55$ in the US using data from 1988–1998, and $p = .3$ in the UK. For the US, if birth and death rates remain constant, the model predicts that obesity rates will plateau in 2030 at 28 % overweight, 32 % obese, and 9 % extremely obese.

Gonzales et. al. perform a similar study focusing on the role of college peer pressure on bulimic students who are not anorexic [11]. Ciarcià et. al. [3] study the effects of peers, media, and education on the dynamics of anorexic and bulimic populations.

References

[1] Brandy Benedict. Modeling alcoholism as a contagious disease: how infected drinking buddies spread problem drinking. *SIAM news*, 40(3):11–13, 2007.

[2] Luís MA Bettencourt, Ariel Cintrón-Arias, David I Kaiser, and Carlos Castillo-Chávez. The power of a good idea: Quantitative modeling of the spread of ideas from epidemiological models. *Physica A: Statistical Mechanics and its Applications*, 364:513–536, 2006.

[3] Carla Ciarcià, Paolo Falsaperla, Andrea Giacobbe, and Giuseppe Mulone. A mathematical model of anorexia and bulimia. *Mathematical Methods in the Applied Sciences*, 38(14):2937–2952, 2015.

[4] Donna Marie Giselle Comissiong, Joanna Sooknanan, and Balswaroop Bhatt. Life and death in a gang-a mathematical model of gang membership. *Journal of Mathematics Research*, 4(4):10, 2012.

[5] EJ Cother and BR Cullis. Tuber size distribution in cv. sebago and quantitative effects ofrhizoctonia solani on yield. *Potato research*, 28(1):1–14, 1985.

[6] NJ Cunniffe, ROJH Stutt, F Van den Bosch, and CA Gilligan. Time-dependent infectivity and flexible latent and infectious periods in compartmental models of plant disease. *Phytopathology*, 102(4):365–380, 2012.

[7] Centers for Disease Control and Prevention. The health effects of overweight and obesity. https://www.cdc.gov/healthyweight/effects/index.html.

[8] Christopher A Gilligan. Sustainable agriculture and plant diseases: an epidemiological perspective. *Philosophical Transactions of the Royal Society B: Biological Sciences*, 363(1492):741–759, 2008.

[9] Christopher A Gilligan, Simon Gubbins, and Sarah A Simons. Analysis and fitting of an sir model with host response to infection load for a plant disease. *Philosophical Transactions of the Royal Society of London B: Biological Sciences*, 352(1351):353–364, 1997.

[10] William Goffman and VA Newill. Generalization of epidemic theory. *Nature*, 204 (4955):225–228, 1964.

[11] Beverly González, Emilia Huerta-Sánchez, Angela Ortiz-Nieves, Terannie Vázquez-Alvarez, and Christopher Kribs-Zaleta. Am I too fat? Bulimia as an epidemic. *Journal of Mathematical Psychology*, 47(5-6):515–526, 2003.

[12] Nicole Gurley and Daniel KN Johnson. Viral economics: an epidemiological model of knowledge diffusion in economics. *Oxford Economic Papers*, 69(1):320–331, 2016.

[13] GA Hide and PJ Read. Effect of neighbouring plants on the yield of potatoes from seed tubers affected with gangrene (phoma foveata) or from plants affected with stem canker (rhizoctonia solani). *Annals of applied biology*, 116(2):233–243, 1990.

[14] William O Kermack and Anderson G McKendrick. Contributions to the mathematical theory of epidemics. I. *Bulletin of mathematical biology*, 53(1-2):33–55, 1991.

[15] Lorelei Koss. Sustainability in a differential equations course: a case study of Easter Island. *International Journal of Mathematical Education in Science and Technology*, 42 (4):545–553, 2011.

[16] Laurence V Madden and Frank Van Den Bosch. A population-dynamics approach to assess the threat of plant pathogens as biological weapons against annual crops: Using a coupled differential-equation model, we show the conditions necessary for long-term persistence of a plant disease after a pathogenic microorganism is introduced into a susceptible annual crop. *AIBS Bulletin*, 52(1):65–74, 2002.

[17] Steady Mushayabasa. Modeling optimal intervention strategies for property crime. *International Journal of Dynamics and Control*, 5(3):832–841, 2017.

[18] Hatson John Boscoh Njagarah and Farai Nyabadza. Modeling the impact of rehabilitation, amelioration and relapse on the prevalence of drug epidemics. *Journal of Biological Systems*, 21(01):1350001, 2013.

[19] Paul Ormerod, Craig Mounfield, and Laurence Smith. Non-linear modelling of burglary and violent crime in the uk. *Volterra Consulting Ltd*, 2001.

[20] Wilfred Otten, JAN Filipe, Douglas J Bailey, and Christopher A Gilligan. Quantification and analysis of transmission rates for soilborne epidemics. *Ecology*, 84(12): 3232–3239, 2003.

[21] SA Simons and CA Gilligan. Factors affecting the temporal progress of stem canker (rhizoctonia solani) on potatoes (solanum tuberosum). *Plant Pathology*, 46(5):642–650, 1997.

[22] SA Simons and CA Gilligan. Relationships between stem canker, stolon canker, black scurf (rhizoctonia solani) and yield of potato (solanum tuberosum) under different agronomic conditions. *Plant Pathology*, 46(5):651–658, 1997.

[23] Diana Maria Thomas, Marion Weederman, Bernard Fuemmeler, Corby Martin, Nikhil Dhurandhar, Carl Bredlau, Steven B Heymsfield, Eric Ravussin, and Claude Bouchard. Dynamic model predicting overweight, obesity, and extreme obesity prevalence trends. *The FASEB Journal*, 27(1 Supplement):360–6, 2013.

[24] UNESCO. Rethinking education. towards a global common good? 2015. URL http://unesdoc.unesco.org/images/0023/002325/232555e.pdf.

[25] Caroline Elizabeth Walters, Brian Straughan, and Jeremy R Kendal. Modelling alcohol problems: total recovery. *Ricerche di Matematica*, 62(1):33–53, 2013.

[26] Emma White and Catherine Comiskey. Heroin epidemics, treatment and ode modelling. *Mathematical biosciences*, 208(1):312–324, 2007.

[27] Jiyoung Woo, Jaebong Son, and Hsinchun Chen. An SIR model for violent topic diffusion in social media. In *Intelligence and Security Informatics (ISI), 2011 IEEE International Conference on*, pages 15–19. IEEE, 2011.

[28] Jiyoung Woo, Sung Ho Ha, and Hsinchun Chen. Tracing topic discussions with the event-driven SIR model for online forums. *Journal of Electronic Commerce Research*, 17(2):169, 2016.

The Mathematics of Gossip

Jessica Deters
Virginia Polytechnic Institute and State University

Izabel Aguiar
Stanford University

Jacquie Feuerborn

Keywords: Fake news, gossip, ODEs, humanistic mathematics, problem-based learning, active learning
Manuscript received on September 27, 2018; published on February 13, 2019.

Abstract: How does a lie spread through a community? The purpose of this paper is two-fold: to provide an educational tool for teaching Ordinary Differential Equations (ODEs) and sensitivity analysis through a culturally relevant topic (fake news), and to examine the social justice implications of misinformation. Under the assumption that people are susceptible to, can be infected with, and recover from a lie, we model the spread of false information with the classic Susceptible-Infected-Recovered (SIR) model. We develop a system of ODEs with lie-dependent parameter values to examine the pervasiveness of a lie through a community.

The model presents the opportunity for the education of ODEs in a classroom setting through a creative application. The model brings a socially and culturally relevant topic into the classroom, allowing students who may not relate with purely technical examples to connect with the material. Including diverse perspectives in the discussion and development of mathematics and engineering will enable creative and differing approaches to the worlds' problems.

1 Introduction

The current instruction of ODEs lacks socially-relevant examples geared towards helping students understand the social implications and applications of their work. By including a broader diversity of examples in current questions in technical fields, we will be able to address social and cultural problems in more creative and inclusive ways.

The term "fake news" has become increasingly culturally relevant as technology and social media further increases the ability for individuals and media groups to make unfounded claims. Furthermore, the phenomena of fake news has pervaded society as a fundamentally epistemic challenge. The ability to judge what is truth and not reaches

beyond evidence and into philosophical arguments. However, the ability to distinguish truth is critical to making informed decisions that inevitably impact society.

The spread of misinformation throughout society has become one of the most pressing issues of our generation. In order to address such an epistemic challenge, we must prepare our future leaders, future developers, future mathematicians to think with this mindset.

The purpose of this paper is two-fold: to provide an educational tool for teaching ODEs and sensitivity analysis through a culturally relevant topic (fake news), and to examine the social justice implications of misinformation. The intentions behind these purposes are to engage students with a culturally relevant example and to encourage students to think creatively about how to apply mathematical tools to societal issues.

The organization of the paper is as follows. In Section 2 we detail the educational foundation behind problem based learning. In Section 3 we discuss the background of the proposed project, develop the Gossip Model used to understand the spread of a rumor, and discuss the use of *anthropomorphized sensitivity analysis* to examine parameter dependence. Suggestions for classroom implementation for the instruction of the Gossip Model are discussed in Section 4. We conclude in Section 5 with discussion and suggestions for future work.

2 Educational Foundation: Problem Based Learning and Student Interest

Active learning approaches have been shown to boost student motivation and student performance. Motivation comes, in part, from interest [1]. Accordingly, if students are interested in the problem and application, they will be more motivated to learn the concept at hand. We posit that many students are interested in the spread of fake news, and more human-centric applications than currently addressed in mathematics classrooms. As a result, by connecting ODEs to the spread of fake news, students will be more motivated to learn ODEs, and more prepared to creatively translate societal issues to mathematical problems.

We provide two classroom implementation suggestions: a **simple implementation** designed for one class period and an **independent work implementation** designed for multiple class periods.

The two implementations offer various levels of an active, problem-based learning pedagogy, meaning students learn by working to understand or solve a problem [3]. Teachers facilitate student learning by guiding their students through the problem and offering help when needed. Students then work in small groups to solve the problem at hand [3]. It is believed that this experience helps students develop problem-solving skills and acquire new information through self-directed inquiry into the problem.

A more detailed explanation of how to implement this project into a class is provided in Section 4.

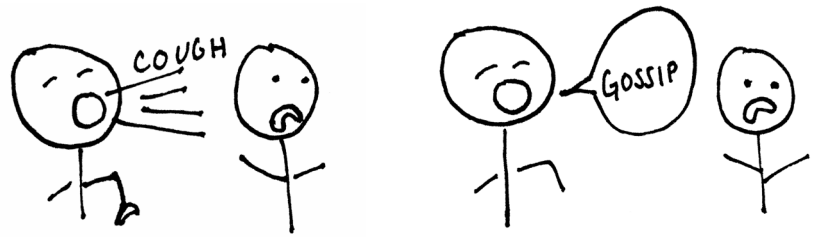

Figure 1: Modeling the spread of gossip with the modeling tools developed to understand infectious diseases.

3 The Gossip Model

In this section we discuss the background, assumptions, and development of the Gossip Model, a system of ODEs used to understand the spread of a lie. The Gossip Model proposed here is that which we use to prompt students to question the societal implications of the spread of a lie, as well as the role of mathematics in addressing such an issue.

3.1 Background and related work

The SIR model for modeling the population biology of infectious diseases was originally developed by Kermack and McKendrick in 1927 [2]. The SIR model describes the dynamics of three populations – those susceptible to (S), infected with (I), and recovered from (R) the infectious disease, and is common in the instruction of ODEs. The system of ODEs describe the following population dynamics: S becomes infected at a transmission rate β when interacting with the I population. I recover (and join the R population) at a rate γ.

When discussing the traditional SIR model, the language used (something *spreading*, people being *infected* and *recovering*) hints toward a more socially-driven application. This shared vocabulary, the idea of the *transmission* of something through interaction (see Figure 1), leads to the next sections wherein we develop and describe the Gossip Model.

3.2 Assumptions of the model

We begin to develop our model by stating our assumptions. Foremost, we assume that the gossip that is spreading is *false*. Similar to the SIR model, we assume that there are three possible populations: those susceptible to the gossip (S), infected with the gossip (I), and recovered from the gossip (R). The S population consists of people who have not yet heard the gossip. The I population consists of people who have heard the gossip *and believe it is true*. The R population consists of people who have heard the gossip *and know it is false*. Furthermore, gossip is only spread through direct interaction with the infected (it's not airborne), and there are a fixed amount of people in the system, $N = S + I + R$.

3.3 The Model

We define four lie-dependent parameters, ρ, β, γ, and α. We assume that, upon hearing the gossip for the first time, $(1 - \rho)$ proportion of the population will immediately know

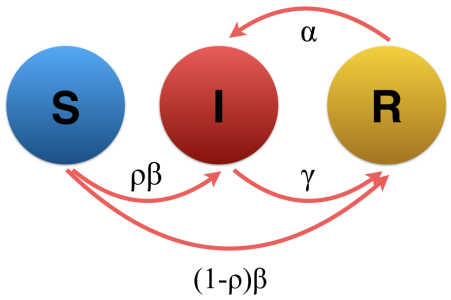

Figure 2: The SIR model described by (3.1). Parameters β and γ describe the rates at which the lie is believed and rejected as false, respectively, ρ describes the percentage of the population immune to the lie, and α describes the rate at which the recovered population become re-infected with the lie.

it is false: that is, they will move directly from S to the R population. This proportion of people describes those in the population who may have existing knowledge counteracting the gossip, or who are perhaps naturally skeptical people.

The rate of transmission, β, describes how "contagious" the gossip is. It is the per-capita rate per unit time that the interaction between populations will lead to infection. This parameter is dependent on the environment in which the gossip is being spread (e.g., maybe gossip spreads faster in a middle school than in an office), the nature of the gossip (e.g., perhaps people will talk more about relationships than ice cream flavors), and the origin of the gossip (e.g., the reliability of the original source).

The rate of recovery, γ describes how easy the gossip is to counteract with other evidence/hearsay. Again, this parameter is dependent on the environment and the nature of the gossip.

The fourth parameter, α, describes how convincing the believers of the gossip (those in the I population) are. This rate acts through the interaction between the I and R populations, and results in the R population becoming re-infected with the gossip.

The system of ODEs for the SIR model described above and shown in Figure 2, is written as,

$$\begin{aligned} \frac{\partial S}{\partial t} &= -\beta \cdot S \cdot I \\ \frac{\partial I}{\partial t} &= \rho \cdot \beta \cdot S \cdot I - \gamma \cdot I + \alpha \cdot R \\ \frac{\partial R}{\partial t} &= \gamma \cdot I - \alpha \cdot R + (1-\rho) \cdot \beta \cdot S \cdot I. \end{aligned} \tag{3.1}$$

3.4 An Example

To demonstrate an example of how the model works, consider the gossip, *"Jo made out with Jaimie last night,"* and assume that this statement is a false rumor started by one jealous friend. The following scenes describe the movement between populations upon hearing the rumor. The scene is also demonstrated in the schematic shown in Figure 3.

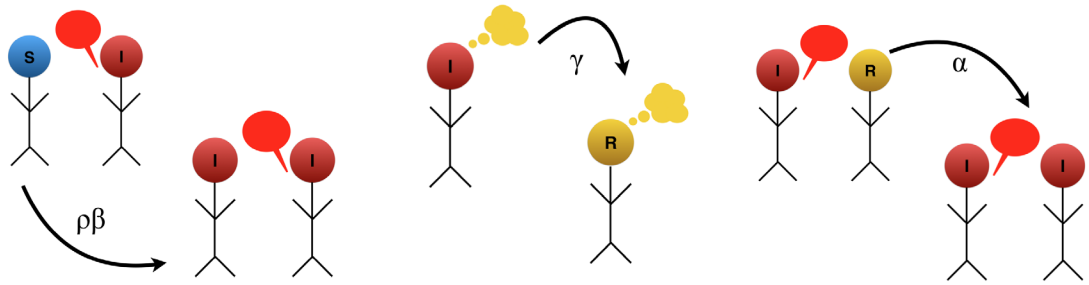

Figure 3: Schematic showing the rates at which the gossip spreads and dies. Leftmost shows the rate $\rho\beta$ at which people who haven't heard the gossip hear and believe it. Middle shows the rate γ at which those who believe the gossip stop believing it. Rightmost shows the rate α at which particularly convincing believers can re-convince nonbelievers of the gossip.

Scene: Susceptible interacting with Infected and becoming Recovered according to $(1-\rho)\beta$
I: Did you hear that Jo made out with Jaimie last night?
S (becoming R): Um no, I was with them both all night.
I: Believe what you want.

Scene: Susceptible interacting with Infected and becoming Infected at $\rho\beta$
I: Did you hear that Jo made out with Jaimie last night?
S (becoming I): OMG I knew they were acting weird.
I: I know right.

Scene: Infected recovering at rate γ
I (becoming R): *(thinking aloud)* It really doesn't make sense for Jo to make out with Jaime... Jo has been home sick with the flu all week.

(Scene: Recovered interacting with Infected and becoming re-Infected at rate α*)*
I: Did you hear that Jo made out with Jaimie last night?
R: You know that's a dumb rumor right?
I: No it's not, I saw them with my own eyes.
R (becoming I): Wow really? I guess it makes sense...

3.5 Anthropomorphized Sensitivity Analysis

As discussed in Section 3.3, parameters ρ, β, γ, and α depend on many characteristics of the gossip scenario. To highlight these differences and how they impact the dynamics of the system, we conduct *Anthropomorphized Sensitivity Analysis*. This approach allows students to observe and practice the purposes of conducting sensitivity analysis, understand the contextual meaning of the parameters, and creatively and humanistically translate social characteristics to mathematics.

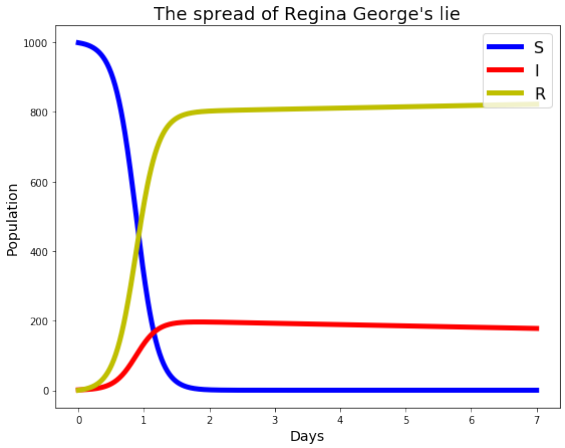

Figure 4: The dynamics of a petty rumor spread by Regina George. We see that by the end of the second day after the gossip started, everybody in the school has heard the rumor. However, by the end of the week, more than 80% of the school knows that the rumor is false.

3.5.1 Regina George

Regina George is one of the main characters in the film *Mean Girls*. Regina George is well-known as a meanspirited, but extremely popular, member of her high school. We assume that Regina George and her gossip have a high priority status at the high school, and thus that the transmission rate, $\beta = 0.03$, is extremely high: each infected person spreads the gossip to 30 other people, per day. Likewise, we assume that the nature of Regina George's gossip is petty, and thus relatively easy to disprove or counteract. This characteristic of the rumor lends to a high rate at which people recover and reject the rumor as false ($\gamma = 0.02$, 20 people per day). We also assume that Regina George is well-known to spread gossip, and thus is relatively unreliable. This unreliability is reflected in that 80% of people ($(1 - \rho) = 0.8$) who hear the gossip automatically discount it as false – they won't be tricked by yet another Regina George rumor.

We run this simulation for 7 days and analyze the situation that has arisen from Regina George's rumor (see Figure 4 for analysis and interpretation).

3.5.2 Dr. Neverheardofher

Dr. Neverheardofher is the top expert in her field. Her field, however, is extremely specific, esoteric, and small (perhaps she studies the ligaments of the Argentine ant). Consider the possibility that Dr. Neverheardofher wants to test her scientific community, and, to do so, introduces a lie in her most recent publication (perhaps that the female Argentine ant is double-jointed). The transmission rate at 1 person per ten days ($\beta = 0.0001$) of this esoteric lie is considerably less impressive than Regina George's (people don't tend to chat about the ligaments of female Argentine ants).

Furthermore, the rate at which people recover from this lie ($\gamma = 0.00001$, one person every one hundred days) is incredibly small – the esoteric and harmless lie does not necessarily inspire independent counter-arguments – and Dr. Neverheardofher is *the*

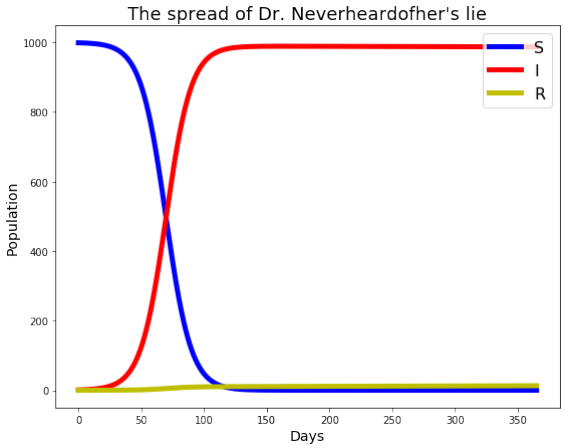

Figure 5: The spread of an esoteric lie started by Dr. Neverheardofher. We see that although it takes considerably longer for her community to be saturated with the lie (about 100 days), by the end of the year, the majority of the community still believes her lie. We do, however, see that the population of the infected is very slowly decreasing.

expert in her field: there is no other evidence counteracting her claim. Finally, because Dr. Neverheardofher is a well-known expert, has her PhD, and has a reputation of producing top-notch science, we assume that only 1% of people who hear the lie ($(1-\rho) = 0.01$) reject it as false. This one percent might represent people who are naturally cynical, people who have some sort of direct experience with the nature of the lie, or have other reasons not to believe it.

We run the scenario for a year to observe the dynamics (see Figure 5 for analysis).

3.5.3 The Conwoman

The Conwoman is charismatic. Her lie, her vision, her movement, is one of which she is so convincing that all of her followers are able to re-convince non-believers of the lie. This charisma is reflected through the parameter, $\alpha = 0.009$. This parameter represents the ability for the Recovered population to become re-Infected upon interacting with the Infected population (see the rightmost picture in Figure 3).

We assume that the Conwoman and her followers' rate of infection ($\beta = 0.003$, three people per day) is higher than that of Dr. Neverheardofher, but lower than that of Regina George–she's popular and influential, but not on the scale as Regina George. We also assume that the Conwoman's lie is easier to recover from ($\gamma = 0.001$, one person per day) than Dr. Neverheardofher's, although not as easy as Regina George's. Furthermore, we assume the Conwoman is a fairly prominent figure with no prior reputation of lying. Thus we assume that only 30% of people ($(1-\rho) = 0.3$) automatically reject the rumor as false. See Figure 6 for the dynamics and analysis.

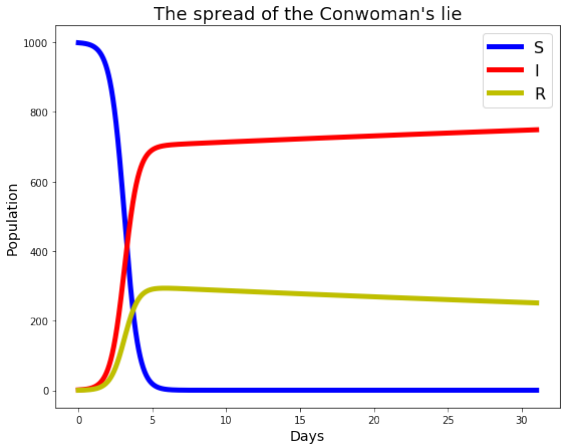

Figure 6: The spread of a lie started by the Conwomanand perpetuated by her charismatic followers. We see that by the end of the month, nearly 80% of the population believes her lie. Furthermore, contrary to the decline in infection we saw in the other two cases, we see that the number of people in the Infected population is increasing.

3.6 Classroom Jupyter Notebook

A jupyter notebook with the code for the above plots, question prompts, and problem discussion can be found on GitHub at
`https://github.com/izabelaguiar/The-Mathematics-of-Gossip`.

4 Classroom Implementation

There are several methods by which the instruction of this model can be implemented in a classroom, depending on the preexisting course content and available time. For classes that spend only a few days on SIR models, it may be best to begin with a general explanation of SIR models and then spend another day looking specifically at this application with the Simple Classroom Implementation. Alternatively, this can be used as an introduction to SIR models, if the course does not plan on going deeply into the topic.

For courses that are planning on spending more time looking into different forms of the SIR model, it can be beneficial to use this example as a method of introducing independent student learning, in the form of an assignment or even a presentation. For this depth of learning, the Independent Work Implementation allows students to gain a deeper understanding of the model, create new sensitivity analysis characters or scenarios, and to extend the model beyond current assumptions.

4.1 Simple Classroom Implementation

For a simple classroom implementation that can be done with just one class period, the problem can be explained and worked through by the professor in front of the class. The professor can begin by explaining the background, walking through the formulas and demonstrating an example or two. Demonstrating the parameter sensitivity is best done

with the provided Jupyter notebook, which the students should have access to as well. This explanation and demonstration will give students an understanding of the system of ODEs, of the model, and how scenarios translate to parameter values.

Then in small groups, the students can choose their own scenarios to represent through parameter values in the model. The choices should reflect the context of their chosen scenario. This will help students understand the meaning behind the parameters and analyze the sensitivity of the model when changing these parameters.

4.2 Independent Work Implementation

Alternatively, if the goal is to have students gain a deeper understanding of the model and its complexities, the initial model can be taught in a series of class periods. First, the instructor can review the background, formulas, and examples the same way as the Simple Classroom Implementation. Then, the students can be placed in groups or work independently to figure out how to add the alpha term – the movement of individuals from the recovered population back to the infected population – to the equations.

This method will work best if students have already been introduced to various forms of the SIR model in previous classes. This will allow them to connect the ideas from those classes with this Gossip Model and help them to understand the complexity of modeling human interactions. For deeper levels of independent work, the students can introduce other terms into the model. Additional terms could include representing: population growth or decrease, the existence of supporting rumours, and any other factors that students devise. Overall, this teaching method will allow students to gain a deeper understanding of the model as they work to adjust and add to it.

5 Conclusions and Future Work

The model developed in this paper has potential to be altered to include more complicated scenarios. There are many possible topics for students to expand upon this model. First, it would be interesting to consider the ability for lies to spread without direct interaction with the infected, accounting for the impact of social media. Second, the incorporation of a separate, counteracting lie/rumor would represent a more complicated scenario. Furthermore, this topic could be studied through a network-science framework to understand how real data could help analyze the spread of a lie.

In this paper we have developed an educational tool to aid in the instruction of ODEs through a socially-relevant application: the spread of lies. We have provided examples for the model application, suggestions for the instruction of the model, and a supplementary Jupyter notebook to aid in the instruction. This educational tool allows students to study the use of ODEs in modeling, to understand the importance of sensitivity analysis and parameter-dependence, and to develop the skills to translate social issues to mathematics. The model is centered around social dynamics and human environments with the hope to make mathematics more accessible and exciting to a diverse group of students, prepared and excited to use mathematics to address the worlds' most pressing challenges.

References

[1] Brett D. Jones. Motivating students to engage in learning: The MUSIC model of academic motivation. *International Journal of Teaching and Learning in Higher Education*, 21:272–285, 2009.

[2] W. O. Kermack and A. G. McKendrick. A contribution to the mathematical theory of epidemics. 115(772):700–721, 1927. doi: 10.1098/rspa.1927.0118.

[3] Karl Smith, Sheri Sheppard, David Johnson, and Roger Johnson. Pedagogies of engagement: Classroom-based practices. *Journal of Engineering Education*, 94, 2005.

An Epidemiological Math Model Approach to a Political System with Three Parties

Selenne Bañuelos, Ty Danet, Cynthia Flores, and Angel Ramos
California State University, Channel Islands

Keywords: Compartment model, epidemiological model, voting, three-party system
Manuscript received on November 12, 2018; published on February 13, 2019.

Abstract: The United States has proven to be and remains a dual political party system. Each party is associated to its own ideologies, yet work by Baldassarri and Goldberg in *Neither Ideologues Nor Agnostics* show that many Americans have positions on economic and social issues that don't fall into one of the two mainstream party platforms. Our interest lies in studying how recruitment from one party into another impacts an election. In particular, there was a growing third party presence in the 2000 and 2016 elections. Motivated by previous work, an epidemiological approach is taken to treat the spread of ideologies and political affiliations among three parties, analogous to the spread of an infectious disease. A nonlinear compartmental model is derived to study the movement between classes of voters with the assumption of a constant population that is homogeneously mixed. Numerical simulations are conducted with initial conditions from reported national data with varying parameters associated to the strengths of political ideologies. We determine the equilibria analytically and discuss the stability of the system both algebraically and through simulation, parameters are expressed to stabilize a co-existence between three parties, and numerical simulations are performed to verify and support analysis.

There is nothing which I dread so much as a division of the republic into two great parties, each arranged under its leader, and concerting measures in opposition to each other. This, in my humble apprehension, is to be dreaded as the greatest political evil under our Constitution.
— John Adams, 1780

1 Introduction

The United States has proven to be and remains a dual political party system. The 2000 and 2016 presidential elections have brought with them a growing number of voters moving into third parties. The goal of this research is to study the movement of voters between political parties, and the population dynamics amongst the voting class. To evaluate these attributes, we will approach the issue using a nonlinear mathematical model employing epidemiological methods with the assumption of a constant population

that is homogeneously mixed. That is, the ideology and influence of a political party is treated as a disease that a person can contract.

A deterministic model of the movement of eligible voters within a constant population is presented. We determine the equilibria analytically and discuss the stability of the system. Parameters are expressed to stabilize a co-existence between three parties, and numerical simulations are presented to verify and support the analysis. This manuscript is concluded with a note to instructors interested in conducting this type of undergraduate research project.

2 Three-Party Voter Model

In [4], a deterministic model of the movement of voters between two political parties is developed with an epidemiological approach. The model presented here is expanded to include a third option that combines the "no party preference" and third parties. The total population size, N, is assumed to remain constant. That is, for every person that enters the system, another leaves the system. In the United States, citizens who turn 18 years of age or immigrants who become naturalized citizens enter the class of eligible voters. Voters enter the system at rate μN into the eligible voter class, V. The standard convention of registering as a member of a political party when registering to vote is followed. It is assumed that the choice an eligible voter makes is influenced by coming into contact with a member of a given party and the probability the eligible voter *contracts* their ideology. That is, an eligible voter enters a political party at a per-capita rate of $\beta = pk$ where k is the average number of eligible voters a member of a political party contacts and p is the probability an eligible voter is convinced to join that party. Hence, the rate at which eligible voters become members of Political Party A, is $\beta_1 V\left(\frac{A}{N}\right)$ where $\frac{A}{N}$ is the probability of coming into contact with a member of Party A. Similarly, the rate at which people join Political Party B from V is given by $\beta_2 V\left(\frac{B}{N}\right)$, and those who choose a third party will enter C from V at a rate of $\beta_3 V\left(\frac{C}{N}\right)$. It is important to note that voter registration or party affiliation is interchangeable here with votes to a presidential candidate from a given party in that the two acts are ultimately attributed to recruitment. As stated above, the population is assumed to be constant, therefore

$$N = V + A + B + C.$$

Variables and parameters in the model are summarized in Tables 1 and 2.

V	Population of eligible voters
A	Population of Political Party A
B	Population of Political Party B
C	Population of Political Party C
N	Total Population
v	Proportion of eligible voters, V/N
a	Proportion of Political Party A, A/N
b	Proportion of Political Party B, B/N
c	Proportion of Political Party C, C/N

Table 1: Description of variables in the model.

Notably, not all people who are eligible voters register to vote. Hence, individuals leave the system with out joining any political party at a rate μV. Once having joined a party, voters may become ineligible due to inactivity, felony convictions, or death. Members of political Party A, B, and C, leave the system at rates μA, μB, and μC, respectively.

The model also accounts for the movement of registered voters between political parties. The per capita recruitment rate from one political party to another is denoted by θ_i, for $i = 1, \ldots 6$. Thus, the rate at which registered voters leave Political Party A and join Party B is $\theta_1 A\left(\frac{B}{N}\right)$. Similarly, the recruitment rate at which members of Political Party B join Political Party A is $\theta_2 B\left(\frac{A}{N}\right)$. Similar recruitment rates are defined for θ_i for $i = 3, \ldots 6$ and can be seen in Figure 1 in the diagram of the three-model system.

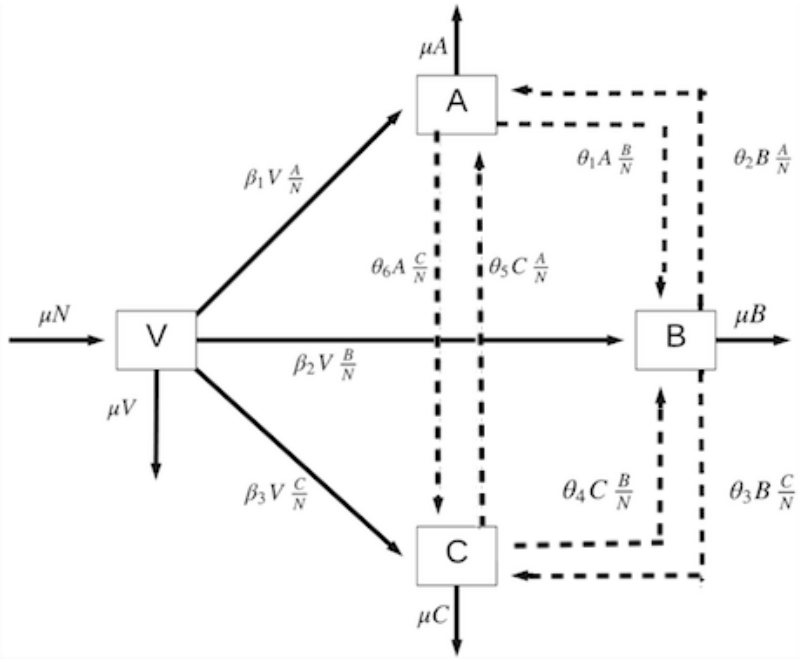

Figure 1: Diagram of the three-model system

μ	rate at which individuals enter and leave voting system
β_1	per capita recruitment rate of Party A from V
β_2	per capita recruitment rate of Party B from V
β_3	per capita recruitment rate of Party C from V
θ_1	per capita recruitment rate of Party B from Party A
θ_2	per capita recruitment rate of Party A from Party B
θ_3	per capita recruitment rate of Party C from Party B
θ_4	per capita recruitment rate of Party B from Party C
θ_5	per capita recruitment rate of Party A from Party C
θ_6	per capita recruitment rate of Party C from Party A
Ω_1	Net Shift between Party A and Party B
Ω_2	Net Shift between Party B and Party C
Ω_3	Net Shift between Party A and Party C

Table 2: Description of parameters in the model.

The solid lines in the diagram represent both the rates at which individuals enter and leave the system and the rates at which individuals initially choose their political parties. This initial choice will determine where most people stay within the system. The dashed lines represent the recruitment rates from one political party to another.

The governing equations to the model are

$$\begin{aligned}
\frac{dV}{dt} &= \mu N - \beta_1 V\left(\frac{A}{N}\right) - \beta_2 V\left(\frac{B}{N}\right) - \beta_3 V\left(\frac{C}{N}\right) - \mu V, \\
\frac{dA}{dt} &= \beta_1 V\left(\frac{A}{N}\right) + \theta_2 B\left(\frac{A}{N}\right) + \theta_5 C\left(\frac{A}{N}\right) - \theta_1 A\left(\frac{B}{N}\right) - \theta_6 A\left(\frac{C}{N}\right) - \mu A, \\
\frac{dB}{dt} &= \beta_2 V\left(\frac{B}{N}\right) + \theta_1 A\left(\frac{B}{N}\right) + \theta_4 C\left(\frac{B}{N}\right) - \theta_2 B\left(\frac{A}{N}\right) - \theta_3 B\left(\frac{C}{N}\right) - \mu B, \\
\frac{dC}{dt} &= \beta_3 V\left(\frac{C}{N}\right) + \theta_3 B\left(\frac{C}{N}\right) + \theta_6 A\left(\frac{C}{N}\right) - \theta_4 C\left(\frac{B}{N}\right) - \theta_5 C\left(\frac{A}{N}\right) - \mu C
\end{aligned} \tag{2.1}$$

where $V(0) > 0, A(0) \geq 0, B(0) \geq 0,$ and $C(0) \geq 0$.

2.1 Simplifying

To simplify the model, parameters are introduced to denote the net shift between political parties:

$$\begin{aligned}
\Omega_1 &= \theta_1 - \theta_2 \\
\Omega_2 &= \theta_3 - \theta_4 \\
\Omega_3 &= \theta_6 - \theta_5.
\end{aligned}$$

The system is rewritten to reflect proportion of populations as opposed to population size. The equation $N = V + A + B + C$ is rewritten as $1 = v + a + b + c$, where, for example, $a = \frac{A}{N}$ (See Table 1). System of equations (2.1) is rewritten as

$$\begin{aligned}
\frac{dv}{dt} &= \mu - \beta_1 va - \beta_2 vb - \beta_3 vc - \mu v \\
\frac{da}{dt} &= \beta_1 va - \Omega_1 ab - \Omega_3 ac - \mu a \\
\frac{db}{dt} &= \beta_2 vb + \Omega_1 ab - \Omega_2 bc - \mu b \\
\frac{dc}{dt} &= \beta_3 vc + \Omega_2 bc + \Omega_3 ac - \mu c.
\end{aligned} \tag{2.2}$$

The system is reduced to three differential equations by substituting $v = 1 - a - b - c$:

$$\begin{aligned}
\frac{da}{dt} &= a[\beta_1(1 - a - b - c) + \Omega_3 c - \Omega_1 b - \mu] \\
\frac{db}{dt} &= b[\beta_2(1 - a - b - c) + \Omega_1 a - \Omega_2 c - \mu] \\
\frac{dc}{dt} &= c[\beta_3(1 - a - b - c) + \Omega_2 b - \Omega_3 a - \mu].
\end{aligned} \tag{2.3}$$

3 Equilibria and Stability

The equilibrium of (2.3) are denoted by (a^*, b^*, c^*), where $a^* = A^*/N$, $b^* = B^*/N$, $c^* = C^*/N$, and (V^*, A^*, B^*, C^*) denotes the equilibrium of the unreduced system (2.1). Equilibria occur in the party-free system $E_0(0,0,0)$, single-party system $E_1(a^*,0,0)$, $E_2(0,b^*,0)$, and $E_3(0,0,c^*)$, dual-party system $E_4(a^*,b^*,0)$, $E_5(a^*,0,c^*)$, and $E_6(0,b^*,c^*)$, and in the interior case $E_7(a^*,b^*,c^*)$. We derive each equilibrium algebraically and include discussion on the stability algebraically in the dictatorship case (single-party equilibrium) and via simulation in the endemic case. The party-free equilibrium $E_0(0,0,0)$ always exists without any conditions on the associated parameters and corresponds to nonpartisan systems where no official political parties exist. Refer to [4] and references therein.

3.1 Single-party equilibrium.

We derive $E_1(a^*,0,0)$, the equilibrium in a dictatorship system. We seek $a > 0$ such that

$$\frac{da}{dt} = \beta_1(1-a-b-c)a - \Omega_1 ab - \Omega_3 ac - \mu a = 0,$$

where $b, c \equiv 0$. That is,

$$\begin{aligned}\frac{da}{dt} &= \beta_1(1-a^*-0-0)a^* - \Omega_1 a^*(0) - \Omega_3 a^*(0) - \mu a^* \\ &= \beta_1(1-a^*)a^* - \mu a^* = 0,\end{aligned}$$

which implies

$$a^* = 1 - \frac{\mu}{\beta_1}.$$

Hence, we find the equilibrium $E_1\left(1-\frac{\mu}{\beta_1},0,0\right)$. The equilibria $E_2(0,b^*,0)$, and $E_3(0,0,c^*)$ are solved using the same strategy. Note that these equilibria only exist if $\beta > \mu$.

3.2 Dual-party equilibrium.

Without the presence of a third-party, we can find the equilibrium $E_4(a^*,b^*,0)$ by solving the following system using Cramer's rule,

$$\begin{bmatrix} -\beta_1 & -(\beta_1+\Omega_1) \\ \Omega_1-\beta_2 & -\beta_2 \end{bmatrix} \begin{bmatrix} a^* \\ b^* \end{bmatrix} = \begin{bmatrix} \mu-\beta_1 \\ \mu-\beta_2 \end{bmatrix}.$$

Thus

$$E_4(a^*,b^*,0) = E_4\left(\frac{\beta_2(\beta_1-\mu)-(\beta_2-\mu)(\beta_1+\Omega_1)}{\beta_1\beta_2+(\Omega_1-\beta_2)(\beta_1+\Omega_1)}, \frac{\beta_1(\beta_2-\mu)+(\beta_1-\mu)(\Omega_1-\beta_2)}{\beta_1\beta_2+(\Omega_1-\beta_2)(\beta_1+\Omega_1)}, 0\right).$$

This is consistent with the results in [4]. Similar computations yield E_5 and E_6,

$$E_5(a^*,0,c^*) = E_5\left(\frac{\beta_3(\beta_1-\mu)+(\beta_3-\mu)(\Omega_3-\beta_1)}{\beta_1\beta_3+(\beta_3+\Omega_3)(\Omega_3-\beta_1)}, 0, \frac{\beta_1(\beta_3-\mu)-(\beta_1-\mu)(\Omega_3+\beta_3)}{\beta_1\beta_3+(\beta_3+\Omega_3)(\Omega_3-\beta_1)}\right),$$

and

$$E_6(0,b^*,c^*) = E_6\left(0, \frac{\beta_3(\beta_2-\mu)-(\beta_3-\mu)(\beta_2+\Omega_2)}{\beta_2\beta_3+(\beta_2+\Omega_2)(\Omega_2-\beta_3)}, \frac{\beta_2(\beta_3-\mu)+(\beta_2-\mu)(\Omega_2-\beta_3)}{\beta_2\beta_3+(\beta_2+\Omega_2)(\Omega_2-\beta_3)}\right).$$

3.3 Three-party equilibrium.

Finally, E_7 is the equilibrium solution of most interest. It is also found using Cramer's Rule. We express $E_7(a^*, b^*, c^*)$ as $E_7(p_1^*/q, p_2^*/q, p_3^*/q)$ where

$$\begin{aligned} q = &-\beta_1\beta_2\beta_3 - \beta_1(\beta_2 + \Omega_2)(\Omega_2 - \beta_3) - \beta_2(\Omega_3 - \beta_1)(\beta_3 + \Omega_3) - \beta_3(\beta_1 + \Omega_1)(\Omega_1 - \beta_2) \\ &- (\beta_1 + \Omega_1)(\beta_2 + \Omega_2)(\beta_3 + \Omega_3) + (\Omega_1 - \beta_2)(\Omega_2 - \beta_3)(\Omega_3 - \beta_1), \end{aligned}$$

and with

$$\begin{aligned} p_1 = &-(\beta_1 - \mu)[\beta_2\beta_3 + (\beta_2 + \Omega_2)(\Omega_2 - \beta_3)] + (\beta_2 - \mu)[\beta_3(\beta_1 + \Omega_1) - (\Omega_3 - \beta_1)(\Omega_2 - \beta_3)] \\ &- (\beta_3 - \mu)(\beta_2(\beta_1 - \Omega_3) - (\beta_1 + \Omega_1)(\beta_2 + \Omega_2)), \\ p_2 = &\beta_1[\beta_3(\mu - \beta_2) - (\beta_2 + \Omega_2)(\mu - \beta_3)] + (\Omega_1 - \beta_2)[\beta_3(\mu - \beta_1) + (\Omega_3 - \beta_1)(\mu - \beta_3)] \\ &+ (\beta_3 + \Omega_3)[(\beta_2 + \Omega_2)(\mu - \beta_1) + (\Omega_3 - \beta_1)(\mu - \beta_3)], \\ p_3 = &\beta_1[\beta_2(\mu - \beta_3) + (\mu - \beta_2)(\Omega_2 - \beta_3)] + (\Omega_1 - \beta_2)[(\beta_1 + \Omega_1)(\mu - \beta_3) + (\mu - \beta_1)(\Omega_2 - \beta_3)] \\ &+ (\beta_3 + \Omega_3)[(\beta_1 + \Omega_1)(\mu - \beta_2) - \beta_2(\mu - \beta_1)]. \end{aligned}$$

3.4 Stability Analysis.

The Jacobian of system (2.3) is given by

$$J = \begin{pmatrix} \Theta_1 & -(\Omega_1 + \beta_1)a & (\Omega_3 - \beta_1)a \\ (\Omega_1 - \beta_2)b & \Theta_2 & -(\Omega_2 + \beta_2)b \\ -(\Omega_3 + \beta_3)c & (\Omega_2 - \beta_3)c & \Theta_3 \end{pmatrix},$$

where

$$\begin{aligned} \Theta_1 &= \beta_1(1 - 2a - b - c) + \Omega_3 c - \Omega_1 b - \mu, \\ \Theta_2 &= \beta_2(1 - a - 2b - c) + \Omega_1 a - \Omega_2 c - \mu, \\ \Theta_3 &= \beta_3(1 - a - b - 2c) + \Omega_2 b - \Omega_3 a - \mu. \end{aligned}$$

We can now find the eigenvalues of J evaluated at each E_i to determine the stability. For instance, in the non-partisan system, the eigenvalues of $J(E_0(0, 0, 0))$ are given by $\lambda_1 = \beta_1 - \mu$, $\lambda_2 = \beta_2 - \mu$, and $\lambda_3 = \beta_3 - \mu$. Relative to the restriction for E_1, E_2, and E_2 to exist, namely $\beta_i > \mu$ for $i = 1, 2, 3$; we conclude that E_0 is unstable. Alternatively, the goal of this manuscript will be to understand the stability of equilibrium using a simulation approach.

3.5 Simulation approach.

Below we take a simulation approach to analyze stability of the equilibrium $E_7(a^*, b^*, c^*)$. The simulations were run using ODE solvers in the SciPy library and plotted with the Matplotlib library.

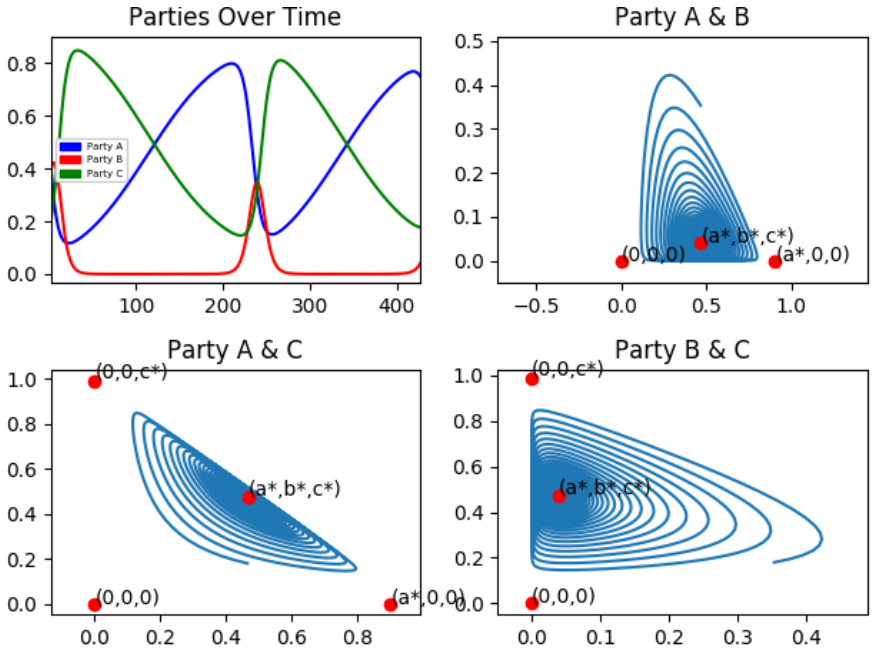

Figure 2: Three-party simulation with $\mu = 0.01$, $\beta_1 = 0.1$, $\beta_2 = 1$, $\beta_3 = 1$, $\Omega_1 = 1$, $\Omega_2 = 1$, $\Omega_3 = 0.1$

In Figure 2 the net-shift parameters are $\Omega_1 = 1.00$, $\Omega_2 = 0.10$ and $\Omega_3 = 1.00$. Hence, the net shift between between Party A and Party B is to Party A, Party C dominates in recruitment between Party A and Party C, and the net shift is to Party C between Party B and Party C.

By setting the net-shift recruitment rate between Party B and Party C low at 0.10 and having the recruitment rates between Party A and Party B, and between Party A and Party C be the same at 1.00, we are simulating a system in which two political parties are initially dominant with the third political party, namely, Party B staying close to 0. Over time, we see oscillatory behavior as the parties tend towards the endemic equilibrium. That is, there is arise in the third party. This choice in particular seemed to capture the recent pattern in which third-parties rise in American politics. Again, for our model there are only three political parties and we consider the third one being made up of many small political parties.

Over a longer simulation, the graph in the top left of Figure 2 shows how all of those parties can chip away at the two major ones as the system approaches $E7(a^*, b^*, c^*)$. The trajectory observed over time and projected in the figures labeled Party A & B, Party A & C, and Party B & C, produces asymptotic behavior towards $E7(a^*, b^*, c^*)$. This could provide insight into they dynamics that were observed in the 2016 Presidential Election. An alternate dynamic is captured in Figure 3, with different parameters. This figure shows that there are limit cycle solutions and has implications about the type of stability displayed by $E7(a^*, b^*, c^*)$.

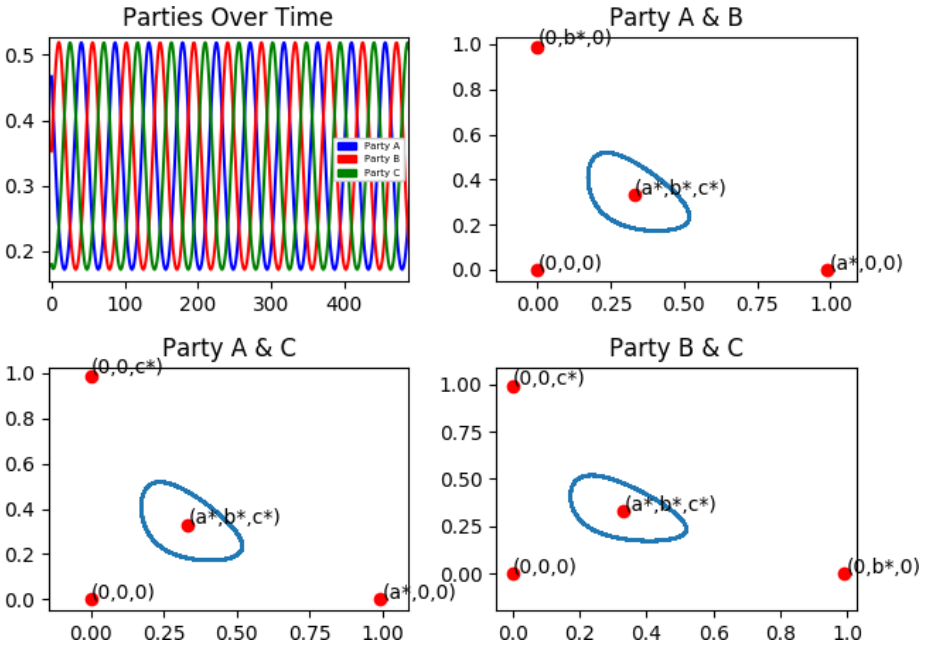

Figure 3: Three-party simulation with $\mu = .01$, $\beta_1 = 1$, $\beta_2 = 1$, $\beta_3 = 1$, $\Omega_1 = -1$, $\Omega_2 = 1$, $\Omega_3 = 1$

4 Discussion

By including an influential third party to the system we were able to study how votes can sway between the two major political parties. According to the Federal Election Commission the 2016 and the 2012 Presidential Elections had very similar voting age population size (N) with 2016 having a 0.9% increase in voting age population. The Republican party attained approximately 2 million more votes in 2016 than in 2012 and the Democratic Party lost 0.1 million votes. However, there was an estimated 7 million increase in the three voting classes. Therefore, the largest increase in population was the third party class who rose from 2 million votes to more than 8 million votes. Hillary Clinton did not visit swing states like Wisconsin, Pennsylvania, and Michigan, implying a lower recruitment rate. However, Donald Trump had a heavy recruitment strategy in these states. Interestingly, the third parties having such an increase in their population suggests they had the highest per capita recruitment from the other two parties.

5 Note to Instructors

The work in this paper was conducted during a one-year long experience with undergraduates during academic semesters with a team of two faculty research supervisors and seven undergraduates with varying previous knowledge of ODE's and programming in MATLAB and Python. The faculty approach is as follows:

1. Build a team with diverse skills; some have seen ODEs before, some have computing skills, others have only seen linear algebra and the calculus sequence,

2. Mini-lectures on MATLAB and math modeling; SIR article from MAA [5],
3. Gather voter data from different counties as well as nationally [2, 3],
4. Once students understand the two-party voter dynamical system [4], allow students to build their own models – to answer their own questions which they formulate,
5. Provide feedback as they *experiment* with their models; i.e., run numerical simulations and interpret outcomes,
6. Compare simulated results with collected data,
7. Write official reports, posters and talks for presenting; faculty period of reflection.

Expanding on point (4), the faculty mentors found that students were very passionate about this project which was conducted during the 2016-2017 academic year. This lead to much subjective writing from the students which faculty members had to channel towards mathematical reasoning. For instance, students often conjectured the motivations of the voter population before analyzing the model mathematically. Ultimately, we found that this student driven interest in the project kept the experience fruitful. One cautionary note: faculty are responsible for providing feedback so that model designs balance complexity and functionality.

The results presented in this article lead to a starting point for a future academic research experience with undergraduates focused mainly on analyzing the stability of the remaining equilibrium both analytically and via simulation. Open questions remain around any chaos present within the model, or present through the numerical methods implemented in studying the model.

Acknowledgements

The authors are grateful for the fruitful contributions with Garrett Lopez and acknowledge the conversations with Matthew Costa, Kristen Godinez, Tiffany Jenkins, and Haley Peña. Moreover, the authors recognize financial support from the California State University Channel Islands Foundation, the Brigham Young University Foundation and, Center for Undergraduate Research in Mathematics (CURM) funded by the National Science Foundation (NSF) grant #DMS-0636648 / #DMS-1148695, Preparing Undergraduates Through Mentoring Towards PhD's (PUMP) funded by a National Science Foundation grant (DMS-1247679), LSAMP supported by the National Science Foundation under Grant No. HRD-1302873 and the CSU Chancellor's Office.

References

[1] Goldberg A. Baldassarri, D. Neither ideologues nor agnostics: Alternative voters' belief system in an age of partisan politics. 120(1):45–95, 2014.

[2] Federal Election Commission. Federal elections 2012: Election results for the U.S. president, the U.S. senate and the U.S. house of representatives, 2012. https://transition.fec.gov/pubrec/fe2012/federalelections2012.pdf, retrieved December 7, 2015.

[3] Federal Election Commission. Official 2016 presidential general election results, Dec. 2017. https://transition.fec.gov/pubrec/fe2016/federalelections2016.pdf, retrieved February 12, 2018.

[4] A.K. Misra. A simple mathematical model for the spread of two political parties. 17:343–354, 07 2012.

[5] Moore L. Smith, D. The sir model for spread of disease—the differential equation model. *JOMA*, 2004. https://www.maa.org/press/periodicals/loci/joma/the-sir-model-for-spread-of-disease-the-differential-equation-model.

[6] Samantha Smith. A deep dive into party affiliation: Sharp differences by race, gender, generation, education, April 7, 2015. Pew Research Center, http://www.people-press.org/2015/04/07/a-deep-dive-into-party-affiliation/.

Consensus Building by Committed Agents

William W. Hackborn
University of Alberta, Augustana Campus

Tetiana Reznychenko
Vasyl` Stus Donetsk National University

Yihang Zhang
East China Normal University

Keywords: Social dynamics, committed agents, bifurcations, center manifold
Manuscript received on October 3, 2018; published on February 13, 2019.

Abstract: One of the most striking features of our time is the polarization, nationally and globally, in politics and religion. How can a society achieve anything, let alone justice, when there are fundamental disagreements about what problems a society needs to address, about priorities among those problems, and no consensus on what constitutes justice itself? This paper explores a model for building social consensus in an ideologically divided community. Our model has three states: two of these represent ideological extremes while the third state designates a moderate position that blends aspects of the two extremes. Each individual in the community is in one of these three states. A constant fraction of individuals are *committed agents* dedicated to the third, moderate state, while all other moderates and those from either extreme are uncommitted. The states of the uncommitted may change as they interact, according to prescribed rules, at each time step with their neighbors; the *committed agents*, however, cannot be moved from their moderate position, although they can influence neighbors. Our main objective is to investigate how the proportion of committed agents affects the large-scale dynamics of the population: in other words, we examine the special role played by those committed to embracing both sides of an ideological divide. A secondary but equally important goal is to gently introduce important dynamical systems concepts in a natural setting. Finally, we briefly outline a model with different interaction rules, a fourth state representing those who loathe the other three states, and agents who may be committed to any one of the four states.

1 Introduction

Never doubt that a small group of thoughtful, committed citizens can change the world. Indeed, it is the only thing that ever has.

— Attributed to Margaret Mead in [11, p. 158]

How can a society build tolerance, respect, and consensus when it is deeply divided along political or religious lines? It can't, we believe, because deep divisions entail, by their nature, intolerance and disrespect between those on opposite sides, and consensus cannot occur in that environment. This paper examines how social consensus might be built in a community sharply divided by two ideological extremes, denoted A and B, representing opinions or beliefs that are oppositional or opposite. In the American political context, some examples might be Democrat and Republican or pro-choice and pro-life. Some examples in the global religious context might be Christian and non-Christian, Muslim and non-Muslim, or even Christian and Muslim. This latter binary ignores other faiths and the fact that Christians and Muslims live amicably in many parts of the world, but it is a semblance of the kind of reality that exists in some communities and to which our model might be applied. Similar statements can be made about the Democrat-Republican binary and other conceivable binaries. In this paper, we assume further that the adherents of A and B rarely examine their own viewpoint and seldom engage in productive dialogue with those who hold the opposing viewpoint. Of course, many Democrats and Republicans think critically about their own opinions and engage in polite and reasoned dialogue with those who hold differing ones. Nevertheless, hard-line Democrat and Republican voters are prevalent in many electoral districts, just as fundamentalist Christians and Muslims are common in various countries, and such extremists often attempt to impose their collective wills on those who hold different views. We make the plausible assumption in this paper (and make no attempt to justify it from the sociology or political science literature) that the polarization in public discourse resulting from ideological extremism obstructs efforts to identify and collectively address inequities in a society and, in some cases, may contribute substantially to those inequities.

Our model is a variation of the *binary agreement model* of Xie et al. [13], which is in turn a two-word version of the naming game [2]. Players in this game may use word A to name an object, word B, or both words, {A,B} (abbreviated as AB), and interactions between a speaker and a listener can cause their name(s) for the object to change according to a prescribed set of rules. Similarly in [13], agents may hold opinion A, opinion B, or opinion AB, and their opinions may change via speaker-listener interactions exactly as in the two-word naming game. However, [13] adds a fourth kind of agent committed to opinion A: *committed agents* cannot be swayed from their opinion but may influence other agents to change their opinions according to the given rules.

The work in [13] is a kind of *mathematical sociology*, also called *social physics*, a subject (born in the mid-twentieth century) that employs mathematical tools, such as graph theory and differential equations, and models often drawn from physics (see Galam [5] for examples) to understand social behavior. Xie et al. [13] provide an informative discussion of the background literature relevant for their work. Like others, they regard the agents in their model as the nodes of a *graph* (also known as a *network*) whose edges indicate relationships conducive to speaker-listener interactions. They simulate social interactions on a finite graph with N nodes; in each unit time step of the simulation, each of the N agents represented in the graph interacts with one of its neighbors, chosen at random (the graph is assumed to be connected, so each node must have at least one neighbor). The main analytical tool used in [13], however, is a limiting case in which $N \to \infty$, called

the *mean-field approximation*[1]. In this limiting case, changes in opinion states can be modeled by a system of ordinary differential equations (ODEs), the *mean-field equations*. The mean-field approximation is often used (usually without much explanation) in a first course on ODEs to model, for example, the interaction of predator-prey populations and chemical reactions that obey the *law of mass action*: it justifies the assumption that the probability of, say, a predator meeting a prey or a molecule of one kind colliding with that of another is proportional to the size of the subpopulations to which they belong.

The most important finding of [13] is the tipping point associated with the proportion of the population committed to belief A: let p be this proportion, so $1-p$ is the proportion of the uncommitted population free to adopt beliefs A, B, or AB in a mutable way as they interact with other agents, some of whom are committed to A. Xie et al. [13] found that when p exceeds a critical value $p_c \approx 0.0979$ (a root of a cubic polynomial), the mean-field equations have only one fixed point, a stable (attracting) *consensus state* in which all uncommitted agents adopt belief A. When $p < p_c$, there are two additional fixed points, a stable non-consensus state and an unstable saddle point; as $p \to p_c^-$, these two fixed points approach and annihilate each other (in what is known as a *saddle-node bifurcation*), leaving only the attracting consensus state. Hence, a sufficient proportion of agents committed to belief A tips the entire population to eventually adopt that belief.

The work in [13] has inspired much subsequent research. Marvel et al. [8], for example, consider models with agents committed to opinion A and others free to adopt A, B, or AB, as in [13], but for which opinion dynamics are governed by simpler rules (e.g. speakers never change their opinions); they examine seven such models, attempting to find conditions that allow the mean-field equilibrium AB subpopulation (regarded as moderates) to thrive rather than be destroyed by those committed to A (seen as revolutionaries). Of these seven models, only one involving an external stimulus (such as a media campaign) that discourages the extremism of opinions A and B permits the equilibrium AB population to thrive. As another example, Verma et al. [12] extend the naming game dynamics used in [13] to the case where there are two subpopulations of committed agents, some committed to extreme A and others to B, in addition to agents free to believe A, B, or AB; they show that in some cases a minority of *zealots* committed to one extreme can win over a majority of the population to their side against a larger group of zealots committed to the other extreme, while in other cases neither extreme wins a majority.

In this paper, as in [8], we want to discourage extremism and encourage an increase in the size of the equilibrium AB subpopulation. This is what we mean by *consensus building*, as opinion AB is a moderate, "consensus" state even at the individual level; by contrast, we do not regard a situation in which the entire population adopts an extreme viewpoint, A or B, as the kind of harmonious consensus (conducive to social justice) that we'd like to achieve. Viewpoint AB represents for us the position of those who are able to understand and critically weigh the merits of both A and B. In the American political realm, AB

[1]The mean-field approximation used here and in [13] involves a *complete* graph, i.e. there is an edge connecting each node to every other node for a total of $\binom{N}{2} = N(N-1)/2$ edges, and each edge is equally likely to be chosen at random. Because there are N social interactions per unit time step, a discrete-time simulation becomes continuous as $N \to \infty$. See [7, pp. 127-130] for mean-field approximations in the context of social network analysis. An idea of how mean-field theory is used in physics can be found at Wikipedia permalink https://en.wikipedia.org/w/index.php?title=Mean_field_theory&oldid=855120670

might represent the viewpoint of an independent or, more generally, anyone who does not vote along party lines but instead casts each ballot only after a careful examination of candidates and ideas; AB might also represent a third, *centrist* political party, as in [9] where it is denoted by C. The approach used here to encourage agents to adopt opinion AB is to assume that a proportion of the total population is committed to AB (and that no agents are committed to A or B). After an extensive search of the literature, we found [9] to be the only other paper that has agents committed to the moderate state situated between extremes A and B. Mobilia [9] uses what we call a *binary persuasion* model (different from our *binary consensus* model, described below) to represent interactions between voters supporting three parties, A, B, and C (the centrist party to which some agents are committed); in his model, supporters of party A and those of party B never interact, but a supporter of A or B might persuade a supporter of C to join their side, and similarly a supporter of C might persuade a supporter of A or B to join side C, but supporters of C are assumed to have less persuasive power than those who support A or B. Therefore, Mobilia describes his model as a struggle between the commitment of those devoted to C and the greater persuasiveness of those who support A and B.

Section 2 presents and analyses the mean-field equations for a *binary consensus* (BC) model, ending with a brief comparison between our results and those of [9]. Section 3 introduces a *binary persuasion* (BP) model, with far more parameters than our BC model. After giving hints about the most significant results of the BP model, we leave the completion of its analysis to the reader (along with a promise to reveal the missing analysis on request). Finally, we make a few final observations and draw some conclusions in Section 4. As we put the finishing touches on this paper, the confirmation hearings for Brett Kavanaugh to become an Associate Justice of the Supreme Court of the United States are taking place. We offer this as an extreme example of the polarization that seems to have gripped American politics and the kind of dysfunction, posturing, and very partisan politics it has produced at the highest levels of that nation's government. In our opinion, social justice suffers in such a bitterly divided country, partly because people often fail to notice suffering when they're fighting a perceived enemy. It is similarly clear from history that religious minorities often suffer from injustice in regions sharply polarized along religious lines. Can those who resolutely straddle both sides of an ideological divide help to build the consensus that seems necessary for communities to move in positive directions? That is the question we explore in this paper.

2 A Binary Consensus Model

> *[T]he test of a first-rate intelligence is the ability to hold two opposed ideas in the mind at the same time, and still retain the ability to function.*
>
> — F. Scott Fitzgerald, from an *Esquire* magazine essay [4, p. 41]

The interaction dynamics for our binary consensus (BC) model are given in Table 1. These rules differ only slightly from those in [13]. The only differences lie in rows 2 and 4 of the table: the results after interaction for the corresponding rows in [13] are A–AB and B–AB, respectively, and 1 is the relative probability of these interactions in [13] compared

to λ in our model, where $0 < \lambda < 1$. In this way, we have made the probability of these two interactions relatively low, as it seems fairly unlikely that transformative conversations will occur between a speaker and listener on opposing ideological sides – imagine, for example, the likelihood of productive dialogue between hard-nosed Republicans and Democrats. We have also chosen the outcomes of these two interactions so that both speaker and listener revise their positions and agree afterwards. This seems more true for the kind of two-way conversation (rather than an alternating one-way argument) that might actually transform hard-line opponents. Notice that the speaker and listener agree after their interaction in all rows of Table 1 and that the opinion of the speaker changes in six of the twelve rows. This is why we call these rules a *binary consensus* model: the speaker and listener come to a consensus (on A, B, or AB) at the end of each transformative interaction.

In most previous studies (e.g. [13] and [8]), the only committed agents are those who hold opinion A. In our BC model, however, committed agents must hold opinion AB. Let

Dynamics of the Binary Consensus Model		
Before Interaction	After Interaction	Relative Probability
$A \xrightarrow{A} A$	A – A	not applicable
$A \xrightarrow{A} B$	AB – AB	λ
$A \xrightarrow{A} AB$	A – A	1
$B \xrightarrow{B} A$	AB – AB	λ
$B \xrightarrow{B} B$	B – B	not applicable
$B \xrightarrow{B} AB$	B – B	1
$AB \xrightarrow{A} A$	A – A	$\frac{1}{2}$
$AB \xrightarrow{B} A$	AB – AB	$\frac{1}{2}$
$AB \xrightarrow{A} B$	AB – AB	$\frac{1}{2}$
$AB \xrightarrow{B} B$	B – B	$\frac{1}{2}$
$AB \xrightarrow{A} AB$	A – A	$\frac{1}{2}$
$AB \xrightarrow{B} AB$	B – B	$\frac{1}{2}$

Table 1: Speaker-Listener interaction rules for our binary consensus model. The speaker may hold any one of three opinions (A, B, and AB), and there is an equal chance of an AB speaker voicing opinions A or B. The *Before Interaction* column indicates the speaker, listener, and the opinion voiced (above the arrow). The *After Interaction* column shows the opinions of speaker and listener after their conversation: note that the opinion of the speaker may change. The final column indicates the relative probability of a transformative interaction per unit time; conversations for which this probability is *not applicable* (as no transformation occurs) are listed for completeness. Note that committed adherents of AB *cannot* be moved from their opinion by their interactions with others, but these interactions *can* change the opinions of others.

q, with $0 \leq q < 1$, be a constant denoting the proportion of all agents committed to AB, and x, y, z be the proportions of agents who hold (but are not committed to) opinions A, B, AB, respectively, at a moment t in time. So, x, y, and z all lie in the interval $[0,\ 1]$, and

$$x + y + z + q = 1\,. \tag{2.1}$$

Consequently, the variables x and y must lie in the triangular region Λ defined by

$$\Lambda = \{\,(x, y) \mid x \geq 0\,,\ y \geq 0\,,\ x + y \leq 1 - q\,\}\,. \tag{2.2}$$

See Figure 1. The last inequality in (2.2) is implied by equation (2.1) with $z \geq 0$.

Now, using the interaction rules in Table 1 and the fact that the mean-field rate of a particular interaction is proportional to the fractions of agents involved in that interaction, we find the mean-field equations to be

$$\begin{aligned} \frac{dx}{dt} &= xz + \tfrac{1}{2}zx - \tfrac{1}{2}zx - \tfrac{1}{2}qx + 2\big(\tfrac{1}{2}z^2\big) + \tfrac{1}{2}qz + \tfrac{1}{2}zq - \lambda xy - \lambda yx\,, \\ \frac{dy}{dt} &= yz + \tfrac{1}{2}zy - \tfrac{1}{2}zy - \tfrac{1}{2}qy + 2\big(\tfrac{1}{2}z^2\big) + \tfrac{1}{2}qz + \tfrac{1}{2}zq - \lambda yx - \lambda xy\,. \end{aligned} \tag{2.3}$$

Each term in system (2.3) corresponds to one row in Table 1. The terms involving q correspond to interactions between agents committed to AB and other agents; committed agents can be involved in interactions that transform other agents but cannot be transformed themselves. Note also that there is no need to include an equation for dz/dt in (2.3), as $z = 1 - x - y - q$ from equation (2.1). Denoting the right-hand sides of equations (2.3)

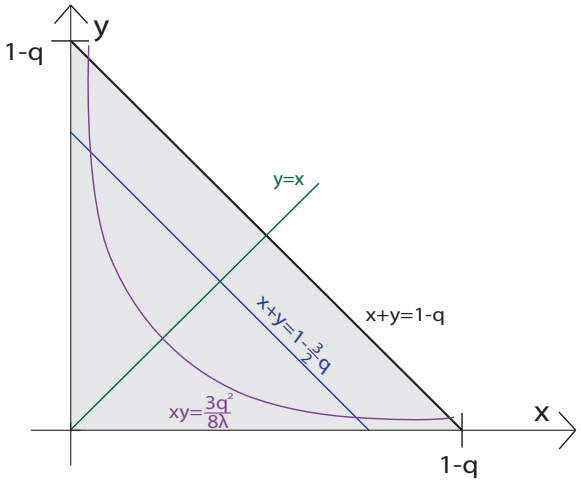

Figure 1: The flow domain Λ in the phase plane associated with our binary consensus model: a triangle bounded by $x = 0$, $y = 0$, and $x + y = 1 - q$. One fixed point in the flow domain lies on the line of symmetry, $y = x$, and two more are placed symmetrically about this line on the hyperbola $xy = 3q^2/(8\lambda)$ when $0 < q < 2/(3 + \sqrt{6/\lambda})$.

by $f(x,y)$ and $g(x,y)$ and eliminating z using (2.1), we find

$$\begin{aligned}\frac{dx}{dt} &= f(x,y) = xz - \tfrac{1}{2}qx + z(z+q) - 2\lambda xy \\ &= 1 - q - (1+\tfrac{1}{2}q)x - (2-q)y + y^2 + (1-2\lambda)xy\,, \qquad (2.4a)\\ \frac{dy}{dt} &= g(x,y) = yz - \tfrac{1}{2}qy + z(z+q) - 2\lambda xy \\ &= 1 - q - (1+\tfrac{1}{2}q)y - (2-q)x + x^2 + (1-2\lambda)xy\,. \qquad (2.4b)\end{aligned}$$

By examining the component of the vector field $\langle f(x,y),\ g(x,y)\rangle$ in the inward-normal direction on each of the boundary lines of the domain Λ and, separately, the direction of this field at each corner point of Λ, we have verified that none of the values of $\langle f(x,y),\ g(x,y)\rangle$ on the boundary of Λ point to the exterior of Λ. Therefore, the flow associated with system (2.4) is trapped within Λ. Now, subtracting (2.4b) from (2.4a) to exploit symmetry yields

$$\frac{d(x-y)}{dt} = -(x-y)(x+y+\tfrac{3}{2}q-1)\,, \qquad (2.5)$$

which reveals that the line of symmetry, $y=x$, is an invariant set of the flow; see [6, p. 33] for more about this concept. We observe from (2.5) that fixed points[2] of the flow (at which f and g vanish) can lie only on the lines $y=x$ or $x+y=1-\frac{3}{2}q$; see Figure 1. Consider the line $x+y=1-\frac{3}{2}q$: it lies in the interior of the flow domain Λ when $0<q<\frac{2}{3}$, and (2.1) implies $z=\frac{1}{2}q$ on this line. But, using (2.4a), $f(x,y)=0$ and $z=\frac{1}{2}q$ imply $xy=3q^2/(8\lambda)$, the equation of a hyperbola. Hence, two fixed points (x,y) lie at the intersections of this hyperbola and the line $x+y=1-\frac{3}{2}q$, where

$$x = \frac{2-3q\pm\sqrt{(2-3q)^2-6q^2/\lambda}}{4}\,,\quad y=\frac{3q^2}{8\lambda x}\,;\quad 0<q<\frac{2}{3+\sqrt{6/\lambda}}\,. \qquad (2.6)$$

These fixed points (x,y), contingent on the intersections that define them, exist when q satisfies the condition in (2.6). If they exist, they are mirror images of each other in the line of symmetry $y=x$, as seen in Figure 1. On the line of symmetry itself,

$$\frac{dx}{dt} = f(x,x) = 2(1-\lambda)x^2 - \tfrac{1}{2}(6-q)x + 1 - q, \qquad (2.7)$$

using equation (2.4a). It follows that the flow has two fixed points (x,x) corresponding to each root x of the quadratic $f(x,x)$ in (2.7). Regarding the invariant set $y=x$ as a phase line, the smaller (larger) root corresponds to a stable[3] (unstable, respectively) fixed point; in other words, the line $y=x$ is a stable (unstable) manifold of the fixed point corresponding to the smaller (larger, respectively) root; see [6, pp. 12-16]. Naming the smaller root x_0,

$$x_0 = \frac{1}{8(1-\lambda)}\left[6-q-\sqrt{(6-q)^2-32(1-\lambda)(1-q)}\right]. \qquad (2.8)$$

[2] In this paper, fixed points are positions at which the right-hand sides of each equation in an autonomous system of ODEs vanishes. They are also known as equilibria or steady-state solutions.

[3] Unless otherwise indicated, the term *stable* means *locally asymptotically stable*, and *unstable* means *not* stable. See [6, p. 3] for more information.

To examine the behavior of x_0 as $\lambda \longrightarrow 1^-$, we find

$$x_0 = \frac{2(1-q)}{6-q} + \frac{16(1-\lambda)(1-q)^2}{(6-q)^3} + \frac{256(1-\lambda)^2(1-q)^3}{(6-q)^5} + O(r^4), \tag{2.9}$$

where $r = 32(1-\lambda)(1-q)/(6-q)^2$, when we write the square root in equation (2.8) as $(6-q)(1-r)^{1/2}$ and use the binomial series. The infinite series indicated in (2.9) converges in all valid cases, since $0 < r < \frac{8}{9}(1-\lambda) < 1$ for $0 < q < 1$ and $0 < \lambda < 1$; its first term is independent of λ and approaches $\frac{1}{3}$ as $q \longrightarrow 0^+$.

Clearly $x_0 > 0$ from (2.8) or (2.9), and $f(x,x) = -\frac{1}{2}qx - 2\lambda x^2 < 0$ on the boundary line $x + y = 1 - q$ (on which $z = 0$) from (2.4a). Hence, the fixed points (x,x) associated with the two roots of $f(x,x)$ in equation (2.7) straddle the line $x + y = 1 - q$: the fixed point associated with the smaller root x_0 lies inside the flow domain Λ and the one associated with the larger root lies outside. We already know that the line $y = x$ is a stable manifold of the fixed point (x_0, x_0). To examine the two-dimensional stability of this point, first observe from (2.5) that trajectories close to the line $y = x$ converge towards it as time proceeds when $x + y > 1 - \frac{3}{2}q$ and diverge away from it when $x + y < 1 - \frac{3}{2}q$. To see this more clearly, we choose coordinates (ξ, η) for which ξ and η are constant along lines parallel to the lines $y = x$ and $x + y = 1 - \frac{3}{2}q$, respectively, and such that ξ and η vanish on these latter lines. Coordinates of this kind, together with their inverse, are given below:

$$\xi = x - y\,, \qquad x = \tfrac{1}{2}(\xi + \eta - \tfrac{3}{2}q + 1)\,, \tag{2.10a}$$

$$\eta = x + y + \tfrac{3}{2}q - 1\,, \qquad y = \tfrac{1}{2}(\eta - \xi - \tfrac{3}{2}q + 1)\,. \tag{2.10b}$$

Using (2.10), system (2.4) becomes

$$\frac{d\xi}{dt} = f(x,y) - g(x,y) = F(\xi,\eta) = -\xi\eta\,, \tag{2.11a}$$

$$\begin{aligned}\frac{d\eta}{dt} &= f(x,y) + g(x,y) = G(\xi,\eta) \\ &= \left[(3q-2)\lambda - \tfrac{5}{2}q - 1\right]\eta + (1-\lambda)\eta^2 + \lambda\xi^2 + K\,,\end{aligned} \tag{2.11b}$$

where $F(\xi,\eta)$ and $G(\xi,\eta)$ denote the right-hand sides of equations (2.11), and

$$K = \tfrac{1}{4}\left[6q^2 - \lambda(2-3q)^2\right]\,. \tag{2.12}$$

A Jacobian matrix represents the linearization of a vector field near a point. For the field $\langle F(\xi,\eta),\, G(\xi,\eta)\rangle$, the Jacobian is

$$J(\xi,\eta) = \begin{pmatrix} \frac{\partial F}{\partial \xi} & \frac{\partial F}{\partial \eta} \\ \frac{\partial G}{\partial \xi} & \frac{\partial G}{\partial \eta} \end{pmatrix} = \begin{pmatrix} -\eta & -\xi \\ 2\lambda\xi & (3q-2)\lambda - \frac{5}{2}q - 1 + 2(1-\lambda)\eta \end{pmatrix}. \tag{2.13}$$

Let η_0 be the η coordinate of the fixed point on the line of symmetry $\xi = 0$ in the flow region Λ defined by (2.2). The (x,y) coordinates of this fixed point are (x_0, x_0), and η_0 can therefore be determined from (2.8) and (2.10b). However, it is better for our purposes to use the fact that $G(0,\eta_0) = 0$: in this way, equation (2.11b) yields

$$\eta_0 = \frac{-C - \sqrt{C^2 - 4(1-\lambda)K}}{2(1-\lambda)}\,, \quad C = -(2-3q)\lambda - \tfrac{5}{2}q - 1\,, \tag{2.14}$$

where K is given in (2.12). On the line $\xi = 0$, the Jacobian matrix in (2.13) is diagonal; the eigenvalues of $J(0, \eta_0)$, namely $-\eta_0$ and $C + 2(1-\lambda)\eta_0$ with C as in (2.14), lie on its main diagonal and correspond to, respectively, eigenvectors parallel to the lines $\eta = 0$ (i.e. $x + y = 1 - \frac{3}{2}q$) and $\xi = 0$ (i.e. $y = x$, the line of symmetry). From an earlier result (i.e. that the line $\xi = 0$ is a stable manifold of the fixed point on this line in the region Λ), we know that the latter eigenvalue must be negative, but it is easy to verify this directly: from the first equation in (2.10b), we see that the boundary line $x + y = 1 - q$ coincides with $\eta = \frac{1}{2}q$, so $\eta \leq \frac{1}{2}q$ in the flow domain Λ, and thus

$$C + 2(1-\lambda)\eta_0 \leq C + 2(1-\lambda)\tfrac{1}{2}q = -2\lambda(1-q) - \tfrac{3}{2}q - 1 < -1\,, \tag{2.15}$$

using the expression for C in (2.14). The sign of the other eigenvalue, $-\eta_0$, is opposite to that of η_0 itself. Since $C < 0$, as seen in (2.15), it follows from (2.14) that $\eta_0 > 0$ if and only if $K > 0$, and the equivalencies below can then be inferred from (2.12):

$$\eta_0 > 0 \quad \Leftrightarrow \quad K > 0 \quad \Leftrightarrow \quad \lambda < \frac{6q^2}{(2-3q)^2} \quad \Leftrightarrow \quad q > q_c = \frac{2}{3 + \sqrt{6/\lambda}}\,. \tag{2.16}$$

For planar flows like those associated with systems (2.4) and (2.11) (see [6, pp. 42-60] for details on such flows), a fixed point is stable if the real parts of both eigenvalues of its Jacobian matrix at that point are negative. If its eigenvalues are real, then it is a (stable) *sink node* if both eigenvalues are negative, an (unstable) *source node* if both are positive, and an (unstable) *saddle* if they have different signs; if its eigenvalues are complex conjugates, it is a *spiral* sink or source, respectively, if the sign of their real parts is negative or positive. Hence, the fixed point $(\xi, \eta) = (0, \eta_0)$ is a sink node when $q_c < q < 1$ because, according to (2.16), $\eta_0 > 0$ in this case and so the eigenvalue $-\eta_0$ is negative; equivalently, it is a sink node when λ satisfies the condition in (2.16) (in addition to the earlier requirement that $0 < \lambda < 1$). When $0 < q < q_c$, however, the fixed point $(\xi, \eta) = (0, \eta_0)$ is a saddle, as the eigenvalue $-\eta_0$ is positive, and two other fixed points (x, y) given in (2.6) also exist in this case. Figure 2 depicts these interesting flow dynamics in the phase plane via two cases, one for $q < q_c$ and the other for $q > q_c$.

To investigate further the emergence of the two fixed points in (2.6) from the fixed point $(\xi, \eta) = (0, \eta_0)$ as q decreases through q_c (holding λ constant), we employ the *center manifold* techniques of Guckenheimer and Holmes [6], pp. 123-138. A center manifold is an invariant set tangent to the eigenspace corresponding to eigenvalues with zero real parts of the Jacobian matrix at a fixed point. Our flow has a center manifold tangent to the line $\eta = \eta_0$ at the fixed point $(\xi, \eta) = (0, \eta_0)$ when $q = q_c$, or equivalently, using (2.16), when $\eta_0 = 0$ or $K = 0$. This center manifold becomes an unstable manifold of fixed point $(0, \eta_0)$ if $0 < q < q_c$ (when $\eta_0 < 0$) and is an invariant subset of the stable manifold of point $(0, \eta_0)$ if $q_c < q < 1$ (when $\eta_0 > 0$), as we have seen. Following [6, p. 130 ff.], we approximate the invariant manifold tangent to the line $\eta = \eta_0$ at the fixed point $(0, \eta_0)$ by

$$\eta = h(\xi) = a + b\xi^2 + O(\xi^4)\,. \tag{2.17}$$

Note that odd powers of ξ need not be included in (2.17), owing to symmetry about the axis $\xi = 0$. The technique for finding the unknown coefficients a and b in (2.17) first

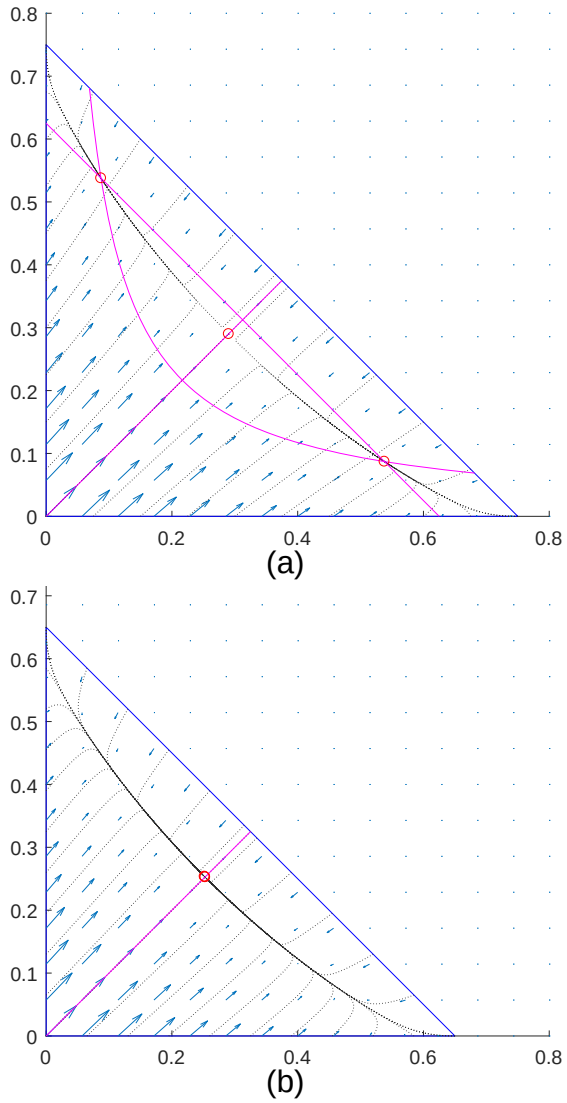

Figure 2: The phase plane flow for two cases of our binary consensus model showing fixed points (circles, red online), some trajectories (dotted), and the direction field (blue online). (a) $q = 0.25,\ \lambda = 0.5$: a fixed point (a saddle) exists on the line of symmetry, $y = x$, connected via its unstable manifold (clearly visible) to two fixed points (sink nodes) lying at the intersections of the line $x + y = 1 - \frac{3}{2}q$ and the hyperbola $xy = 3q^2/(8\lambda)$ (violet online). (b) $q = 0.35,\ \lambda = 0.5$: only one fixed point (a sink node) lies on the line $y = x$. A pitchfork bifurcation occurs at $q = q_c$, where $q_c = 2/(3 + \sqrt{6/\lambda})$; $q_c \approx 0.3094$ for $\lambda = 0.5$.

involves differentiating (2.17) with respect to t, substituting the expression for $d\xi/dt$ in equation (2.11a) into the result, and using (2.17) again. This produces

$$\frac{d\eta}{dt} = \frac{dh}{d\xi}\frac{d\xi}{dt} = -\frac{dh}{d\xi}\xi\eta = -\xi\frac{dh}{d\xi}h(\xi) = -\xi\left[2b\xi + O(\xi^2)\right]\left[a + b\xi^2 + O(\xi^4)\right]\ . \qquad (2.18)$$

However, we obtain another expression for $d\eta/dt$ by combining (2.11b) and (2.17):

$$\begin{aligned}\frac{d\eta}{dt} &= Ch(\xi) + (1-\lambda)\left[h(\xi)\right]^2 + \lambda\xi^2 + K \\ &= C\left[a + b\xi^2 + O(\xi^4)\right] + (1-\lambda)\left[a + b\xi^2 + O(\xi^4)\right]^2 + \lambda\xi^2 + K\,, \end{aligned} \tag{2.19}$$

where K and C are given in (2.12) and (2.14). Equating the coefficients of corresponding powers of ξ in (2.18) and (2.19) yields

$$a = \eta_0\,, \quad b = \frac{\lambda}{(2-3q)\lambda + \frac{5}{2}q + 1 + (2\lambda - 4)\eta_0}\,, \tag{2.20}$$

with η_0 as in (2.14). The value of a in (2.20) is exactly what we would expect from (2.17). Furthermore, in the same way as we proved the inequality in (2.15) using the fact that $\eta \le \frac{1}{2}q$ in the flow domain Λ, we can show that the denominator of b in (2.20) is bounded below by $2\lambda(1-q) + \frac{1}{2}q + 1 > 1$. So $0 < b < \lambda$, and the resulting concavity in the curve described by (2.17) is evident in Figure 2.

Although the manifold tangent to the line $\eta = \eta_0$ at the fixed point $(\xi, \eta) = (0, \eta_0)$, as given in (2.17), is a center manifold of system (2.11) only if $q = q_c$ (when $K = 0$ and $\eta_0 = 0$), Guckenheimer and Holmes [6], p. 134 point out that it can be regarded as a "family of center manifolds" parametrized by K within the center manifold of a larger system that includes the equation $\frac{dK}{dt} = 0$ (which has its own zero eigenvalue) in addition to system (2.11). Provided that K, ξ, and η are sufficiently close to zero, the power series in (2.17) approximates this family of center manifolds that vary with K via the coefficients a and b in (2.20), which depend on η_0 and thus K due to (2.14). Since this family is associated with the eigenvalue $-\eta_0$, which is close to zero and therefore associated with much *slower* flow dynamics than those associated with the strongly negative eigenvalue $C + 2(1-\lambda)\eta_0$, the local evolution of the flow described by system (2.11) can be reduced to what happens on this family; the slow dynamics implied by the fact that eigenvalue $-\eta_0 \approx 0$ also explains why these center manifolds are so visible in Figure 2. The following equation, obtained by substituting η in (2.17) into (2.11a) and using $a = \eta_0$ in (2.20), thus captures the local evolution (i.e. when ξ and η are sufficiently close to zero, and q is sufficiently close to q_c) of the flow projected onto the family of center manifolds:

$$\frac{d\xi}{dt} = -\xi\left[\eta_0 + b\xi^2 + O(\xi^4)\right]\,. \tag{2.21}$$

Equation (2.21) represents a *pitchfork bifurcation* [6, pp. 145-150] at $q = q_c$. If $q > q_c$ then $\eta_0 > 0$ from (2.16), and so the expression $\eta_0 + b\xi^2 + O(\xi^4)$ in (2.21) is positive for sufficiently small ξ values since $b > 0$; in this case, (2.21) has an evidently stable fixed point at $\xi = 0$; note that $\eta_0 = 0$ when $q = q_c$, and so this fixed point is stable, but only marginally so, in this case too. However, if $q < q_c$ then $\eta_0 < 0$, and the right-hand side of (2.21) vanishes when $\xi \approx \pm\sqrt{-\eta_0/b}$; these two ξ values are stable fixed points of (2.21) in this case and $\xi = 0$ is unstable. This shows that, as q decreases through q_c (holding λ constant), the sink node at $(\xi, \eta) = (0, \eta_0)$ in system (2.11) becomes a saddle and two new sink nodes emerge from it.

Our analysis of the flow associated with system (2.11) [or equivalently, system (2.4)] will be complete after we employ one more important tool: the divergence of the flow

field, $\mathrm{div}\langle F(\xi,\eta), G(\xi,\eta)\rangle = \frac{\partial F}{\partial \xi} + \frac{\partial G}{\partial \eta}$, which is identical to the trace of the Jacobian (2.13). Using the fact that $\eta \leq \frac{1}{2}q$ in the flow region Λ, as seen earlier, and that $\eta \geq \frac{3}{2}q - 1$, from the first equation in (2.10b) with $(x, y) = (0, 0)$, it is easy to show from (2.13) that $\mathrm{div}\langle F(\xi,\eta), G(\xi,\eta)\rangle \leq -2q - 1 < -1$ on Λ. Bendixson's Criterion [6, p. 44] can thus be used to infer that the flow has no closed orbits. This indicates that the flow is characterized by the pitchfork bifurcation and fixed points we have examined above. Note that, although our analysis of the bifurcation is necessarily localized to values of q near q_c, the absence of closed orbits and existence of the saddle at point $(0, \eta_0)$ for all $0 < q < q_c$ indicate (and would be key parts of a rigorous proof) that the two fixed points (x, y) given in (2.6) persist as sink nodes for all $0 < q < q_c$. This is supported by computations of the trace $T = \mathrm{trace}[J(\xi,\eta)]$, the determinant $D = \det[J(\xi,\eta)]$, and the discriminant $T^2 - 4D$ at numerous such points (x, y) [associated with (ξ,η) via (2.10)] using the fact that the eigenvalues of $J(\xi,\eta)$ are real and negative if $T < 0$, $D > 0$, and $T^2 - 4D > 0$.

We are now in a position to summarize the results of our binary consensus model. In the event that $q \geq q_c$, there is only one fixed point, $(x, y) = (x_0, x_0)$, a global attractor to which all flow trajectories are drawn. Moreover, it is clear from equation (2.9) that $x_0 \to 0^+$ monotonically as $q \to 1^-$ (while holding λ constant). But equation (2.1) implies that the total (stable for $q \geq q_c$) equilibrium proportion of AB supporters, both committed and uncommitted, is $1 - 2x_0$, and $1 - 2x_0 \to 1^-$ as $q \to 1^-$. Hence, in the mean-field limit of our binary consensus model with a given proportion q committed to opinion AB, a consensus on AB is continuously built towards total consensus as q grows (with λ held constant); this seems possibly more realistic than the model of [9] for which a consensus on C (the centrist position) occurred discontinuously at a tipping point.

When $q < q_c$, there are three fixed points and only the two placed symmetrically about the line $y = x$ are stable (see Figure 1). In this case, making q larger (while holding λ constant) serves to bring these stable fixed points closer together; this can be seen from the hyperbola, $xy = 3q^2/(8\lambda)$, on which these points lie. Since flow trajectories are drawn to one or the other of these fixed points (except trajectories that start on the line of symmetry $y = x$), this indicates that the equilibrium results (in an election, say) are less volatile when q is larger (which is probably a good thing for an election). Making λ smaller (while holding q constant, with $q < q_c$) also pushes the two stable fixed points closer. This seems counter-intuitive, as λ is the relative probability of producing an AB supporter in interactions between adherents of A and B (see rows 2 and 4 of Table 1): larger values of λ imply more AB supporters produced in this way. On the other hand, an interaction between uncommitted supporters of AB always converts them to A or B (see the final two rows of Table 1, which come directly from the two-word naming game). So, high numbers of uncommitted AB supporters are hard to sustain, and it is therefore tempting to change the relative probability of transformation in the last two rows of Table 1 from $\frac{1}{2}$ to $\frac{1}{2}\mu$, where $0 < \mu \leq 1$; we leave this possible modification as an exercise for the reader. The wonderful thing about our model (and models in general) is that they can be modified and explored. Breaking the symmetry with respect to A and B in our binary consensus model would be an interesting exploration. One of the commendable features of [9] is the symmetry-breaking included in its model: supporters of opinion A are more persuasive (at converting supporters of C) than are supporters of B.

3 A Binary Persuasion Model

Don't vote: It just encourages the bastards.

— P. J. O'Rourke, from the title of his book [10]

Our second model, which we only outline in this section, is a significant departure from our BC model in Section 2. One important difference is the addition of a new kind of opinion, ∅, that represents the absence of any opinion (i.e. the null opinion: neither A nor B nor any opinion in between). In the American context, for example, those who despise politicians of all stripes and wouldn't consider voting for any of them might be said to hold viewpoint ∅. We think there is some merit to a political model that includes non-voters, as otherwise they are ignored, despite the fact that they usually represent a significant proportion of citizens (more than 40% of eligible voters in recent Canadian federal elections). Counting those who choose not to vote because they are, say, appalled by political corruption or because no candidate truly represents their position might actually lead to better government, as election campaigns might begin to court these potential voters by, respectively, refusing to accept donations from powerful lobbies or revising their platforms to accord more with the views of the disenchanted. It is worth noting that four Canadian provinces [3] and some other jurisdictions[4] allow voters to publicly decline their vote or indicate "none of the above" on their ballots. In the realm of religious beliefs, the ∅ viewpoint might include atheists or at least those who are repulsed by mainstream religious systems represented by A and B. It is important to count such people, we think, because even some religious leaders[5] have argued that it's preferable to abandon religion when it harbors bigotry and fosters discord. Furthermore, as with non-voters, religious non-conformists form a large segment of many societies.

While the ∅ opinion is an important new feature of the *binary persuasion* (BP) model considered here, the essential difference between our BP model and the BC model of Section 2 lies in the disparity between the words *persuasion* and *consensus*. The interaction rules for our BC model involve speaker and listener reaching a consensus (on A, B, or AB) at the end of each transformative interaction: the opinion of the speaker and that of the listener may change to achieve this consensus. In contrast, for our BP model, only the opinion of the listener (never that of the speaker) changes at the end of a transformative interaction. Our BP model is therefore more like proselytization than dialogue. In any case, one of the reasons we have chosen to consider a persuasion model in addition to a consensus model is to illustrate the diverse possibilities for speaker-listener models. Another reason is that the interaction rules for a binary persuasion model can be represented visually, and more simply, using a *compartment diagram*. One further simplification we make in our BP model is to combine states A and B. How can we do this? We assume that the relative probabilities of transformative interactions between opinions A, ∅, and AB are identical to the relative probabilities of such interactions between opinions B, ∅, and AB; in other words, we assume that the compartments for

[4]See Wikipedia permalink https://en.wikipedia.org/w/index.php?title=None_of_the_above&oldid=847838101

[5]For example, 'Abdu'l-Bahá states, "If religion becomes a cause of dislike, hatred and division, it were better to be without it, ..." [1, p. 130]

A and B (in a compartment diagram) are linked to those for ∅ and AB in the same way, so we can combine the compartments for A and B into a single compartment, which we label A△B (i.e. the symmetric difference of A and B, denoting agents holding opinion A or opinion B but not both). What happens inside the A△B compartment (such as whether an agent can change her opinion from A to B or vice versa) need not concern us, as far as our binary persuasion model is concerned: we have combined the extremists into a single compartment and can think of the residents of that compartment as having the same opinion, namely one-sided extremism. Figure 3 thus represents our BP model.

Our BP model has three parameters, α, β, and γ, which are regarded as positive. These three parameters make our BP model more complicated than our BC model, but several simplifying assumptions were still required to reduce the number of parameters to three. The model represented in Figure 3 is the simplest, analytically tractable model that we were able to handle, within the context of persuasive interactions between agents of the three states ∅, A△B, and AB. For example, our decision to make *gamma* the relative probability for conversions from state ∅ to state AB and for the opposite conversions simplifies our BP model, and it seems realistic. Note also that, because $\alpha > 0$ and $\beta > 0$ (so $1 + \alpha > 1$ and $1 + \beta > 1$), agents in the extremist state A△B are more persuasive at converting those in states ∅ and AB than the other way around. This reflects our perception that opinions A and B offer a kind of social safety that ∅ and AB do not offer. In the American political realm, this might mean that voting Democrat or Republican is socially safer than not voting at all or voting for some fringe party of independent thinkers. Mobilia [9] does something similar: he makes supporters of parties A and B more persuasive at converting centrists (party C) to their side than vice versa (but the similarity of our BP model to that of [9] is coincidence – we built and completely analyzed the former before we discovered the latter).

Unlike the BC model of Section 2, our BP model allows for committed agents of all kinds: let p, c, and q be constants in the interval $[0, 1)$ denoting the proportions of all agents committed to opinions ∅, A△B, and AB, respectively. Also, let w, u, and z

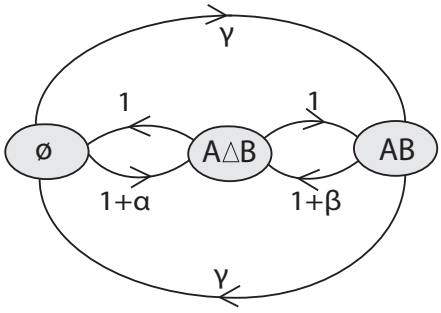

Figure 3: Compartment diagram for our binary persuasion model showing the relative probabilities of transitions between compartments ∅, A△B, and AB. The label on a directed edge from compartment X to compartment Y is the relative probability (per unit time) of a speaker in compartment Y persuading a listener in compartment X to move to compartment Y. Compartments represent sets of agents of the same type.

be the proportions of all agents who hold (but are not committed to) opinions $\emptyset$, A$\triangle$B, and AB, respectively, at a given time t; each of these variables lies in the interval $[0,\ 1]$. Furthermore, all of these proportions must add up to 1, so

$$w + z + u + p + q + c = 1\,. \tag{3.1}$$

The mean-field equations for our BP model can now be written and analyzed as we did for the BC model in Section 2. We have included with this paper (at https://scholarship.claremont.edu/codee/vol12/iss1/2/) MATLAB code that plots phase portraits for our BC and BP models; the mean-field equations for the latter can be seen in a MATLAB function. It is not difficult to show that the resulting flow has at most three fixed points. Furthermore, in the case when $c = 0$ (i.e. no agents are committed to state A$\triangle$B) but $p > 0$ and/or $q > 0$, one fixed point lies on the line $u = 0$ (a boundary of the flow domain where support for opinion A$\triangle$B is zero); this fixed point is stable in some cases, unstable in others, and there is a sharp boundary between these cases (a set of tipping points) that can be described in a simple, geometric way; the transition of this fixed point from stability to instability occurs as it collides with another fixed point in a *transcritical bifurcation* on a center manifold. As we do not want this paper to be overlong and want others to enjoy the thrill of discovery, we leave the (sometimes messy) analysis of our BP model as an exercise for the reader. We are happy to make our results available to anyone who requests them from the corresponding author.

4 Some Observations and Conclusions

The results of this paper give some insight into human social behavior. Although our binary consensus model is only an imitation of reality, it indicates that consensus in a divided community can be gradually achieved if enough people are committed to embracing both sides of the divide. It also suggests that the distance between two stable but opposing equilibria can be reduced by a group of committed moderates. These results make this paper relevant to creating an environment in which social justice might flourish.

Finally, we hope that our paper helps students and others understand some of the beautiful aspects of flows associated with systems of nonlinear ODEs. We have identified three different kinds of bifurcations that can occur as a parameter is varied. In Section 1, we mentioned the saddle-node bifurcation that occurs in the model of [13]; the center manifold on which the three fixed points exist when $p < p_c$ can be seen clearly in Fig. 2(a) of [13]. A pitchfork bifurcation arises in the BC model of Section 2; these bifurcations often occur naturally in flows that have a line of symmetry. We also mentioned the transcritical bifurcation that occurs in the BP model of Section 3. Bifurcations and center manifolds are two important keys for understanding the deeper aspects of flows associated with ODEs.

References

[1] ‘Abdu’l-Bahá. *Paris Talks: Addresses Given by ‘Abdu’l-Bahá in 1911*. UK Bahá’í Publishing Trust, London, 11th edition, 1979.

[2] Andrea Baronchelli, Maddalena Felici, Vittorio Loreto, Emanuele Caglioti, and Luc Steels. Sharp transition towards shared vocabularies in multi-agent systems. *Journal of Statistical Mechanics: Theory and Experiment*, 2006(06):P06014, 2006. http://stacks.iop.org/1742-5468/2006/i=06/a=P06014.

[3] Terra Ciolfe. Ontario election 2018: How to decline your vote. *Maclean’s Magazine*, June 2018. This did not appear in print. It is from the 2 June 2018 online edition of *Maclean’s* magazine available at https://www.macleans.ca/politics/ontario-election-2018-how-to-decline-your-vote/.

[4] F. Scott Fitzgerald. The Crack-Up. *Esquire*, page 41ff, Feb 1936. The first part of a three-part essay published in the February, March, and April 1936 issues of *Esquire* magazine.

[5] S. Galam. Sociophysics: A review of Galam models. *Int. J. Mod. Phys. C*, 19(3): 409–440, 2008. https://doi.org/10.1142/S0129183108012297.

[6] J Guckenheimer and P. Holmes. *Nonlinear Oscillations, Dynamical Systems, and Bifurcations of Vector Fields*. Springer, New York, 1st edition, 1983.

[7] Matthew O. Jackson. *Social and Economic Networks*. Princeton University Press, Princeton, 2008.

[8] Seth A. Marvel, Hyunsuk Hong, Anna Papush, and Steven H. Strogatz. Encouraging moderation: Clues from a simple model of ideological conflict. *Phys. Rev. Lett.*, 109: 118702, Sep 2012. https://link.aps.org/doi/10.1103/PhysRevLett.109.118702.

[9] M. Mobilia. Commitment versus persuasion in the three-party constrained voter model. *J. Stat. Phys.*, 151:69–91, 2013. https://doi.org/10.1007/s10955-012-0656-x.

[10] P.J. O’Rourke. *Don’t Vote: It Just Encourages the Bastards*. Grove/Atlantic, New York, 2010.

[11] F.G. Sommers and T. Dineen. *Curing Nuclear Madness: A New-age Prescription for Personal Action*. Methuen, London, 1984.

[12] Gunjan Verma, Ananthram Swami, and Kevin Chan. The impact of competing zealots on opinion dynamics. *Physica A: Statistical Mechanics and its Applications*, 395:310–331, 2014. ISSN 0378-4371. https://doi.org/10.1016/j.physa.2013.09.045.

[13] J. Xie, S. Sreenivasan, G. Korniss, W. Zhang, C. Lim, and B. K. Syzmanski. Social consensus through the influence of committed minorities. *Phys. Rev. E*, 84(1):011130, 2011. https://doi.org/10.1103/PhysRevE.84.011130.

Kremer's Model Relating Population Growth to Changes in Income and Technology

Dan Flath
University of Arizona

Keywords: Economic growth, population model, Kremer's Model
Manuscript received on September 16, 2018; published on February 13, 2019.

Abstract: For thousands of years the population of Earth increased slowly, while per capita income remained essentially constant, at subsistence level. At the beginning of the industrial revolution around 1800, population began to increase very rapidly and income started to climb. Then in the second half of the twentieth century as a demographic transition began, the birth and death rates, as well as the world population growth rate, began to decline. The reasons for these transitions are hotly debated with no expert consensus yet emerging. It's the problem of economic growth. In this document we investigate a mathematical model of economic growth proposed by Michael Kremer in 1993.

1 The Malthus Model

Thomas Malthus, working in England in the 1790s, created the first mathematical model of economic growth [9]. The classic statement of his finding is that annual food production, Y, increases linearly and population p, unless checked, increases exponentially.

$$\begin{aligned} p &= me^{rt} \\ Y &= nt \end{aligned} \qquad \text{(Model 0)}$$

The parameters m, n, and r are positive constants.

Malthus realized that the growth he described is unsustainable because it leads to ever-decreasing average food production that falls below the amount required for life.

$$\text{Food per person} = \frac{Y}{p} = kte^{-rt}.$$

Malthus's conclusion was that mass starvation on a continuing basis, or death by perpetual war or disease, is inevitable.

Malthus did not actually run the assumptions of Model 0 out to their logical conclusion (predicting zero living standards); his whole point was that positive and preventative checks (essentially, mortality and fertility changes) would ensure that the population

growth slowed down as people had less to eat and in the long run we will all remain at constant, never increasing, near subsistence level incomes. This dismal situation has been called the Malthusian trap.

At just the time Malthus was working, development of technology took off, spurring increases in food production sufficient to support an ever more rapidly growing population. Thus technology became the way out of the trap. Can we produce a growth model that incorporates technology in a meaningful way?

2 Kremer's Model: The Variables

Kremer's theory of economic growth [8] is a mathematical model of the time evolution of three variables:

- p: population of a community
- A: level of technology of the community
- y: per capita income of the community

Note that $y = Y/p$, where Y is the income of the entire community, an annual gross national product (GNP). You can think of Y as equivalent to a quantity of food, perhaps measured in calories, since for most of human history all our income was hunted or gathered and eaten right away.

The three variables y, A and p are linked by a production function for Y. In the Kremer model the value of Y is determined by the population's ability to use two resources: (1) labor, which is the population p itself, and (2) a second resource X. Often X is interpreted as a fixed quantity of land. We model X as a constant and hence set it to 1. Assuming a standard Cobb-Douglas model[1] Kremer postulates that

$$Y = Ap^{1-\beta}X^{\beta} = Ap^{1-\beta}$$
$$y = \frac{Y}{p}.$$

The Cobb-Douglas exponent β is a constant parameter for the model, with $0 < \beta < 1$. Kremer suggests a very rough estimate of $\beta = 1/3$ based on tenants' shares in traditional sharecropping contracts. The level of technology, A, functions as a multiplier in the production function. If technology is greater, then the same number of people can produce more from the land.

Thus p, y and A are related via the yAp equations

$$y = Ap^{-\beta}$$
$$p = \left(\frac{A}{y}\right)^{1/\beta}.$$

Let's look at the implications for growth rates, by which we always mean relative growth rates. Taking logarithmic derivatives of the yAp equations we get

$$\frac{\dot{y}}{y} = \frac{\dot{A}}{A} - \beta\frac{\dot{p}}{p}.$$

[1] https://en.wikipedia.org/wiki/Cobb-Douglas_production_function

The growth rate of per capita income is a linear combination of the growth rates of technology and population. Per capita income y is dragged down by increasing population with fixed technology because the same wealth is divided among more people. But income grows more quickly as technology improves with fixed population as the same number of people can use the better technology to extract more wealth from the land.

We have specified one relation among the three variables y, A and p, so we need two more equations to complete a model. They will be growth equations. We will give equations for two of $\dot{y}/y$, $\dot{p}/p$ and $\dot{A}/A$. There are of course many ways to do this. Different choices can be appropriate for different populations, or for a single population in different stages of its growth.

Problem 2.1. Consider Model 0, the naive Malthus model, which does not involve A.

(a) Show that it can be expressed in terms of growth rates as follows:

$$\frac{\dot{p}}{p} = r$$
$$\frac{\dot{Y}}{Y} = \frac{n}{Y}$$

(b) Show that

$$\frac{\dot{y}}{y} = \frac{n}{py} - r.$$

(c) How does the growth rate, $\dot{y}/y$, of per capita income y change when population p increases? When y increases?

(d) Explain how this model shows that per capita income eventually decreases.

(e) Assuming that $y = Ap^{-\beta}$, show that

$$\frac{\dot{A}}{A} = \frac{n}{py} - (1-\beta)r.$$

3 A Modern Interpretation of Malthus

Malthus's main point is that in the long run population will grow but per capita income will be constant. To see this conclusion arise from a plausible differential equation model for A, p and y, consider Model 1, as follows:

$$p = \left(\frac{A}{y}\right)^{1/\beta}$$
$$\frac{\dot{p}}{p} = \theta(y - y_0) \qquad \text{(Model 1)}$$
$$\frac{\dot{A}}{A} = k$$

The parameters θ, k and y_0 are positive constants.

We interpret y_0 as an acceptable per capita income. For most of history and prehistory y_0 may have been a subsistence level income, but it is probably higher than that now. When income is above the acceptable level, the population increases. When income is below the acceptable level, the population decreases, due for example to malnutrition or misery leading to increased mortality and decreased fertility. The parameter $\theta > 0$ governs how quickly p responds to deviations in per capita income from y_0. The level of technology A increases at a constant relative rate k as humans make discoveries, supporting a greater population at the same per capita income y. The model implies that A grows exponentially,

$$A = C_1 e^{kt}$$

where C_1 is a positive constant.

The implications of Model 1 for income y are most easily revealed by recasting the model as a system of differential equations for p and y. We have

$$\begin{aligned} A &= yp^\beta \\ \frac{\dot{p}}{p} &= \theta(y - y_0) \\ \frac{\dot{y}}{y} &= k - \beta\theta(y - y_0). \end{aligned} \qquad \text{(Model 1, alt. form)}$$

The equation for y is a logistic differential equation of the form

$$\begin{aligned} \frac{\dot{y}}{y} &= s\left(1 - \frac{y}{L}\right) \\ s &= k + \beta\theta y_0 \\ L &= \frac{s}{\beta\theta} = \frac{k}{\beta\theta} + y_0. \end{aligned}$$

with limiting value L, so

$$y(t) = \frac{L}{1 + C_2 e^{-st}}$$

where C_2 is constant. For all initial conditions, per capita income eventually becomes essentially constant, $y \approx L$. Indeed, one exact solution to Model 1 to which all others are asymptotic as $t \to \infty$ is given by

$$\begin{aligned} p &= \left(\frac{C_1}{L}\right)^{1/\beta} e^{kt/\beta} \\ y &= L \\ A &= C_1 e^{kt}. \end{aligned}$$

The population ultimately grows exponentially, enabled to do so by the increasing level of technology. But there is no exit from the Malthusian trap. Per capita income does not grow at all. The ever greater populations remain forever at subsistence level.

4 The Malthusian Era

Kremer called the period from 1 million BCE to about 1800 the Malthusian era. It was characterized by three properties.

1. Population: Continual slow population growth.

   Relevant world population estimates are

Year	1 million BCE	0 CE	1800
Population	125,000	230 million	1 billion.

   Global population doubled fewer than 11 times in the first million years, on average about once every 100 thousand years. Contrast that with the present. World population doubled in just 47 years from 3.8 billion in 1971 to 7.6 billion in 2018.

   Problem 4.1. Assuming exponential growth at a constant rate, find the population growth rates for the periods from

   (a) 1 million BCE to 0 CE

   (b) 0 CE to 1800

   (c) 1971 to 2018.

2. Income: Nearly constant per capita income.

   Global per capita income, expressed in contemporary currency, is estimated to have been about $450 per year from 1 million BCE to 1000 BCE only rising to $670 per year by 1800. During this time per capita food consumption did not rise at all.

3. Technology: Slow but steady improvement.

   During this period tools were invented, language was developed, fire was tamed, agriculture and herding were invented, animals were domesticated, first settlements were created.

Let's convert the Malthusian Era characteristics into Kremer's first mathematical model, given by three equations:

$$\begin{aligned} p &= \left(\frac{A}{y}\right)^{1/\beta} \\ \frac{\dot{y}}{y} &= 0 \\ \frac{\dot{A}}{A} &= gp \end{aligned} \qquad \text{(Model 2)}$$

The parameter g is a positive constant.

It is a model assumption that per capita income remains constant over time, as Malthus expected and as was the case for a million years. This assumption takes as a permanent feature the longterm stagnation in y from Model 1.

The technology equation for $\dot{A}/A$ in Model 2 differs from the analogous equation in Model 1. The new equation asserts that the growth rate of technology increases with population. This reflects the thought that with more people, it is more likely that someone will hit on a great idea that spurs technological development. We interpret g as research productivity. If g is higher then the same population improves technology faster.

The differential equation for y makes $y = y_0$, a constant. As for p, we have

$$\frac{\dot{p}}{p} = \frac{1}{\beta}\frac{\dot{A}}{A} - \frac{1}{\beta}\frac{\dot{y}}{y} = \frac{g}{\beta}p$$

Therefore,

$$\frac{dp}{dt} = \frac{g}{\beta}p^2.$$

In Model 2 population grows faster than exponentially. Increasing population p causes the growth rate of technology A to increase, which makes A climb ever faster. Since y is constant, the ever increasing rate of A drives a runaway increase in p. This may sound unsustainable, and it is, even mathematically. Solving explicitly we have

$$p(t) = \frac{p_0}{1 - gp_0t/\beta}$$

where $p_0 = p(0)$. The solution for p runs off to infinity by finite time $t = \beta/(gp_0)$. This is not necessarily a flaw in the model, since the model was only designed to capture global population growth during the Malthusian Era, not for all time.

Postulating that per capita income is constant may seem a little drastic, since income eventually did begin to rise. Let's move on to a fancier model.

5 The Industrial Revolution

In the late 1700s and very early 1800s the Industrial Revolution began in England, then rapidly spread first to Europe and then to the whole world.[2] During this time period population and per capita income growth rates both exploded. Kremer's second model frees y to vary, as in Model 1, enables technology to grow at an increasing rate with increasing population, as in Model 2, and captures the transition from the Malthusian era to the industrial revolution.

$$\begin{aligned} p &= \left(\frac{A}{y}\right)^{1/\beta} \\ \frac{\dot{p}}{p} &= \theta(y - y_0) \\ \frac{\dot{A}}{A} &= gp \end{aligned} \qquad \text{(Model 3)}$$

The parameters θ, g and y_0 are positive constants.

[2] https://en.wikipedia.org/wiki/Industrial_Revolution

We interpret y_0 as an acceptable per capita income, as in Model 1. In Model 3, if $y = y_0$, then p is momentarily constant, but A is still growing and hence so is y, which leads to further growth in p. The monotonic growth of technology enables population to continue growing, too.

We can recast Model 3 as a system of differential equations for p and y. We have

$$\begin{aligned} A &= yp^{\beta} \\ \frac{\dot{p}}{p} &= \theta(y - y_0) \qquad \text{(Model 3, alt. form)} \\ \frac{\dot{y}}{y} &= gp - \beta\theta(y - y_0). \end{aligned}$$

Figure 1 shows a nulllcline analysis in the py phase plane and solution trajectories.

The $\dot{p} = 0$ nullcline is the line $y = y_0$. The $\dot{y} = 0$ nullcline is the line $y = y_0 + gp/(\beta\theta)$. The nullclines separate the quadrant $p > 0$, $y > 0$ into three regions.

- Region I: per capita income y is less than the threshold y_0. Population therefore declines and income rises.
- Region II: income y is greater than y_0. Population increases and income falls.
- Region III: income y is greater than y_0. Population increases and so does income. This is the region of the post-Malthusian boom, the Industrial Revolution. Population is so large that technology increases fast enough to keep production ahead of population growth and thus provides a way out of the Malthusian trap. All solutions eventually cross one of the nullclines into Region III after which both population and income rise forever. The solutions move through Region III at an ever increasing speed, which means faster and faster increases in both y and p.

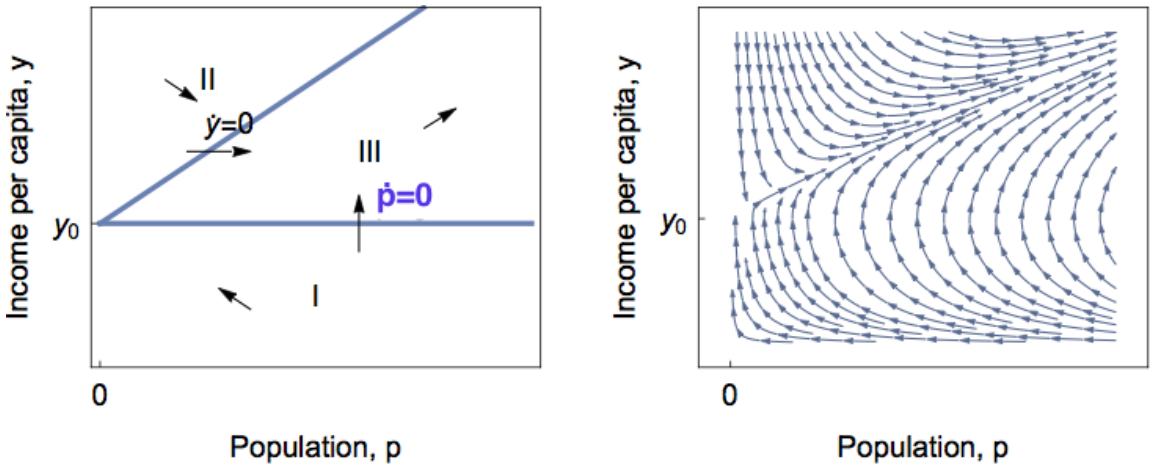

Figure 1: Model 3: Nullclines and trajectories. If per capita income is below y_0 then population decreases. If income is above y_0 then population increases. Increasing population causes a decrease in income when population is low (Region II) but an increase in income when population is high (Region III). The larger population spurs more technological growth. The equations of the nullclines are $y = y_0$ and $y = y_0 + gp/(\beta\theta)$.

Perhaps the most important thing to say about Model 3 is that it predicts that all populations, if left long enough, will eventually enter Region III of continual population and income growth. In this model, something like the Industrial Revolution was inevitable, the result of the human proclivity to improve their technology. Whether this simple explanation truly solves the question of the causes of the Industrial Revolution is a matter of debate.

The numerical solutions of an example of Model 3 with $y_0 = 1$ and $y(0) = 1.5$ is shown in Figure 2. Initially income and population are in Region II. The initial income is above the minimal acceptable level so supports a rapid population increase. Once the income drops near y_0, we enter Region III. Population slowly increases due to slowly improving technology then begins to increase faster. At a later time income begins to explode. The increase in income signals that the transition from the Malthusian Era to the period of the Industrial Revolution has been achieved.

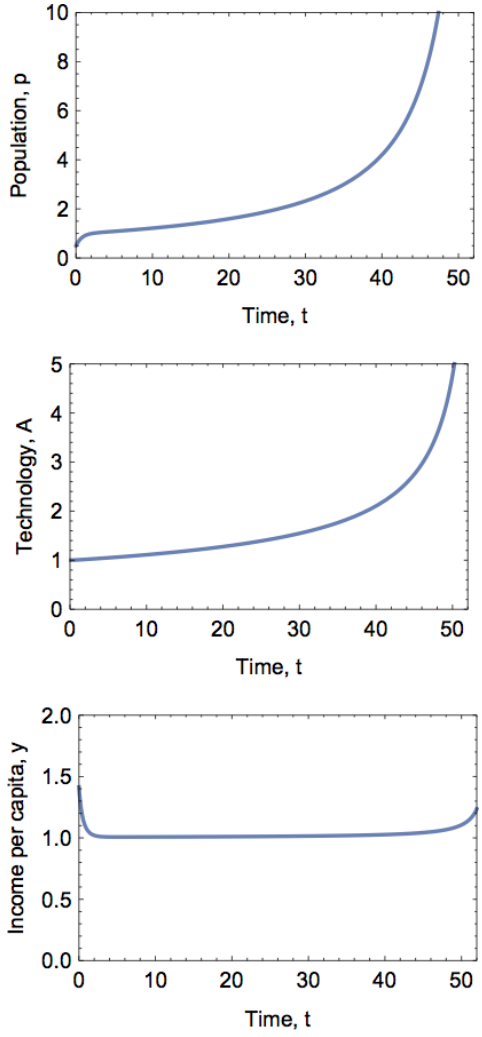

Figure 2: Model 3: After a long period of nearly constant per capita income, income begins to rise and both population and technology surge. This is a possible model for the transition from the Malthusian Era to the Industrial Revolution. Parameter values are $\beta = 0.5, \theta = 3, g = 0.01, y_0 = 1, p(0) = 0.5, A(0) = 1$.

6 The Demographic Transition

The world population growth rate has not continued to increase. It had begun to decline by 1970, at which point global population was around 3 billion. No one knows the reason for sure. One line of thought is that increasing wealth changes the economics of the decision about whether to have more children or to have educated children, an issue referred to in the literature as a quantity versus quality tradeoff. Perhaps when individual incomes become high enough, people are opting for fewer but educated children. Whatever the reasons may be, all the world over birth rates have declined as incomes have risen.

Model 3 does not model this demographic transition. The reason is that the population equation for Model 3

$$\frac{\dot{p}}{p} = \theta(y - y_0)$$

describes the population growth rate $\dot{p}/p$ as a monotonically increasing (linear) function of income. It does not describe a drop in the growth rate as the response to sufficiently high y. To capture this effect Kremer postulates a new population equation, which can be described by a function $f(y)$. We have

$$\begin{aligned} p &= \left(\frac{A}{y}\right)^{1/\beta} \\ \frac{\dot{p}}{p} &= f(y) \\ \frac{\dot{A}}{A} &= gp \end{aligned} \qquad \text{(Model 4)}$$

or equivalently

$$\begin{aligned} A &= yp^{\beta} \\ \frac{\dot{p}}{p} &= f(y) \\ \frac{\dot{y}}{y} &= gp - \beta f(y). \end{aligned} \qquad \text{(Model 4, alt. form)}$$

The function $f(y)$ is to be a function whose graph resembles that in Figure 3. The population growth rate increases for low incomes, just as in Model 3. As income continues to increase, $\dot{p}/p$ reaches a maximum then decreases, approaching a constant value that could be either positive or zero.

The nullclines in the py phase plane with some streamlines for Model 4 are shown in Figure 4. As was the case for Model 3 there are three regions. If income is below y_0 then population decreases, and if it is above y_0 it increases. But the bend in the $\dot{y} = 0$ nullcline causes an effect not seen in Model 3. It is possible for a sudden increase in income to move a population vertically in the phase plane from Region II, where income is declining, to Region III, where income is increasing. Such a jump could be, for example, a technological breakthrough such as the discovery of inexpensive nuclear fusion power, artificial efficient photosynthesis or some other source of cheap power.

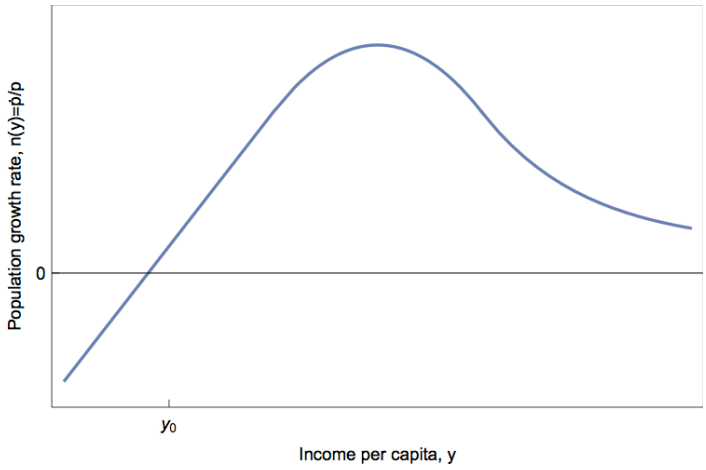

Figure 3: Model 4: When per capita income is high enough, the population growth rate declines with increasing income.

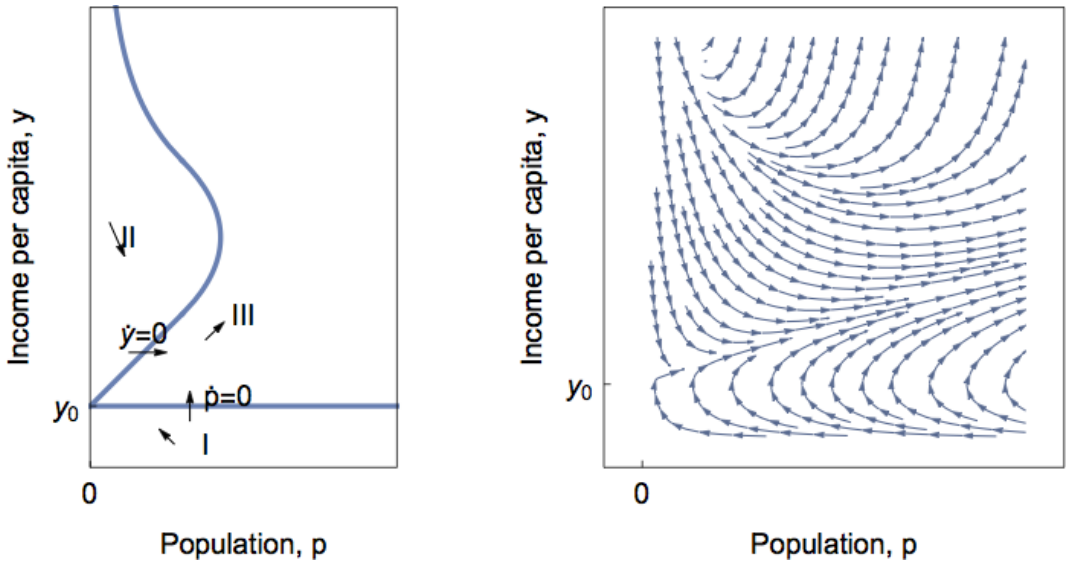

Figure 4: Model 4: Nullclines and trajectories. Population falls in the low income Region I and grows in the high income Regions II and III. A technological breakthrough could move a population overnight from Region II to Region III, thus reversing a downward trend in per capita income. The equations of the nullclines are $y = y_0$ and $gp = \beta f(y)$.

A population drop at a moderate income may take the population from Region III to Region II, where income stops growing and begins decreasing. On the other hand, the same population drop in a wealthier level may stay in Region III, so income continues to grow. This phenomenon was not seen in Model 3.

In Model 4 all populations eventually enter Region III after which their incomes grow forever. If the incomes get high enough, the rate of population growth declines and a demographic transition begins. A sample solution is shown in Figure 5. The figure is meant to be qualitatively correct, but not numerically so. The function $f(y)$ and model

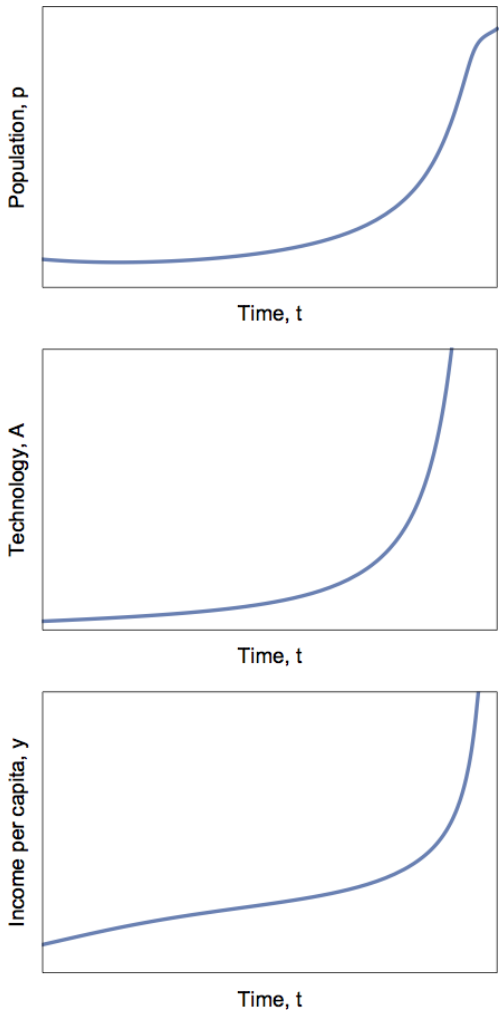

Figure 5: Model 4: When income is high enough, population growth slows, though income and technology continue to increase dramatically.

parameters were not fit to real data.

Model 4 is intended to capture the demographic transition, not to model the future forever. As $f(y)$ decreases with increasing y, per capita income y continues to increase without bound, an unsustainable trajectory. As always, building and refining a model is an iterative never-ending process.

7 Additional Reading

Malthus wrote, "Population, when unchecked, increases in a geometrical ratio. Subsistence increases only in an arithmetical ratio. A slight acquaintance with numbers will shew the immensity of the first power in comparison of the second." For this and more, see [9].

For Kremer's original very clear article (with an awe-inspiring title) see [8]. An elementary textbook exposition appears in Chapter 8 of [7]. An extension to the controversial Unified Growth Model of Oder Galor is given in [5].

In this article we do not tackle directly the question of why birth rates decline in sufficiently wealthy populations. We merely postulate the general shape of the graph of the modeling function $f(y)$. But economists have proposed models to explain declining fertility with increased income, for which see [3] and [4].

There has been a great deal of discussion about the technology equation $\dot{A}/A = gp$. Is the research productivity parameter g really a constant? It's partly an empirical question. Some evidence is that large technologically advanced populations innovate rapidly, and some large less developed populations (for example China in the 1980s) innovated slowly. Perhaps g should depend on A. This led Jones to propose an alternative technology equation: $\dot{A}/A = gp^{\psi}A^{\phi}$ where g is again a constant parameter. See [6].

For alternative explanations of the cause of the Industrial Revolution see [1], [2] and [10].

Acknowledgments

Robert Borrelli and I first crossed paths years ago when I began teaching differential equations from *Differential Equations: A Modeling Perspective* by Borrelli and Coleman. About a month into the course it hit me just how much I loved teaching from his book. Borrelli made it easy to keep the focus on mathematical modeling, with differential equations in a supporting role. I sent Bob some fan-mail, he responded and attracted me into the CODEE orbit. At the next JMM I met Bob and was soon working on the presentation of CODEE sponsored MAA minicourses "Teaching differential equations with modeling." I will forever be grateful for my friendship with Bob. It is a joy for me to contribute to a volume in honor of all that he gave to so many people for so many years.

Borrelli was always on the lookout for interesting mathematical models for students to explore. In this paper we suggest Kremer's model of economic growth as a good way to lead students beyond the exponential and logistic population models that they may have seen in earlier courses. The exponential and logistic models do not capture the global transition to rapid growth at the time of the industrial revolution. Nor do they model the more recent demographic transition to declining population growth rates due to reduced birth rates associated with increasing wealth. Kremer's economic growth model tackles both of these transitions. His model includes a time dependent variable that represents the level of technology of a population. The Kremer model is a 2-dimensional continuous dynamical system appropriate for a first course in differential equations.

I want to thank economist Dietrich Vollrath (University of Houston) for helpful expert comments on the first draft of this paper.

References

[1] Daron Acemoglu. *Introduction to Modern Economic Growth*. Princeton University Press, 2009.

[2] Robert Allen. *The British Industrial Revolution in Global Perspective*. Cambridge University Press, 2009.

[3] Gary S. Becker and H. Gregg Lewis. On the interaction between the quantity and quality of children. *Journal of Political Economy*, 1973.

[4] Matthias Doepke. Gary Becker on the quantity and quality of children. *Journal of Demographic Economics*, 2015.

[5] Oder Galor. *Unified Growth Theory*. Princeton University Press, 2011.

[6] Charles I. Jones. R&D based models of economic growth. *Journal of Political Economy*, 1995.

[7] Charles I. Jones and Dietrich Vollrath. *Introduction to Economic Growth*. 3rd edition, 2013.

[8] Michael Kremer. Population growth and technological change: One million B.C. to 1990. *The Quarterly Journal of Economics*, 1993.

[9] Thomas Robert Malthus. *An Essay on the Principle of Population*. 1798.

[10] Joel Mokyr. *A Culture of Growth: The Origins of the Modern Economy*. Princeton University Press, 2016.

Language, Technology, and Engagement in the Haitian Classroom: An Interim Report on the MIT-Haiti Initiative

Haynes Miller
Massachusetts Institute of Technology

Keywords: Education, Haiti, language
Manuscript received on May 15, 2018; published on February 13, 2019.

Abstract: Since 2013 I have been traveling to Haiti as part of the "MIT-Haiti Initiative."[1] This initiative, led by Professor Michel DeGraff of the MIT Department of Linguistics and Philosophy, aims to encourage active learning strategies, enabled by technology when possible and appropriate, and strongly stresses the importance of the use of the one language spoken by all Haitians, namely Haitian Creole (or *Kreyòl*). To use a Haitian metaphor, these three components form the three stones on which the cook-pot of our educational approach rests. We have focused our attention on the higher education sector.

In this note I will begin with a review of the educational landscape that forms the background for our efforts. Then I will describe the work of the MIT-Haiti Initiative and some of the efforts undertaken in Haiti by participants in our workshops. I will discuss the mathematical material developed for these workshops and what we learned in leading them, and then describe the findings of a site visit to a campus of the State University of the Haiti. I will end by discussing how the typography of equity spelled out by Gutiérrez [10] applies in the Haitian educational setting.

Author's Note: It is a pleasure to thank Michel DeGraff for his assistance in preparing this report, as well as for his leadership of the MIT-Haiti Initiative. I also thank the referee for calling attention to Gutiérrez's work.

1 The political and educational background

The Haitian educational landscape is both complex and resource constrained. Only around 15% of the K-12 education is funded by the government; the rest is either offered by small for-profit organizations or comes from charities of various sorts, mainly Protestant or Catholic religious institutions. This basically eliminates the possibility of governmental

[1] Much of the material created under the auspices of this Initiative is collected on the website https://haiti.mit.edu. This website contains parallel English and *Kreyòl* pages.

accreditation of either institutions or teachers. There are also great disparities between urban and rural education, and, of course, between wealthier and poorer institutions. Overall, there is an enrollment rate of around 88% in primary school, 20% in secondary school, and 1% in university level study.[2] Many students from the elite high schools go abroad (to Dominican Republic, Canada, Mexico, Cuba, the US, and elsewhere) [6],[12, p. 4].

Issues of language play a critically important role in determining who receives an education in Haiti. Despite the fact that only 5% of the population speak French as a mother tongue (alongside *Kreyòl*), a great deal of Haitian education, even at the primary level, is conducted in French rather than in *Kreyòl*,[3] and high-stakes examinations are invariably written in French.[4] This is a major factor in the very low educational level in the country overall, and effectively disenfranchises the large majority of Haitian citizens. A *Kreyòl* expression for the French language is *lang achte* (the "bought language") whereas *Kreyòl* is considered *lang rasin* (the "language of roots") [2, p. 570].

Haitians place a high value on education. Any visitor to Port-au-Prince or other Haitian cities will notice the many storefronts offering instruction in computer technology, business, or English. School uniforms are the rule in elementary schools even in remote sections of the country. This very faith in the value of education somewhat paradoxically poses its own obstacles. Parents are not mistaken in their conviction that acquisition of French is a prerequisite for advancement in most professions in Haiti today. They see a very narrow window in which fluency in French can be acquired: Only a fifth of Haitian school children graduate into secondary school. This lends credibility to the argument that formal education, even at the elementary level, should be conducted in French; what could be better than an immersive experience for young children? Besides, the vast majority of available textbook material is published in French.

There are crippling flaws with this approach, however. The cognitive demands imposed by interpreting a language one is not fluent in compete and conflict with the process of learning subject matter. Most Haitian K-12 educators are not comfortable with the French language themselves. The textbooks in use exemplify French culture, not Haitian, and the references they contain are either meaningless to Haitian students or re-inforce a negative cultural self-image [16, p. 34], [7], [14]. Most critically, the use of a foreign language in the classroom discourages student creativity, especially since it is often coupled with

[2] https://en.wikipedia.org/wiki/Education_in_Haiti

[3] It is hard to get accurate statistics on the predominance of the use of French in Haitian classrooms, partly because it varies widely from one school to another and from one instructor to another. Some relatively current insight can be gleaned from an entry in an "operational plan" [9] published by the Haitian Ministry of Education. Among the problems facing the Haitian educational system, there is a "pronounced imbalance in bilingualism (predominance throughout of the use of French, generally poorly mastered by teachers, over Creole)." Later, this document prescribes an "equilibrium" between French and Creole. Despite the neutral tone of this diagnosis, and unrealistic vision of the cure, the document has some revealing comments later on (p 43): "Finally, if the education system is not at the origin of the crisis of individual and collective identity, it contributes to at the least accentuating it, on the one hand, by [contributing to] the prevailing confusion as regards the use of Creole and French in education and, on the other hand, by promoting the knowledge of national history without making room for the beliefs and customs of the population. This set of findings . . . makes even more palpable a certain paradox in the analysis of the Haitian educational system, namely: it confers little use to individuals, but remains very socially relevant." (My translations.)

[4] . . . with the signal exception of the exams on *Kreyòl* itself!

an authoritarian and rote pedagogical style. We often heard it said that if the goal was understanding, the teacher would use *Kreyòl* ; if discipline was the aim, then French was the language of choice.

There are important Haitian examples of enlightened educational models in K-12 education. One, which is affiliated with the MIT-Haiti Initiative, is the Matènwa Community Learning Center,[5] MCLC, or, in *Kreyòl*, *Lekòl Komiotè Matènwa, LKM*. Its location on the island of Lagonav means that it serves a distinctly rural population. Founded in 1996, the school states that "Our mission is to be a democratic model of hands-on education that reflects the learning and growing possible in one's local environment. MCLC uses methodologies that have been tailored to their culture through experimentation, evaluation, and modifications, resulting in the present implementation of highly successful practices." Its associated Institute for Learning offers training in the methods they have developed. At this school, all education begins in *Kreyòl*, with French taught as a second language. A careful comparative study [3] shows substantially larger learning gains – in speed of reading and in comprehension – at MCLC than at traditional schools.

There has been a long succession of attempts to improve the educational system in Haiti.[6] A governmental initiative known as the "Bernard Reform" contained one of the first official recognitions of the importance of the use of *Kreyòl* in education. Promulgated in 1979 with effect intended for 1982, it was in part a genuine response to an ossified educational system and in part intended to shore up international support for the dictatorship of Jean-Claude "Baby Doc" Duvalier.[7] It ran into inevitable political obstacles and most of its provisions were never widely implemented; "Indeed, the different actors (ministry executives, school directors, teachers, parents and pupils) on which the process of setting up this educational reform should be based were not sufficiently imbued with the aims and contents of the new curriculum. This gave rise to the expression and organization of some very fierce resistance, particularly regarding the official integration of Creole into the curricula as a language of instruction and language to teach."[8, p. 81] (my translation).

Be that as it may, "the Bernard Reform was . . . the first attempt to develop a language policy for teaching in Haiti. According to the regulations established by this reform, it is essential that teaching 'be in a language that the child understands, in this case Creole.' " [8, p. 81] (my translation). The document continues: "The first and second cycle Creole communication program includes knowledge, skills, attitudes and habits that one wishes to develop in the child, particularly the ability to express oneself properly in one's mother tongue and to acquire the mental mechanisms that are at the base of all knowledge: to listen, to speak, to read and write. On the other hand, the recommendation is made for French to be taught as second language at the first and second cycles, with a focus on oral in the early years."

The higher education sector is no less complex. We quote from a study done soon after the 2010 earthquake. "While precise statistics are unavailable, it is clear that the pre-earthquake higher education system served only a tiny fraction of secondary school

[5] https://www.matenwa.org

[6] For an excellent general history of Haiti, see [5].

[7] For accounts of the history of this reform see [1, 16, 11].

graduates. In 2007, the Ministry of National Education and Professional Formation (*MENFP*) reported the university population of Haiti was approximately 40,000 students. Of this number 28,000 (70%) were in public universities and 12,000 (30%) in private ones." [12, p. 4] "Before the January 12, 2010 earthquake, the Haitian system of higher education comprised at least 159 institutions .... This system was divided into disparate public and private sectors. The former consisted of a small network of 14 public, government-run institutions of higher education (*Instituts d'enseignement supérieur, IES*) including the State University of Haiti (*Université d'État d'Haïti, UEH*). The *UEH* has 18 campuses, of which 11 were located in the metropolitan area of Port-au-Prince, and 7 located outside the capital .... Besides the *UEH*, the public university sector also includes 13 *IES* either affiliated with or independent of *UEH*. In contrast, the private higher education sector consists of a vast array of 145 institutions of varying quality. Of the 145 private universities, 10 provide high quality, accredited education; of the remaining 135 (often religious-based institutions), 67% (97) do not have permission to operate from the governmental Agency of Higher Education and Scientific Research (*DESR*)." [12, p. 93].

The recognition of the central place of *Kreyòl* in Haitian society was strongly affirmed in the 1987 Constitution,[8] adopted during a period of military rule following the deposition of Jean-Claude Duvalier. It contains the following clauses:

> *Article 5*: All Haitians are united by a common language: Creole. Creole and French are the official languages of the Republic.
>
> *Article 40*: The State has the obligation to publicize in the oral, written and televised press in the Creole and French languages all laws, orders, decrees, international agreements, treaties, and conventions on everything affecting the national life, except for information concerning national security.

Though the 1987 Constitution was duly published in both *Kreyòl* and French, adherence to the requirements of Articles 5 and 40 over the past thirty years has been spotty at best. Even the amendments, in 2011, to the 1987 Constitution were written in French only, thus violating the very Constitution that was being amended!

2 The MIT-Haiti Initiative

The fact that elementary and secondary schools are often failing Haitian students in their choice of language and pedagogy cannot be used as an excuse for inaction in higher education. The MIT-Haiti Initiative set out to work with university level faculty, because this is our area of expertise. But in fact many university faculty members also teach in primary or secondary schools or in teaching colleges, so our work has had an impact at many educational levels.

A turning point in Haitian history occurred on January 12, 2010, in the form of a catastrophic earthquake. Centered near the capital, it killed hundreds of thousands of people and left large parts of the city in ruins. Most of the institutions of higher education

[8] Translation by http://pdba.georgetown.edu/Constitutions/Haiti/haiti1987.html.

were located in Port-au-Prince and were heavily impacted both by destruction of physical infrastructure and human casualties. It is estimated [12, p. 137] that 90% of the higher education infrastructure in the capital was destroyed. The economic cost of this disaster was immense and long-lasting, and generated a great deal of international attention. While the failings of much of the international relief and rebuilding response are well-documented,[9] one of the more hopeful outcomes has been an upsurge in contributions to their homeland by the large Haitian diaspora, often by returning to Haiti to work. The increased awareness of the needs of the Haitian population was a precipitating factor in the creation of the MIT-Haiti Initiative.

2.1 Kickoff Symposium and NSF grant

The MIT-Haiti Institute was launched by a Symposium in Cambridge, MA, on October 21 and 22, 2010, nine months after the earthquake. Funded by MIT and the Port-au-Prince-based Foundation for Knowledge and Liberty, *FOKAL*, it brought a highly distinguished group of Haitian leaders, including a former prime minister, deans from the Faculty of Sciences at the University of Haiti, rectors or presidents from a number of private institutions, and high tech industry representatives, together with MIT educational leadership and faculty. Momentum was born, and based on ideas emerging from the Symposium Michel DeGraff along with then director of MIT's Office of Educational Innovation and Technology Vijay Kumar (now Associate Dean for Open Learning at MIT) applied for and won an NSF grant entitled INSPIRE: Kreyol-based Cyberlearning for a New Perspective on the Teaching of STEM in local Languages.[10] This grant has underwritten the bulk of the activities of the MIT-Haiti Initiative over the past six years.

2.2 Workshops

Over the life of this grant we conducted seven academic workshops – five in Port-au-Prince and two at the *Campus Henri Christophe de Limonade, CHCL*, a branch of the *UEH*, occupying a beautiful new campus in the north of the country near Cap-Haïtien.

Our approach has been to work with individual faculty members directly, rather than through institutional or governmental agencies. This reflects a realistic assessment of the historical effectiveness of reforms promulgated by these structures, as well as a faith in the enormous potential of human resources in the country. We required of our participants at least a Masters Degree or enrollment in a Masters Degree program, though we made some exceptions to that rule. A number of our participants had received PhDs from various institutions. Altogether we had over 250 participants from 146 institutions.

The seven workshops had the following enrollments [4, p. 142]:

	3/2012	1/2013	8/2013	3/2014	1/2015	8/2015	6/2016
Attendance	47	58	38	22	74	31	39
Returnees		8	29	13	22	8	20

[9] See for example [13].

[10] https://kreyonomi.com/2018/08/31/derive/

Figure 1: Group photo of the MIT-Haiti Initiative Workshop at SHCL in August, 2015. Credit: Kendy Verilus.

One of our principal objectives was to contribute what we could to the formation of a community of educators with a common experience and approach. The high number of returning participants suggested that we have had some success in this. See Figure 1.

Our workshops followed a common pattern. They would last three or four days. We would typically open with a demonstration of an engaged classroom. As an example, Peter Dourmashkin, Senior Lecturer in the MIT Department of Physics, came with a bag of yoyos and handed them out to groups of three or four participants. He carefully set up the following experiment. Put the yoyo down on a horizontal flat surface, with the string coming up from underneath. Here is the question: When you pull the string, will the yoyo roll towards you or away from you? This is a great question, for many reasons. There is no right answer: It turns out to depend on the angle the string makes with the table, as you can see by examining extreme cases. Then it becomes quantitative: what is the critical angle? This has a very simple and verifiable answer, relying on a basic principle of mechanics.

Each day, much of the morning was taken up by a lecture to the entire group, by Dr. Glenda Stump (then Associate Director for Assessment and Evaluation of MIT's Teaching and Learning Laboratory, now Education Research Scientist at MIT's Open Learning), in which the principles of modern educational theory were brought out, and general ideas about how to implement them in the classroom were discussed.

The afternoons were largely devoted to disciplinary sessions in Mathematics, Physics, Biology, and most recently Chemistry. This was a time when active learning techniques could be modeled and participants could develop lesson plans for use in their own classroom.

The pedagogical and disciplinary sessions were conducted in English with consecutive translation (except for the Physics sessions run by Dr. Paul Belony, a native *Kreyòl* speaker). We depended on the services of a superb group of translators, who contributed immensely to the vibrancy and excitement of the classroom. The Workshop in January 2015 was opened by Nesmy Manigat, then head of *MENFP*, and that office provided some financial

support and simultaneous translation at that workshop. Overall, however, our interaction with *MENFP* was difficult to say the least, and confirmed our sense that it was better to work independently of the government.

In two of the workshops we organized panel discussions: In one, participants at earlier workshops reported on activities they had put into effect in their classrooms; in the other, several leaders in Haitian education described some of their work and vision.

The workshops would end with a communal wrap-up. These events elicited passionate and moving testimony to the importance of this work, and expressions of commitment and optimism that played a critical role in maintaining the momentum of the MIT-Haiti Initiative.

2.3 Fellowship and Konbit

The MIT-Haiti Initiative workshops were by design brief and broad-based. A number of participants came to several workshops in succession, and we wanted to provide them with more opportunities to develop material for use in their classrooms. We invited a group of six of these most committed participants to visit MIT. All six accepted this invitation, and spent two weeks at MIT in September 2015. We designed a rich menu of talks and classroom observations, and spent a lot of time working with these individuals on refining their skills at creating student-engaged lesson plans in their respective subjects.

When this group returned to Haiti, five of the six formed an organization they called the "*Konbit MIT-Ayiti*." This is one of the most significant outcomes of the MIT-Haiti Initiative to date. This group, augmented more recently by a sixth member, consists of the following educators.

- Abdias Augustin, Physics and Chemistry, *UEH/Faculté des Sciences (FdS)*
- Jean Genis Dorvilien, Mathematics, *Catts Pressoir and Lycée de Cité Soleil*
- Jimmy Fedna, Biology, Quisqueya University and *UEH*
- Étrenne François, Chemistry, *Lycée Toussaint Louverture* and *MENFP*
- Guerda Jean-Guillaume, Mathematics, *Centre de Formation pour l'École Fondamentale*
- Adler Thomas, Physics and Chemistry, *UEH/FdS* and *Faculté de Médecine et de Pharmacie*

In the year following their visit to MIT this group ran four workshops in Haiti, including one at *LKM* on Lagonav, and are still very active in disseminating the principles of the MIT-Haiti Initiative.

2.4 Leadership and Teamwork Workshop

In June 2014, then Prime Minister Laurent Lamothe visited MIT with several of his deputies to prepare the way for a workshop later that month. This three-day workshop was conducted in Port-au-Prince under the leadership of MIT Sloan Professor Deborah

Ancona, Michel DeGraff, and MIT Sloan Executive Education Project Manager Rebecca Roseme Obounou. This extraordinary workshop reached a leadership group within the Haitian government whose membership transcends Haiti's endemic political turbulence, and made a real contribution to a progressive stabilization of the Haitian administrative structure.

2.5 CHCL Consultancy

The MIT-Haiti Initiative came to know the *Campus Henri Christophe at Limonade (CHCL)* branch of the *Université d'État d'Haïti (UEH)* in detail through a week-long consultancy in June 2016. This visit, following one of our standard workshops at that campus, was initiated by then *CHCL* President Jean-Marie Théodat and consummated by his successor Audalbert Bien-Aimé. It operated under a grant from the US Embassy in Port-au-Prince. We made a detailed study of the program of study at that university, especially the "*Propédeutique*" or foundational program. We visited many classrooms, interviewed faculty and administration, and wrote a report on our findings. This experience greatly deepened our understanding of the challenges facing Haitian institutions of higher education, and, we hope, helped the *CHCL* faculty improve their program. We will summarize some of what what we learned below.

2.6 Port-au-Prince Symposium

In March 2017 a Symposium was held in Port-au-Prince, bookending the NSF grant and opening the way for the next stages of the MIT-Haiti Initiative. It attracted many participants from our workshops, but also representatives from a wide range of academic administrators, language rights activists, NGOs, and publishers. Working groups on various topics were formed, and at least one, on translation, has become a major social media presence. The leader of that translation working group, Stevens Azima, is now helping us with the *Kreyòl* translation of an online calculus course on MITx (see below, in Section 2.9).[11] Material from that symposium is available on the MIT-Haiti website.

2.7 Library Project

As we ran our workshops, a major need quickly became clear and was reinforced repeatedly by our participants: there is very little textbook material written in *Kreyòl*, and a great demand for more at all levels and in all subjects – especially in STEM disciplines at high-schools and universities. This is not a need that the MIT-Haiti Initiative can address; this is work that has to be done by Haitian educators with first hand knowledge of the social and curricular demands that must be addressed. But as material for use in our workshops, we did produce quite a body of modern educational theory, and examples of how it can be put into practice in STEM disciplines (many produced by Haitian participants in the workshops, with specific classes in mind). We would always have all of this loaded onto memory sticks that were distributed to the participants. We encouraged our participants

[11] Azima has also created *Kreyòl* introductions to various mathematical concepts; see for example https://kreyonomi.com/2018/08/31/derive/, where the notion of the derivative is introduced.

to disseminate this material at their own institutions. Much of it is available now on the MIT-Haiti website. But we felt that it could be better organized, and formed into something appropriate for guidance in teaching practice more generally. Moreover, we discovered that hard copy is still more accessible in many places than electronic formats. So we are currently in the process of producing a series of pamphlets — on Biology, Chemistry, Mathematics, Physics, and Pedagogy — containing material developed for or during our workshops. These will be mirrored and enriched by web-based versions.

2.8 *Kreyòl* Glossary

In each of the workshops, and in subsequent work, the MIT-Haiti Initiative has assembled an extensive glossary of *Kreyòl* technical terms. This is available on the Initiative website and some of it will appear in the Library pamphlets. It is also being integrated into the Google Translate lexicon.

2.9 Calculus Translation

Under a grant from MITx, the MIT-Haiti Initiative is overseeing a *Kreyòl* translation of Calculus 1A: Differentiation. This prize-winning online course will be made available in a variety of formats for use for free by *Kreyòl* speakers.

3 The Mathematics Workshops

The experience of running workshops in Haiti has been both rewarding and surprising.

In support of my own undergraduate teaching, I had developed, with Hubert Hohn, of the Massachusetts College of Art, the "MIT Mathlet" collection.[12] I have used these tools regularly in lecture, and just about every homework assignment requires students to explore some concept or algorithm using the Mathlets. They are not simulations. I prefer to call them computational manipulatives, with reference to the Montessori learning tools. Students adjust parameters and witness the effect. The student acts with power, controlling many aspects of a mathematical situation by means of sliders that can be grabbed and adjusted. This agency contributes to the learning impact of these tools. The Mathlets also provide a variety of representations of the same data, and observing how these representations change together reinforces the connections between them. Keyboard entry is replaced by continuous adjustment of parameters. The effect is to situate any given example within a general family of examples that together produce a visualization of a "general" case. More recently, these tools have been seamlessly integrated into the MITx presentation of this course, used both residentially and in a MOOC setting.

Part of what I felt I could contribute to university-level education in Haiti was an awareness of this resource and some training in how to use it effectively in lecture and in support of group or individual work by students. We translated a half dozen of the Mathlets into *Kreyòl*. (See Figure 2.)

[12] http://mathlets.org

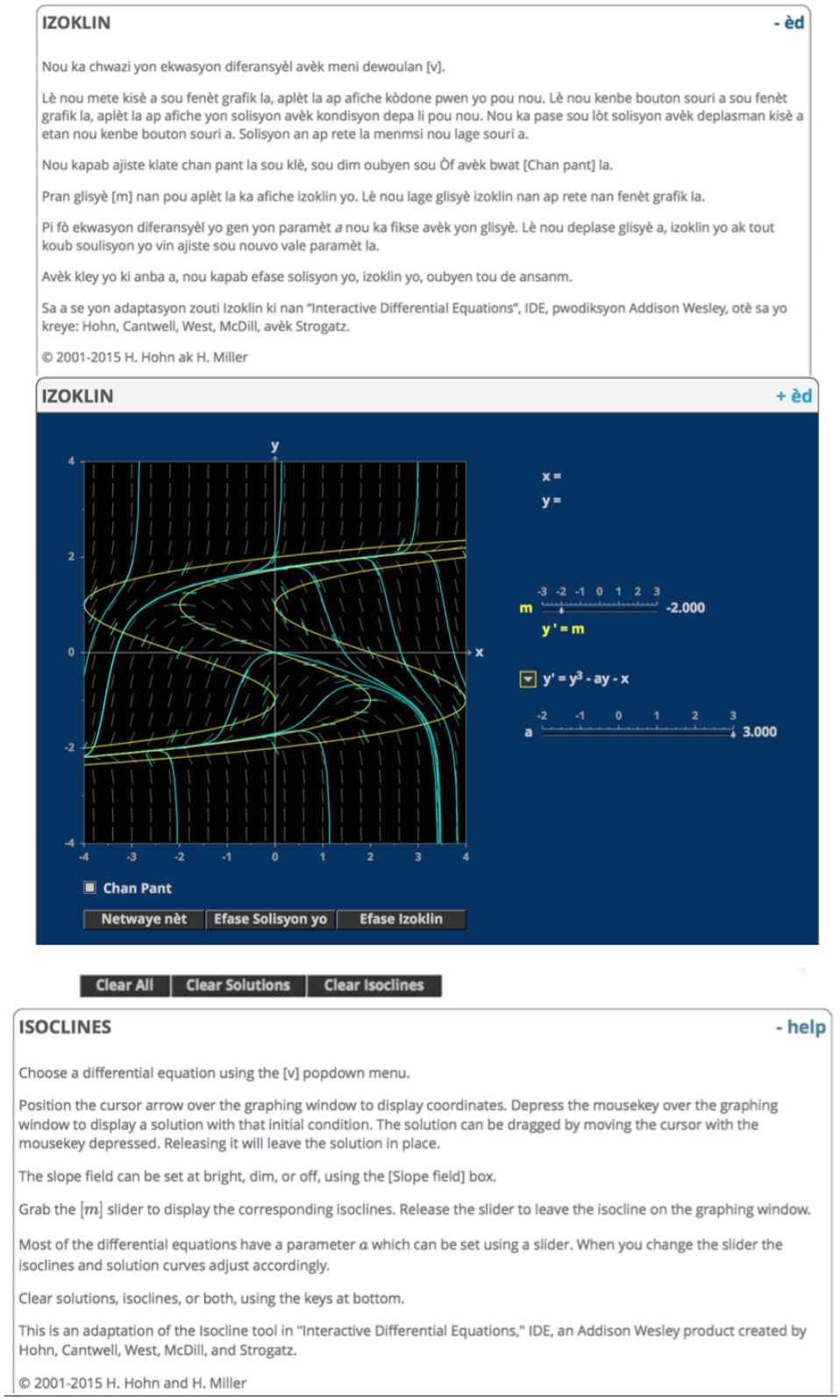

Figure 2: A sample mathlet in Kreyol, with English below. These are easily accessed at https://haiti.mit.edu/resources/mathlets/

One of the pedagogical and aesthetic principles underlying the design of the Mathlets was that they should be simple and direct. They often picture physical systems – spring-mass-dashpot systems or RLC circuits for example – but the screen contains very few words. The result is a minimization of cultural references, and this served us well when we came to export them to the Haitian context. (One cultural reference that we had to remove was the image of a thrown football. By this we meant American football, of course. But in Haiti as in many other countries in the world, "football" means "soccer," a sport in which the ball is thrown only in special situations. We learned from this and improved the main English collection by renaming the Mathlet "Ballistic trajectory.")

The Mathlets were first designed for and implemented in a course in ordinary differential equations. This course is taken by 75% of MIT undergraduates, and consequently has an engineering slant. Subsequently Mathlets have been written to support learning in Calculus, Linear Algebra, Probability and Statistics, among others.

So at the outset the Mathematics workshops in Haiti were focused on the use of Mathlets, especially in a differential equations course. I chose to focus on the standard "LTI package," computing the complex gain and hence gain and phase lag of a system controlled by a linear constant coefficient differential equation. This was partly because it was central to the differential equations course I taught at MIT, partly because the concepts and methodology were well illustrated by Mathlets, and partly because I thought it might correspond to a use-oriented syllabus in Haitian university curricula.

I discovered, however, that my participants did not teach differential equations. They taught courses in calculus or analysis; or in pedagogical practice to education majors; or more basic mathematics in primary and secondary schools. It was also unclear how frequently they would be able to actually use computer technology of any kind in their own teaching. In subsequent workshops the focus shifted away from technology and subjects typically taught in the first year of university in the United States, and more towards promulgating progressive pedagogical practice. We did enlarge the collection of *Kreyòl* Mathlets, including several built following suggestions made by participants in our workshops ("Graphing Rational Functions," "Linear Programming").[13] We added an introduction to the widely used package of mathematics tools GeoGebra,[14] and provided *Kreyòl* translations of a dozen GeoGebra Worksheets based on Judah Schwartz's excellent geometric explorations. In March 2014 Drs. Jeremy Orloff and Jonathan Bloom used their newly developed syllabus[15] on basic probability and Bayesian statistics as a basis for modeling an active learning classroom.

The faculty coming to these workshops almost always carried several jobs. The faculty we worked with in Limonade, for example, typically taught there on Monday and Tuesday, took a bus to Port-au-Prince on Wednesday, taught there on Thursday and Friday, and bussed back to Limonade over the weekend. The energy and commitment required to organize attendance at a four-day workshop in the face of these demands was impressive.

[13] These were both subsequently rendered in English and entered into the Mathlets website: http://mathlets.org/mathlets/graphing-rational-functions, http://mathlets.org/mathlets/linear-programming.

[14] https://www.geogebra.org

[15] A description of this course and the courseware for it can be found at https://ocw.mit.edu/courses/mathematics/18-05-introduction-to-probability-and-statistics-spring-2014/.

Figure 3: Guerda Jean-Guillaume guiding students in a classroom at *ESIH*. Credit Guerda Jean-Guillaume.

We have little information about what aspects of our message were brought back into the classrooms of our participants. One striking piece of evidence was provided by a video made by Guerda Jean-Guillaume of a class in which she formed the students into groups and led them through a script using the Mathlet "Graph Features[16]" in a first year Management class at *Ecole Supérieure d'Infotronique d'Haïti, ESIH*. (See Figure 3.)

And there is evidence [4] that the Workshops had the effect of increasing participants' comfort with using *Kreyòl* in teaching and in technical discussion.

4 The CHCL Program

The week in June 2016 spent at the *Campus Henri Christophe de Limonade (CHCL)* was very revealing of real educational conditions in Haiti, at least at this campus of the *Université de l'État d'Haïti*.

We were struck by the analogies between *CHCL* and our own home institution, MIT. Both are largely but not exclusively engineering schools. (One important difference is that *CHCL* has a large population of students preparing to be teachers, something MIT lacks.) Both institutions have a collection of courses that are required of all students. In both institutions, many of these courses are science or mathematics courses taught by scientists and mathematicians.

Admission to *CHCL* is very competitive: only around 20% of the students who take the entrance exam ("*concours*") are admitted. At the time of our visit, applicants were linearly ordered by a weighted sum of their scores on six exams (in mathematics, physics,

[16] http://mathlets.org/mathlets/graph-features/

chemistry, biology, earth science, and French, with mathematics given four times the weight of the others), and the top group (400 in the year we studied) were accepted. This system had the virtue of clarity and simplicity, but it produced a student body with a very wide range of preparation and ability. About 100 rejected students actually achieved scores on the mathematics exam that were above the median score achieved by the accepted students; and, conversely, fully 10% of the accepted students scored below the median of the scores achieved by the rejected students. The range of total scores among the students admitted on the basis of the 2014-2015 concours was quite wide: A factor of 2 separated the top scores from the bottom, and within the mathematics test the separation was by a factor of 10. These data all bear witness to the extreme variation in mathematics preparation within the applicant pool. The faculty expressed great concern about how best to bring weaker students up to par, revealing a belief that it is their responsibility to help all students admitted to *CHCL*.

The *CHCL Propédeutique* or *Cycle Préparatoire Integré (CPI)* mathematics syllabus seemed to be based on a traditional French *école préparatoire* model. It was relentlessly formal, beginning with the general and gradually becoming more specific. Great emphasis was placed on precise notation and definitions.

Classes were typically lectured in *Kreyòl* with blackboard writing and worksheet material in French. Lectures were often augmented by "*travaux dirigés*," sometimes taught by the lecturer immediately following the lecture, in which students, perhaps in groups, worked on problems illustrating the concepts introduced in the lecture.

All the lecturing we witnessed was well-organized, clear, and energetic. The students were by and large attentive. We noted two common traits that are shared by university teachers across the world. There was a tendency to lecture to the top group, the most attentive group, and let the back of the class drift; and quite often the problems students were asked to work on seemed repetitive. We found ourselves wishing that the faculty would propose activities developing cognitive skills higher in Bloom's taxonomy, offering students more developmentally appropriate challenges.

We found that the performance expected of students in examinations was much more conceptual and challenging than what was expected in the classroom. Given this disparity, we were actually quite impressed with the level of performance on the examinations we saw. Indeed, some of the students struck us as simply brilliant, based on their examination performance.

5 Equity

An interesting framing of the notion of equity spelled out by Rochelle Gutiérrez [10] illuminates the importance of efforts such as ours. She identifies four "dimensions," or poles, of the concept of equity: *Access* and *Achievement* form the ends of the "dominant axis," which intersects the "critical axis" that terminates in *Identity* and *Power*.

Linguistic barriers form extremely effective obstacles to access, perhaps especially to education. As Gutiérrez points out, aspects of access within mathematics education include "resources that students have available to them to participate in mathematics, including such things as: quality mathematics teachers, adequate technology and supplies in the

classroom, a rigorous curriculum, a classroom environment that invites participation, and infrastructure for learning outside of class hours." All of these are for the most part available to only a tiny élite student group in Haiti.

Access makes achievement possible, but of course more is required. The example of *LKM* shows that the introduction of French as a second language results in higher achievement than early school immersion does. The linguistic barrier is one part of a broader characteristic of the Haitian educational system, as we understand it: much of it seems to be designed as a filter not a pump. Examinations are systematically set to be very difficult, for example, with low passing rates.

The critical axis captures underlying societal structures, of which the dominant poles are symptoms. Gutiérrez posits that identity "…includes whether students have opportunities to draw upon their cultural and linguistic resources (e.g., other languages and dialects, algorithms from other countries, different frames of reference) when doing mathematics, paying attention to the contexts of schooling and to whose perspectives and practices are 'socially valorized' …." This describes the alienating presumptions present in much of Haitian education. We have spent much effort encouraging incorporation of local cultural references and the rich supply of *Kreyòl* idioms. *Kreyòl* is in fact at the very core of Haitian identity.

And Power is to Identity as Achievement is to Access. From the educational perspective, power has various faces. The existing structures are maintained through the exercise of power, from positions that are generally accessible only to the élite. At the level of the classroom, the power imbalances that permeate the dominant contemporary educational model in Haiti leave little room for personal agency, well known as a key student motivator. Systematic use of a language not easily spoken by the students is a principal cause of this limitation. A shining exception to this is the *LKM* system.

Overall, the suppression of *Kreyòl* in the Haitian educational system presents a textbook example of *elite closure*, in the terminology of the linguist Carol Myers-Scotton [15]: "Elite closure is a type of social mobilization strategy by which those persons in power establish or maintain their powers and privileges via linguistic choices." These methods are both powerful and difficult to combat.

6 Conclusion

We found in Haiti an energetic and committed cadre of university-level teachers, eager to learn about and put into practice "active learning" methodologies in the Haitian mother tongue *Kreyòl*. They often face serious political, administrative and cultural hurdles in implementing these ideas, but we also encountered forward-looking administrators eager to advance this agenda.

We look forward to further collaboration with these individuals, and enlarging the scope of our efforts. We see several very attractive opportunities.

- One of the most impressive outcomes of our work to date was the formation of the *Konbit*. The two week visit to MIT had a dramatic long-term effect. We would like to do this again, learning from the first experience, to expand the capacity of the team working full time in Haiti.

- There is enormous need for courseware that is culturally relevant, supports active learning pedagogies, and is available in *Kreyòl*. The ideal goal would be to create courseware in *Kreyòl* that is simply better than what is available in French.
- One way to support the creation of this material is to arrange for semester long visits by Haitian academics to US institutions. This would tap into untested creative potential. One model might be to have the visitor follow an existing course, learning the strategies and philosophy in detail and adapting it in real time to the Haitian local context.
- We hope to maintain our relationship with *CHCL*, and extend our engagement to other institutions. Institutional commitments in Haiti can be fragile, but are nevertheless critical if reforms are to take root. We came to feel that a combination of direct contact with faculty and collaboration with administration is the most effective approach.

Haiti is by no means alone in suffering from this form of linguistic apartheid; it is estimated[17] that some 40% of children in the world receive education in a language other than their mother tongue. The typical situation involves rather localized languages, spoken by just a fragment of the national population. Haiti, in contrast, is blessed with a national language, spoken by all Haitians. This is a major untapped national resource, and exploiting it constitutes a great opportunity for Haiti. The MIT-Haiti Initiative represents a modest contribution to the movement to unlock this potential.

References

[1] Guy Alexandre, *La politique educative du Jean-Claudisme: Chronique de l'échec "organisé" d'un projet de réforme," Le Prix du Jean-Claudisme: Arbitraire, parodie, désocialisation*, Haiti, C3 Editions, 2013.

[2] Michel DeGraff, Linguists' most dangerous myth: The fallacy of Creole Exceptionalism, *Language in Society* 34, 533–591. http://bit.ly/1EowtV4.

[3] Michel DeGraff, Mother-tongue books in Haiti: The power of Kreyòl in learning to read and in reading to learn, *Prospects: Comparative Journal of Curriculum, Learning, and Assessment* 46 (2016) 435–464.

[4] Michel DeGraff and Glenda Stump, Kreyòl, pedagogy, and technology for opening up quality education in Haiti: Changes in teachers' metalinguistic attitudes as first steps in a paradigm shift, *Language* 94 (2018) e127–e157.

[5] Laurent Dubois, *Haiti: The Aftershocks of History*, Picador, 2013.

[6] Harry E. Dumay, The Paradox of High Satisfaction and Low Choice: A Study of Student Satisfaction and University Access in Haiti, PhD thesis, Boston College, 2009. http://hdl.handle.net/2345/726.

[17] http://unesdoc.unesco.org/0024/002437/243713E.pdf

[7] Jacques-Michel Gourgues, *Les manuels scholaires en Haïti: Outils de la colonialité, Documentation haïtienne, Education Monde Caraïbes Haïti*, 2016.

[8] *Groupe de Travail sur L'Éducation et La Formation, Jacky Lumarque, coordonnateur, Pour un Pacte National pour l'Education en Haïti*, 2010.

[9] *Groupe de Travail sur l'Éducation et la Formation, Vers la Refondation du Système Éducatif Haïtien Plan Opérationnel 2010-2015*. https://www.ifadem.org/sites/default/files/divers/Planrefondation-Haiti.pdf.

[10] Rochelle Gutiérrez, Framing Equity: Helping Students "Play the Game" and "Change the Game," *Teaching for Excellence and Equity in Mathematics* 1 (2009) 5–7.

[11] Bernard Hadjadj, Education for All in Haiti Over the Last 20 years: Assessment and Perspectives, Eduation for all in the Carribean: Assessment 2000 Monograph Series 18, UNESCO, 2000. http://unesdoc.unesco.org/0013/001363/136393e.pdf

[12] The Interuniversity Institute for Research and Development, The Challenge for Haitian Higher Education, http://www.inured.org/uploads/2/5/2/6/25266591/the_challenge_for_haitian_higher_education.pdf.

[13] Jonathan M. Katz, *The Big Truck that Went By: How the world came to save Haiti and left behind a disaster*, St Martin's Griffin, 2014.

[14] Gérarde Magloire, Haitian-ness, Frenchness and History: Historicizing the French component of Haitian National Identity, in Sciences sociales et Caraïbe, special edition of Pouvoirs dans la Caraïbe, 1997, pp 18–40.

[15] Carol Myers-Scotton, Elite closure as a powerful language strategy: the African case, *Intl. J. Soc. Lang.* 103 (1993) 149–163.

[16] Marc Prou, Attempts at reforming Haiti's education system: The challenges of mending the tapestry, 1979–2004, *Journal of Haitian Studies* 15 (2009) 29–69.

A Note on Equity Within Differential Equations Education by Visualization

Younes KarimiFardinpour
Islamic Azad University, Ahar Branch

Keywords: Visualization, mathematical communication, bilingualism, dynamic method, equity education, differential equations
Manuscript received on May 17, 2018; published on February 13, 2019.

Abstract: The growing importance of education equity is partly based on the premise that an individual's level of education directly correlates to future quality of life. Educational equity for differential equations (DEs) is related to achievement, fairness, and opportunity. Therefore, a pedagogy that practices DE educational equity gives a strong foundation of social justice. However, linguistic barriers pose a challenge to equity education in DEs. For example, I found myself teaching DEs either in classrooms with a low proficiency in the language of instruction or in multilingual classrooms. I grappled with a way to create an equity educational environment that supported students both with social justice mathematics and satisfaction for the students. According to the 2000 NCTM (National Council of Teachers of Mathematics) *Principles and Standards for School Mathematics*, mathematics instructors should strive to meet the demands of Principles and Standards. However, meeting the standards such as the Equity Principle can be a daunting task. DE student diversity in language proficiency might enrich the educational environment, but it also raises challenges. This brief report summarizes a way to build an equity learning environment by providing visualization support.

1 Linguistic barriers in DEs education

For the past decade, I have taught DEs with an eye toward promoting multiple representations [8]. In line with [3, 11], I encouraged my students to access notation by mathematical communication. Mathematical communication, verbally or in writing, is challenging for many students, especially multilingual students, and poses barriers on exams ([4, 5]). I found that students who were strong in mathematics in their native language (such as Azari) often find themselves handicapped in using a second language (such as Farsi) to communicate their mathematical thoughts. I noticed that those who passed my DE exams (in Farsi, the official language for instruction) were mostly native speakers of Farsi, even though the student population was mostly multilingual, with different native languages (such as Azari, Farsi, and Kurdish). The main problem for multilingual students was

in language proficiency. In the same vein, Martiniello, in a study comparing students' performance, showed that nonnative speaking students performed significantly lower than their native speaking peers despite the fact that they had the same level of mathematical knowledge [9]. So nonnative speaking students were challenged by lacking the language skills ([1, 2]). In fact, it was hard to distinguish whether my DE exams measured a student's language proficiency or his or her knowledge of differential equations. For multilingual students who may have appropriate DE knowledge but who had difficulty explaining their mathematical thinking, my exams were a gatekeeper. Thus, it required me to be knowledgeable about potential linguistic bias.

2 Translating verbalization into visualization

I found that my multilingual students' ways of thinking, although different from that of native speakers, were correct. Therefore I asked all students to translate verbal expressions into visual aspects. It engaged my students in thinking and communicating in any language. Using visualization to express their mathematical thinking helped them feel empowered and excited by mathematical communication ([6, 10, 12, 13]). Even though some students' visualization may not be perfect, the mathematical thinking and mathematical communication derived from this exercise was very helpful ([7, 8]). One of the aims of the paper reported in [8] was to determine the extent to which visualization might enable multilingual students to improve themselves. The following briefly describes how visualization could be useful, for example, to better understand autonomous DEs.

KarimiFardinpour and Gooya [8] highlighted two students' difficulties: long-term prediction and coordinating graphs in different coordinate planes. The former concerns students' attempts to visualize the graphs of solution curves of autonomous differential equations for predicting the long-term behavior for various initial conditions. The latter involves the coordination of two or more graphical representations in different coordinate planes and is the focus of this report. In this same report, we outlined three different geometric approaches for visualizing autonomous differential equations and their effectiveness for overcoming student difficulties. The three approaches are referred to as Standard, Traditional, and Dynamic. The authors came to the conclusion that the positive effect of the Traditional method was more than the Standard method, and the Dynamic method had better results than the Traditional method. In the following, these three methods are briefly described for the autonomous differential equation

$$dy/dt = -r(1 - y/T)(1 - y/K)y$$

where r, T and K are constants.

With the Standard geometrical approach, students are provided with an autonomous differential equation in the form $dy/dt = f(y)$ and the corresponding graph of $f(y)$ vs. y. Then they are requested to draw sample solution curves in the $[t, y(t)]$ plane that are coordinated with that graph. For example, Fig. 1(a) is the graph of $f(y) = -r(1 - y/T)(1 - y/K)y$ versus y that is given to the students, and Fig. 1(b) is what the students are asked to draw.

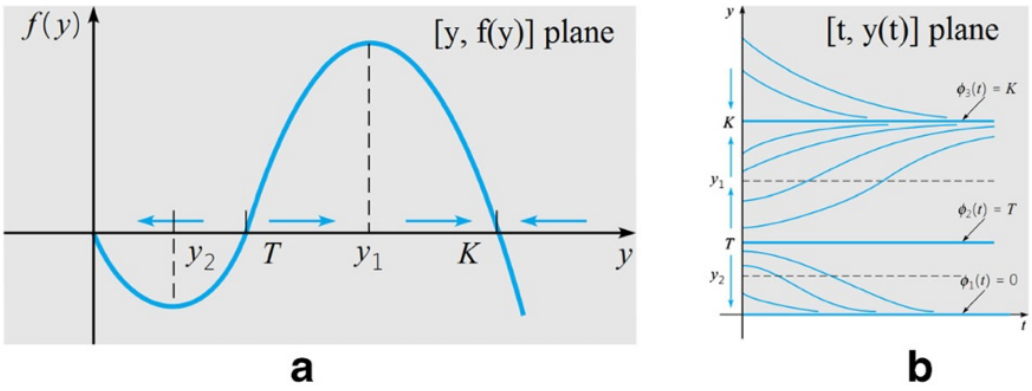

Figure 1: The Standard geometrical approach for $dy/dt = -r(1 - y/T)(1 - y/K)y$. Graph **a** is given, graph **b** is the task for students.

In the Standard method, I preferred to use $[y, f(y)]$ and $[t, y(t)]$ instead of the yy'-plane and ty-plane in order to emphasize the dual role of y. It is very important that students be aware of this dual role, as the y is meant to represent the function of t in the $[t, y(t)]$ plane, as well as to act as a variable in the $[y, f(y)]$ plane.

In the Traditional geometrical approach (as shown in Fig. 2), the phase-line has also been drawn (part c), coordinated with the given $[y, f(y)]$ plane.[1] Now students are requested to draw the sample solution curves in the $[t, y(t)]$ plane, coordinated with the phase-line, which has been isolated from the y-axis in the $[t, y(t)]$ plane. This visual connection helps students to understand the phase space of y as $t \to +\infty$.

The new Dynamic method (shown in Fig. 3) has the following unique features:

- the $[y, f(y)]$ plane is rotated counterclockwise 90 degrees;
- a sign-chart is put between $[y, f(y)]$ and $[t, y(t)]$ giving the positive/negative values of $f(y)$,$f'(y)$ and $f(y) \cdot f'(y)$;
- horizontal dotted lines partition the whole solution space at the equilibria and inflection points;
- small solid circles and small hollow circles respectively represent equilibrium solutions and inflection points of solutions.

In the Dynamic method, the horizontal dotted lines play two different roles. Those connecting solid circles have partitioned the whole solution space according to initial conditions, to help students understand the structure of the solution space. Thus the critical points, the zeros of $f(y)$ in the $[y, f(y)]$ plane, are linked to the equilibrium solutions (as

[1]Fig. 1 is taken from the 7th edition of the Boyce and DiPrima's textbook *Elementary Differential Equations* and Fig. 2 is taken from the 9th edition. Although diagrams similar to Fig. 1 appeared earlier in the text by Blanchard, Devaney, Hall, it is unclear who first isolated the phase-line from the y-axis in the $[t, y(t)]$ plane.

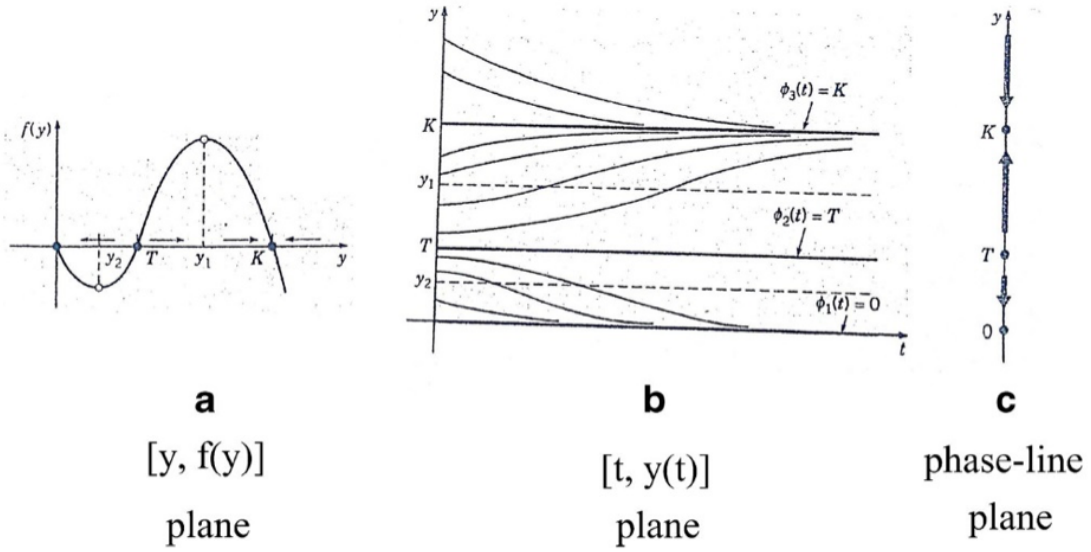

Figure 2: The Traditional geometrical approach for $dy/dt = -r(1 - y/T)(1 - y/K)y$. Here graphs **a** and **c** are given, graph **b** is the task for students.

fixed value functions in the $[t, y(t)]$ plane), which enhances students' understanding of the concept of equilibrium solution.

The dotted lines between open circles connect the extreme points in the $[y, f(y)]$ plane to the inflection points in the $[t, y(t)]$ plane. Seeing these inflection points helps students to understand the concavity of the sample solution curves.

The originality of the Dynamic method is its ability to connect planes, and make a visual coordination between them. These visualization components of the Dynamic

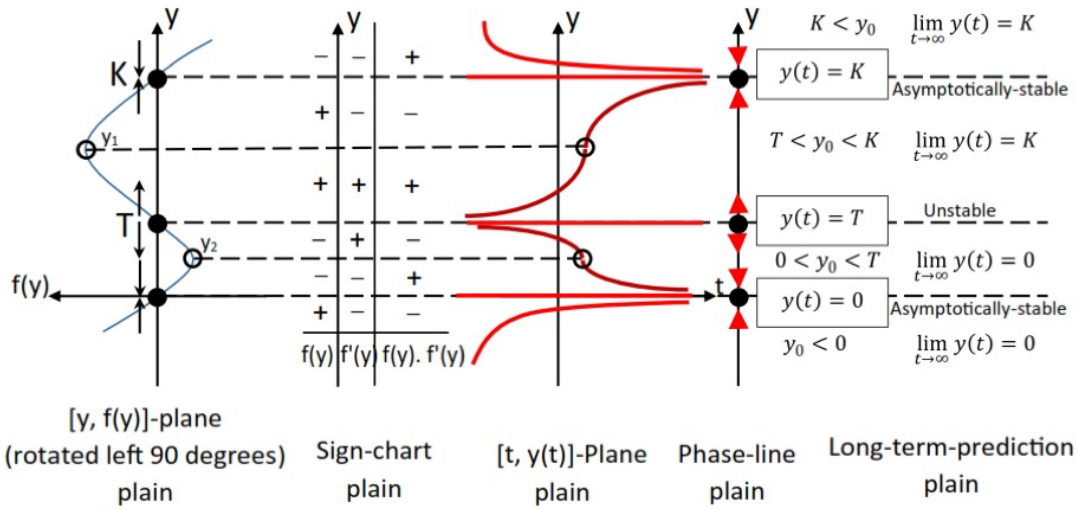

Figure 3: The Dynamic geometrical approach for $dy/dt = -r(1 - y/T)(1 - y/K)y$. The graph at far left is given; the students are asked to add the dotted lines, circles, sign chart, and solution curves, and arrows on the phase line.

method help students to make sense of the connections between the differential equation and the long term behavior of its solutions.

3 The Last Word

I have found that the Dynamic method supports my students who have a low language proficiency in Farsi, so that all of my students could find themselves belonging to the classroom group and achieving understanding of the mathematics. That is a foundation of social justice. I also turned the mirror back on myself to examine my pedagogy and my exams. I asked myself what I did about the equity lens, and this note summarizes the research results described in [8]. I continue my attempt to observe social justice regarding equity within differential equations education by visualization.

References

[1] R. Barwell. Integrating language and content: issues from the mathematics classroom. *Linguistics and Education*, 16(2), 2005.

[2] R. Barwell. Mathematical word problems and bilingual learners in England. *Multilingualism in Mathematics Classrooms: Global Perspective*, 63(77), 2009.

[3] S. Habre. Improving understanding in ordinary differential equations through writing in a dynamical environment. *Teaching Mathematics and Its Applications: An International Journal of the IMA*, 31(3), 2012.

[4] Y. KarimiFardinpour. Mathematics teachings' experiences in bilingual classrooms in North-West Iran. *Pre-proceeding of ICMI Study 21 conference*, 2011.

[5] Y. KarimiFardinpour. Educational challenges on geometric approach in differential equations: coherent qualitative behavior analysis. *12th Seminar on Differential Equations and Dynamical Systems (SDEDS-Tabriz-2015)*, 2015.

[6] Y. KarimiFardinpour. Factors to predict the engineering students' satisfaction with the quality of the differential equations curriculum: factor analysis. *Journal of Curriculum Studies (Iranian Curriculum Studies Association)*, 6(11), 2015.

[7] Y. KarimiFardinpour and Z. Gooya. Analysis of educational challenges of geometric approach on autonomous differential equations: task based interview. *Journal of Curriculum Studies (Iranian Curriculum Studies Association)*, 6(12), 2016.

[8] Y. KarimiFardinpour and Z. Gooya. Comparing three methods of geometrical approach in visualizing differential equations. *International Journal of Research in Undergraduate Mathematics Education*, 1(19), 2017.

[9] M. Martiniello. Language and the performance of English-language learners in math word problems. *Harvard Educational Review*, 78(2), 2008.

[10] C. Rasmussen and H. Blumenfeld. Reinventing solutions to systems of linear differential equations: A case of emergent models involving analytic expressions. *The Journal of Mathematical Behavior*, 26(3), 2007.

[11] C. Rasmussen and O.N. Kwon. An inquiry-oriented approach to undergraduate mathematics. *The Journal of Mathematical Behavior*, 26(3), 2007.

[12] C. Rasmussen, M. Zandieh, and M. Wawro. How do you know which way the arrows go? *Mathematical Representation at the Interface of Body and Culture*, 2009.

[13] E. Yackel, C. Rasmussen, and K. King. Social and sociomathematical norms in an advanced undergraduate mathematics course. *The Journal of Mathematical Behavior*, 19(3), 2000.